Eutrophication and bottom water hypoxia in the northern Gulf of Mexico: reconstructing their development over the last century using palynological and geochemical tools

Imke Smeets
4271882
i.smeets@students.uu.nl

Master's thesis
Program "Earth, Life and Climate"
Utrecht University
December 2021

1st supervisor: Dr. Francesca Sangiorgi, Utrecht University, f.sangiorgi@uu.nl
2nd supervisor: Yord IJdema MSc, Utrecht University, y.w.ijdema@uu.nl
3rd supervisor: Dr. Francien Peterse, Utrecht University, f.peterse@uu.nl

Contents

Abstract

Marine hypoxia in bottom shelf waters (<2 mg oxygen per liter) is caused by a combination of eutrophication, caused by high (river) nutrient input in the top waters, and stratification preventing oxygenated waters to reach the bottom of the shelf. Human activities in the watershed, such as the use of fertilizer and municipal wastewater discharge, can cause a strong increase in this nutrient load. Bottom-water hypoxia is often problematic, causing biodiversity to decline and toxic substances, such as H_2S and As^{3+}, to be produced.

The northern Gulf of Mexico (nGoM) is home to the second-largest hypoxic zone in the world. Although hypoxia was present before the 1950s, since the 1950s hypoxia has significantly worsened due to increased (anthropogenic) nutrient input via the Mississippi and Atchafalaya rivers, mostly in the form of nitrogen originating from fertilizer use in the watershed. The nGoM's natural inclination to stratification also helps the formation of hypoxia. To prevent eutrophication and hypoxia from worsening, the Action Plan for Reducing, Mitigating, and Controlling Hypoxia was formulated in 2001. However, to date, the successful integration of the Action Plan has proven to be a challenge, despite its solid scientific backing. The extend of the hypoxic zone has risen, not decreased, since 2001.

To battle hypoxia, it is essential to understand the nGoM and its history in high detail. It is useful to extend our range of vision beyond the era of direct hypoxia measurements (from the 1970s onward) to investigate when, how and under which conditions hypoxia formed and developed. Therefore, the aim of this study is to reconstruct the history of nutrient loading and hypoxia over the last ~100 years in the northern Gulf of Mexico, using core "80b" from the 64PE467 expedition to the nGoM in 2020. The core was analyzed for dinocyst assemblages, and additionally for geochemical parameters ($\delta^{13}C$, $\delta^{15}N$, %N, TOC), colour parameters, and pollen assemblages to very roughly reconstruct vegetation changes.

Of the parameters, %N and $\delta^{15}N$ are used as proxies for terrestrial nitrogen input, a* (the red-green colour parameter) for clastic input, $\delta^{13}C$, TOC, TIC and, to a lesser extent, the absolute abundance of autotrophic dinocysts for primary production, and the absolute abundances of *Lingulodinium machaerophorum*, *Brigantedinium spp*. and heterotrophic dinocysts for eutrophicaton. For some of these proxies, Principal Component Analysis was used to investigate their relationship to other proxies and determine what they indicated. Since heterotrophic dinocyst are selectively vulnerable to oxic degradation, all relative abundances of dinocysts (including the %heterotroph proxy) are deemed unreliable.

The proxies indicate that the first signs of enhanced productivity appear in the 1950s. The first signs of (slight) eutrophication appear in the late 1960s. Productivity gradually increases, until the 70s-80s boundary, where it increases sharply, most certainly related to nitrogen loading. Productivity remains high during the 80s and 90s, where the system seems to have experienced peaks of eutrophication. In the 2000s and 2010s, productivity rises again and eutrophication becomes more permanent. The exception is 2018, where productivity and eutrophication shortly fall (possibly because of low river discharge, but this is uncertain).

For hypoxia, there is evidence that this was at least present in the 1970s, 1980s, 2000s and 2010s. The absence of signs of hypoxia before the 1970s is probably due to relatively low levels of N loading and productivity. For the 90s, when N loading and productivity are high, the absence of signs of hypoxia would have been caused by other (unknown) means. This suggests that widespread hypoxia started in the 1970s.

Introduction

The phenomenon of hypoxia

Marine hypoxia is a state of very low oxygen concentrations in the water: lower than 2 mg oxygen per liter. Marine anoxia, a related phenomenon, refers to seawater in which no oxygen is present. Although hypoxia and anoxia can also occur in marine sediments, in other bodies of water such as lakes, this study focuses on a particular type: hypoxic (or anoxic) marine bottom waters on continental shelves.

The causes of such bottom-water shelf hypoxia are already well understood: it is a combination of eutrophication caused by high nutrient input in the top waters, and stratification preventing oxygenated waters to reach the bottom of the shelf. Organic matter, produced at the top of the water column, sinks down and is remineralized. This process uses oxygen, so hypoxia develops when much organic matter is produced and when oxygen is not sufficiently renewed because of reduced mixing with oxygen-rich waters, often caused by strong stratification. As organic matter is less effectively remineralized, more organic carbon is buried in the sediment.

The specifics of this process differ per region, and in the "hypoxia in the GoM" section, I will digress on the constraints specific for the northern Gulf of Mexico, which is the focus of this study. However, it is a universal given that organic matter production is high in coastal systems where (riverine) nutrient supply is also high, often combined with stratification. Human activities in the watershed, such as the use of fertilizer and municipal wastewater discharge, can cause a strong increase in this nutrient load. As virtually all human influences have intensified over the last decades, hypoxia, all over the globe, has worsened (Breitburg et al. 2018). This coincides with other anthropogenic forcings which have intensified, including global warming and ocean acidification.

Bottom-water hypoxia can be problematic. In hypoxic shelf waters, electron acceptors that replace oxygen (such as Fe^{3+} and sulfate) yield less energy, causing more energy in the ecosystem to be transferred to microbes; the ecosystem's ability to support larger and more organisms is severely hampered. Biodiversity declines. Migrations of different taxa and trophic groups caused by the changing seawater conditions can cause crowding and therefore food competition in other areas, increased vulnerability to predation, increased stress, and local extinctions. Low oxygen levels can even interfere with reproduction, also in generations after the hypoxia has seceded, and may weaken the immune system.

It is especially the combination of hypoxia with other related ecosystem pressure, such as aforementioned anthropogenic warming and ocean acidification, that is so dangerous. More energy is needed within the ecosystems to withstand these pressures, but hypoxia reduces the amount of energy available. Unbalanced ecosystems may also yield less (shell-)fish for human consumption, threatening the livelihood of millions. The Baltic cod, for example, fared far worse when it experienced increased food competition caused by ecosystem compression (Breitburg et al. 2018). Breitburg et al. (2018) points out that the harm done by extensive hypoxia extends further than organisms alone. When oxygen levels above the sediment's face are low, more phosphorus and iron are released from the sediment and into the water column, even further enhancing the biological productivity responsible for causing the hypoxia in the first place. When little oxygen is available, organic matter is remineralized by means of denitrification and annamox. This removes biologically available nitrogen out of the ocean as N_2 gas. When this nitrogen is not sufficiently renewed by nitrogen fixation, this will affect total biological production on millennial timescales.

Denitrification, especially in suboxic rather than anoxic environments, also produces the greenhouse gas NO_2. According to Breitburg's review, low-oxygen zones contribute largely to the total flux of NO_2

to the atmosphere. Also, when circumstances worsen and anoxia replaces suboxia, H_2S gas may be produced, which is toxic to aerobic organisms. Another toxic substance that may form is As^{3+}. Cadmium, copper and zinc form sulfides and precipitate in anoxic sediments, possibly altering worldwide cycling of these important micronutrients. Anoxic sediments also excrete methane, a powerful greenhouse gas.

In hypoxic waters, organisms that are unable to move out of the hypoxic zone die, while organisms that migrate away may cause crowding and increased food competition in other ecosystems (Breitburg et al. 2018). Toxic substances such as H_2S and As^{3+} might be produced. This harms ecosystems that provide a livelihood in (shell-)fish for millions of people.

Hypoxia in the GoM

The northern Gulf of Mexico (nGoM), an area where the outflow of the great North American Mississippi river and related Atchafalaya river is most felt, is a continental shelf with the second largest hypoxic zone in the world (Van Meter et al. 2018) and the largest zone of oxygen-depleted coastal waters in the entire western Atlantic Ocean (Rabalais and Turner 2001). The zone of hypoxic bottom water encroaches to an area of around 20 000 km^2 at midsummer, with only the hypoxic zone of the Baltic Sea (70 000 km^2) surpassing it in size. It extends up to 125 km off the shore and to 60 m water depth (Dale et al. 2010). Hypoxia does not only occur close to the seabed, but permeates 20 to 50 percent of the water column above, sometimes up to 80 percent (Rabalais et al. 2002). The hypoxic area is south and southwest (down current) of the deltas of the Mississippi and Atchafalaya rivers.

Hypoxia occurs continually from mid-May to mid-September (Rabalais et al. 2002). In these months, the outflow of the rivers is greatest. This results in a larger input of nutrients than in the winter months, causing enhanced eutrophication. Also, the river's freshwater induces enhanced stratification, which is also a factor in the development of hypoxia. The stratification is occasionally broken down by (multiple) large tropical storms and hurricanes occurring in the area, in which cases oxygen can reach the deeper waters and the extend of the hypoxic zone will diminish.

Today, the system is more sensitive to nutrient inputs than in the past, due to a regime shift in the ecosystem. So, the same amount of nutrients now invokes more intense hypoxia than it would in the past. This is reason for concern: benthic and fish communities find it hard to survive in hypoxic zones. The recovery of the ecosystems may only be possible after a long period of reduced nutrient input (CENR, 2010).

Action Plans and Policy

To protect the Gulf's ecosystem, improve water quality in the Gulf as well as in the rivers, and to reduce anthropogenic nutrient input in the river basins, much research has been conducted and action plans have been devised. After scientists started to realize that "something was wrong" in the late 70s, yearly monitoring of the midsummer extend of the hypoxic zone has started in 1985. Later, the Mississippi River/Gulf of Mexico Watershed Nutrient Task Force was formed (Dale et al. 2010). The Task Force asked the White House Office of Science and Technology Policy for a thorough scientific assessment of the causes and consequences of Gulf Hypoxia, and this resulted in the *Integrated Assessment of Hypoxia in the Northern Gulf of Mexico* (CENR 2000). Informed by this Integrated Assessment, the Task Force created their Action Plan for Reducing, Mitigating, and Controlling Hypoxia in the Northern Gulf of Mexico, which was brought before the US congress in 2001 (Nutrient Task Force 2001). The Action Plan contained:

1. Ten management actions to be implemented, and

2. A plan to reassess actual nutrient load reductions, hypoxic zone extend, water quality, ecosystem health, and economic and social effects every five years.

However, to date, the reassessments have painted a bleak picture. The successful integration of the Action Plan has proven to be a challenge, despite its solid scientific backing (further strengthened by the findings of an independent research panel requested by the Task Force (Dale et al. 2010) and despite a new, updated Action Plan issued in 2008 (Nutrient Task Force 2008). Economic interests have often interfered with the hypoxia action plans. For example, corn-based ethanol production has been encouraged in the basin since the *Integrated Assessment*, as part of a plan to produce renewable fuels. It is expected that 6,5 million hectares of corn will be planted, most of which in the Mississippi and Atchafalaya river basins. This would mean a large increase in N loadings to the river basins (Dale et al. 2010, x1vi).

The related goal of reducing nitrate river load by 60 percent was also far from reached, because of a phenomenon termed "nutrient legacy". Some nutrients tend to linger in the soils of the river basin. These "old" nutrients only slowly leach into the groundwater and rivers, but they do add to the present-day nutrient loads. This means that a lag exists of about 30 years between implementation of reduction strategies and their observable effects (Van Meter et al. 2018).

Factors like these have caused the extend of the hypoxic zone to rise, not decrease. The Action Plan's goal for 2015 was a reduction of the hypoxic zone to 5,000 km^2 (5-year running average). This would take a reduction of at least 45% in total riverine N flux (with the greatest emphasis on the spring flux) and, also, at least a 45% reduction of total riverine P flux, based on model predictions (Dale et al., 2010, x1iv). But in 2015, the real extend of the hypoxic zone was three times as large.New research suggests that the situation will only get worse: climate change may cause the need for even greater nutrient reductions, such as 50-60% for N (Dale et al., 2010).

Nitrogen or phosphorus

Apart from N, P may also be an important nutrient contributing to primary production, as is the case in other systems such as lakes and the open ocean (Fennel and Laurent 2018). P has also been on the rise: since the mid-1950s, P load has become twice as large (Justic et al. 1995). In contrast, the N load has become three times as large during the same time period (Turner and Rabalais 1991). However, since the 2000s, N has only increased slightly (Stets et al. 2015). Still, the size of the hypoxic zone has not gone down. Is this due to the still very high N load (regardless of a rise in this load of not), or may the influence of P play a role here? Indeed, in anoxic bottom waters, sediments may release P into the water column, causing more primary production and creating a positive feedback loop (Adhikari et al. 2015). But although P input does play a role in the development of hypoxia, N input seems to play the bigger role.

Turner and Rabalais (2013), using algal cultivations, found that phytoplankton in the nGoM is mostly N limited. Another portion was N *and* P limited. Only a very small portion (less than 10 percent of samples) appeared to be only P limited. Therefore, they conclude that limiting N input is vital in the reduction of hypoxia, but that P should not be completely overlooked. A later study (Fennel and Laurent 2018) confirms this and adds to it. They make a distinction between the ultimate and proximate limiting nutrient. While the proximate limiting nutrient is only locally or temporarily limiting, the ultimate limiting nutrient determines the productivity of a system over longer timescales, in this case years to centuries. Their model simulations show that, on this timescale, P is the proximate limiting nutrient, N the ultimate one. Reducing P would decrease hypoxia on a short timescale, but for lasting and bigger effect, we would need N reduction. This is consistent with other observations (US Environmental

Protection Agency 2007): P limitation almost exclusively occurs in the Mississippi river plume and estuaries, not further out to sea, and then only during spring and summer.

However, P limitation may become more important for the whole system. According to the models of Fennel and Laurent (2018), the system is almost N saturated. Now, the system is still far more sensitive to changes in N than in P, but after saturation, the sensitivity to N might decrease and P might become the most important limiting nutrient. Still, also then, focusing on N reduction would have more far-reaching effects than focusing on P.

Over the past 50 years, the system has indeed become more P limited (mainly close to the coast) because the excessive input of N has altered N:P ratios dramatically (Dale et al. 2000). Still, N and P are both responsible for increased production and hypoxia. They should both be reduced in order to truly reduce hypoxia, with P reductions comparable in percentage terms to N reductions (Dale et al. 2000, Turner and Rabalais 2013, Adhikari et al. 2015, Scavia et al. 2017, Fennel and Laurent 2018).

History of hypoxia in the northern GoM

The nGoM's sediment record shows a strong increase in hypoxia since the 1950s. In the 1970s, problems arising from hypoxia were first noticed, and from 1985 onward, with the monitoring of the midsummer hypoxic extend, the low-oxygen zone has doubled in size after 1995 compared to the period 1985-1995 (Rabalais et al. 2002) and has grown even more after 2002: the maximum extend until now was reached in 2017, when the hypoxic zone was larger than the state of New Jersey (Van Meter et al. 2018). This clearly rising trend is only punctuated by drought-related minima (such as in 1998), flood-related maxima (1993) and minima caused by the disruption of stratification by storms (2003, 2005) (Rabalais et al. 2002).

Coinciding with this trend, from 1960 to 2000 commercial use of fertilizer -rich in nitrate- saw a more than six-fold increase in the Mississippi catchment area. Meanwhile, the extend of croplands in the same area increased by 20 percent (Van Meter et al. 2018). So, hypoxia in the nGoM seems strongly related to human activity in the watershed, particularly to nitrate-producing activities such as fertilizer use and municipal wastewater discharge.

There are other factors contributing to hypoxia development in the nGoM, most notably strong stratification preventing ventilation of the lower water regions. For example, hypoxic conditions in autumn are only lifted because passing stormfronts disrupt salinity-induced. However, since these are natural features of the system, recent concerns are focused on preventable, human-induced increases in the river's nutrient (particularly nitrate) load (Van Meter et al. 2018).

Dinoflagellates and their cysts

Dinoflagellates are planktonic protists, living mostly in marine settings (although they are also common in fresh water). Generally, they are roughly cone-shaped, with a pointy "head" (or apex) and two pointy "legs" (or antapex). They possess two flagella, thread-like appendages protruding from the middle of their bodies, which are used for locomotion. Today, over 2000 species have been described (Góme, 2012). Approximately half of the species in this large group are heterotrophic, while the other half consists of autotrophic and mixotrophic species (Dale 2009). Around 10 percent of marine dinoflagellate species produce cysts, mostly organic-walled cysts made of carbohydrate polymers (Versteegh et al. 2012, Bravo and Figueroa 2014). Cysts are produced as part of the dinoflagellate's normal life cycle (related to sexual reproduction) or when under unfavorable environmental pressures to protect itself (Itakura et al. 1997). In a cyst, a dinoflagellate can remain dormant in the sediment for

decades or even centuries (Lundholm et al. 2011; Ribeiro et al. 2011), exiting their cysts again when conditions are more suitable. The dinoflagellates then migrate upwards toward the top of the water column to reproduce, where they may contribute significantly to the start of algal blooms (e. g. Anderson 1998; Garcés et al. 2002; Hense 2010).

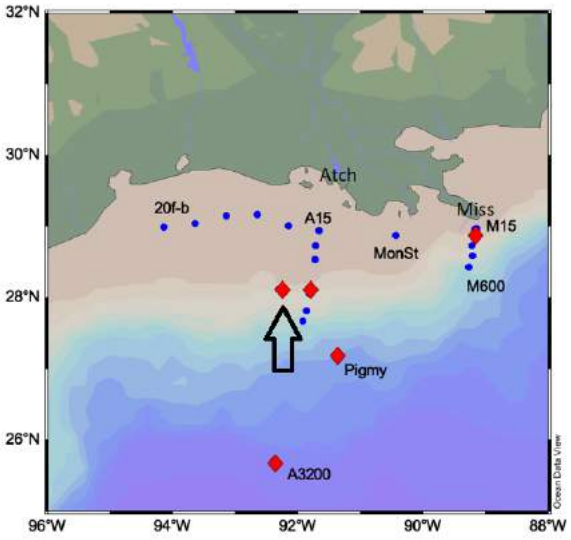

Fig. 1 All coring locations of expedition 64PE467 in the northern Gulf of Mexico. Blue dots indicate the locations were a box core was taken, red diamonds indicate piston cores. The black arrow indicates the location of core 80b. Taken from *64PE467 Cruise Report*, see Appendix 1.

Organic-walled dinoflagellate cysts assemblages are known to reflect environmental factors such as sea surface temperature, sea surface salinity, nutrient availability and productivity (e. g. Dale 1996; Matsuoka 1999; de Vernal et al. 2001; Radi et al. 2007; Price et al. 2013) and are often used to track eutrophication) (e.g., Dale and Fjellså 1994; Matsuoka 1999; Pospelova et al. 2002; Dale 2009; Price et al. 2017b). They are very fit to use as (paleo)environmental indicators, because they tend to be well preserved in the sediment and are not subject to dissolution. There may be an exception to this in the case of several species of dinoflagellates, mostly heterotrophs, and this may influence the dinocyst record (Dale 2001, Reichart and Brinkhuis 2003, Zonneveld et al. 2007, Versteegh et al. 2010).

Some autotrophic dinoflagellates can release toxins in harmful blooms, such as *Pyrodinium bahamense*, *Lingulodinium polyedrum*, and *Gymnodinium breve*. Especially this last species has great impact on marine wildlife, human health, fisheries and tourism (e.g. Davis 1948; Van Dolah 2000; Steidinger 2009)

The aim and scope of this study

Although the signs of hypoxia have been noted from the 70s onwards, it is possible that hypoxic conditions were already present before the 70s. In order to trace the onset of hypoxia and its relationship with nutrient input (particularly nitrate) into the nGoM, it is useful to extend our range of vision beyond the era of direct hypoxia measurements (the 70s onward) and use sediment cores and proxy records to investigate when, how and under which conditions hypoxia developed.

Therefore, the aim of this study is **to reconstruct the history of nutrient loading and hypoxia over the last ~100 years in the northern Gulf of Mexico**, focusing on one specific location. This location is fit for this aim as it is particularly affected by hypoxia in recent times (See the cruise report of the coring expedition in Appendix 1). It is downstream of the two most important river outlets in the area (the Mississippi and Atchafalaya rivers) while also being relatively far off to the open sea, on the edge of the continental shelf. So, it is most probably affected by both terrestrial (river-induced) influence and marine influence, both of which have an impact on the development of hypoxia. On this location, a 47 cm core has been taken during the 64PE467 expedition of 2020. This is core 80b, and its location is indicated by a black arrow in Figure 1. The report of the coring of 80b (and other cores of this expedition) can be found in Appendix 1. Core 80b contains sediment from roughly the first two decades of the 20th century up until 2019.

The main method in determining the past extend and intensity of these environmental factors is the assessment of dinocyst assemblages in samples taken at regular intervals in the core. This is relatively novel for this area, as only few studies have examined dinocyst assemblages from

nGoM surface sediments (Limoges et al. 2013; Edwards and Willard 2001) or late Quaternary sediment cores (e.g., Wrenn 1988; van Soelen et al. 2010; Limoges et al. 2014, 2015), and none (known) studies have focused on dinocysts in northern GoM shelf sediments that are directly influenced by the discharge of the Mississippi River (Price et al. 2018).

In addition to dinocyst assemblages, I will use geochemical proxies ($\delta^{13}C$, $\delta^{15}N$, %N, %TOC, %TIC), colour data of the core (specifically a*, the red/green parameter) and pollen assemblages. The latter are used to construct a very rough vegetation reconstruction, to possibly couple vegetation changes on land to changes in the coastal system.

Regional setting

Geological formation and basin fill

The sedimentary basin which came to be known as the Gulf of Mexico first formed in a period of rifting during the Late Triassic to Middle Jurassic (Buffler and Sawyer 1985). However, the main part of the formation of the Gulf of Mexico can be attributed to a short extensional phase in the Middle to Late Jurassic (Stern and Dickinson, 2010).

The first sedimentary deposits in the basin were Middle-Jurassic evaporites, widely occurring over the while basin. In the Late Jurassic, another, but brief period of oceanic crust formation occurred in the deep central Gulf, followed by cooling and resulting subsidence of the crust (Buffler and Sawyer 1985). This enabled the deposition of very widespread carbonate platforms that surrounded the deep basin. The northern part of the Gulf of Mexico was such a carbonate platform: broad, shallow, and restricted to open marine. Apart from carbonates, the platform saw clastic sedimentation, as the northern margin propagated (Galloway 2008).

In the middle Cretaceous, a large unconformity, the Middle Cretaceous Unconformity, developed as a consequence of a large eustatic sea level drop of 60-100 m (Faust 1990). The Late Cretaceous is a complex period in the history of the Gulf of Mexico, especially its northern part. It saw igneous activity and many dome-shaped uplifts that overlapped each other, resulting in a large number of regional unconformities (Ewing 2009). Clastic and carbonate aggradation continued at the continental margins, however, and this intensified in the Paleogene. The north and northwest of the basin were gradually filled with clastics (Galloway 2008). The Paleogene was relatively quiet in tectonic terms, apart from post-Eocene uplift in the northern part due to sediment loading in the south- and southeastern basin (Ewing 2009). Clastic filling of the basin continued into the Miocene, now spreading to the central and northeastern Gulf, until today. It resulted in a continuous Cenozoic record of sediment supply for the past 65 million years (Galloway et al. 2011). Only the Florida margin seems to be an exception to this trend of propagation: it is primarily a carbonate platform (Galloway 2008).

Mississippi and Atchafalaya deltas

The northern GoM is fed (in terms of sediment, nutrients and terrestrial carbon) mainly by two rivers, the Mississippi and Atchafalaya rivers, of which the latter is a tributary of the former. They run over the same delta plain, which is a mud-dominated, birdfoot-like delta which slowly builds out into the sea (Hijma et al. 2017). The growth of the delta is hardly hindered by tidal processes, as the mean tidal range is only 0,3-0,4 m.

The large delta system consist of subdelta's, which grow and are abandoned over millennial timescales in response to the changing courses of the rivers. The stratigraphy of these subdelta's is well constrained, for example in Coleman et al., 1998, and Blum and Roberts, 2012. The five most recent subdelta's have formed in a period of continuous sea level rise, so that little erosion has taken place and the subdelta's are well preserved. Generally, they formed in relatively shallow water of less than 10 meter deep. An exception is the most modern subdelta, which has formed in over 50 meter water depth. Two of the lobes are active, which are the lobes occupied by the Mississippi and Atchafalaya rivers (Draut 2005). Since the 16th century, the Mississippi is in the process of shifting its main course to the Atchafalaya. Water discharge through the Mississippi would have decreased and the Atchafalaya's discharge increased, and lakes and marshes behind the coastline filled with Atchafalaya sediment. Today, these form the largest continuous marsh in the United States, and by running through it, the Atchafalaya river gains 10% more total carbon and 28% more total phosphorus, although the total amount of nitrogen does not seem affected (Turner et al. 2007).

When the marshes were filled, a delta lobe began to form, emerging above sea level in the 1970s. This process has been slowed down by the dam built by the US Army in 1963. This dam prevented the flow of the Mississippi to be further directed into the Atchafalaya, so that now only 30 percent of the Mississippi's discharge can pass through the Atchafalaya river. Furthermore, both rivers have today been completely embanked. This has consequences for the evolution of the delta. Embanking of the rivers prevents delta lobe switching, but also causes a large part of the delta to become sediment-starved. The result is erosion and subsidence, so that, over the past two decades, the delta loses 30-50 km2 every year to the sea (Couvillion et al. 2017).

Mississippi and Atchafalaya input into the northern GoM

The discharge of the two rivers accounts for 90% of the total freshwater input into the northern GoM (Limoges, 2013). The discharge varies on a decadal timescale due to droughts and floods (Turner et al. 2007). The dams have caused the flood peaks to be more frequent and more severe, however, no large-scale changes have occurred during the 20th and 21st century. According to Turner et al. 2007, the discharge "has remained within its historical upper and lower bounds."

With this discharge comes a yearly load of approximately 175 megatonne of for the two rivers combined. Before the damming of the Mississippi, this was much higher: 400-500 megatonne per year. Compared to the past 12 kyr average of 230-290 megatonne/year, the load before damming had been much higher than the average, but the load after damming has remained under that average (Hijma et al. 2017). This sediment load is brought to the continental shelf of the northern Gulf of Mexico, where both rivers terminate (Draut 2005). Of course, clastic sediment is not the only load the rivers bring to the Gulf: the two rivers combined deliver 91% of all yearly N and 88% of all yearly P to the northern Gulf of Mexico (Turner et al. 2007). This amounts to roughly 1,37 million tons per year for N and 170 000 tons per year for P, measured by the US Geological Survey over 2001-2005, which (although this is a 21% decline in N compared to 1980-1996), is still very high (Anderson, Howarth and Walker 2010, x1iv). It leads, combined with stratification, to strong seasonal hypoxia in the bottom waters, as described in the introduction.

Results and discussion

Dinocyst assemblage

The most common species of dinoflagellates are *Spiniferites spp* (specifically *Spiniferites ramosus/bulloides, hyperacanthus,* and *mirabilis), Operculodinium centrocarpum, Pentapharsodinium dalei, Polyspaeridium zoharyi* and *Lingulodinium machaerophorum.* Other species often found, but not dominant, are *Nematospaeropsis labyrinthus,* several species of *Impagidinium,* other species of *Spiniferites (delicanthus, belerius, bentorii, pachydermus), Operculodinium israelianum, Melitaspaeridium choanophorum* and *Tuberculodinium vancampoae.* The dinocyst assemblage is dominated by autotrophs, forming 80-93% of the assemblage.

The heterotrophic component consists of *Selenopemphix quanta/Protoperidinium nudum* (counted together), *Selenopemphix undulata* and *nephroides, Brigantedinium spp, Echinidinium spp, Lejeunecysta paranella* and *sabrina*, and to a lesser extend *Polykrikos schwarzii* and kofodii, Echinidinium aculeatum, Quinquecuspis concreta and *Trinovantedinium applanatum*.

Of all counts, a substantial part (12-20%) consists of lagoonal species, namely Operculodinium israelianum, Polyspaeridium zoharyi and Tuberculodinium vancampoae. Since core 80b was taken at a rather open marine site, this shows that the system displays some characteristics of a lagoonal setting, without being truly lagoonal. The typical "lagoonal" factor might be a high amount of nutrients.

We can compare my counts for core 80b with the count for 80b as performed by PhD-student Yord IJdema (Utrecht University), who counted surface samples of all coring locations of expedition 64PE467 (Figure 1). This allows me to check the robustness of my findings. As counts and absolute abundances cannot be compared, I compare relative abundances. The results are mostly similar, with a few differences:

- The percentage of autotrophs in my samples is somewhat higher than in IJdema's count (80-93 versus 69), but it is not a large difference.
- My counts reveals a higher abundance of *O. centrocarpum* than in IJdema's counts, while the abundance of *P. dalei* is lower. I might have underestimated the amount of *O. centrocarpum* by identifying some *P. dalei* as *O. centrocarpum*. For the remainder of this study, this is of minor importance, as none of these species are used as indicative species, and are grouped together as "autotrophs".
- IJdema's *Lingulodinium* percentage is somewhat lower than mine. IJdema's percentage resemble those of the samples close to the shore (and quite far away from 80b), while my percentages more resemble surface samples A100, A30 and A50, all located very close to 80b. Therefore, I will consider my *Lingulodinium* counts to be roughly correct.

Autrotrophic vs heterotrophic dinocysts

The %heterotroph proxy might be used to assess eutrophication. However, doubts can be cast on the reliability of the %heterotroph proxy, since heterotrophic dinocysts seem to be selectively vulnerable to oxic degradation compared to autotrophs. Reichart and Brinkhuis (2003) have assesses the reliability of the heterotrophic dinocyst *Protoperidinium* as a proxy for productivity. They found that the cysts of *Protoperidinium* indeed degrade more strongly in the presence of bottom water oxygen than autotrophic cysts, but that "downcore patterns in *Protoperidinium* cyst concentration still primarily reflect changes in sea surface productivity." This means that we may use the overall, absolute trend in *Protoperidinium* cysts as a reflection of productivity, but we should be very wary of using the relative abundance of *Protoperidinium*.

Similarly, Versteegh, Zonneveld and De Lange (2010) found a strong and highly selective aerobic degradation of heterotrophic dinocysts. Zonneveld, Bockelmann and Holzwarth (2017) even try to establish a useful tool for quantifiying bottom water oxygenation using this fact. The abundance of dinocysts sensitive to degradation ("S-cysts") may be compared to that of resistant dinocysts ("R-cysts"), where the sensitive cysts's accumulation rate is correlated with bottom water oxygenation. Of the species I encountered in core 80b, five are cited by Zonneveld, Bockelmann and Holzwarth as resistant cysts: *Nematospaeropsis, Operculodinium israelianum, Pentapharsodinium dalei*, all *Impagindinium* species, and *Polyspaeridium zoharyi*. Sensitive cysts in my assemblage are *Brigantedinium, Protoperidinium nudum* and *stellatum, Echinidinium Lejeunecysta, Quinquecuspis, Selenopemphix, Trinovantedinium* and *Votadinium*, in short, all heterotrophic species. Zonneveld, Bockelmann and Holzwarth advise to only use R-cysts as proxy's for productivity.

For my study, this means that I must regard the relative abundances of these S-cysts, including the relative proxy %heterotrophs, as unreliable proxy's for productivity. I may use their absolute abundances, since they, according to Reichart and Brinkhuis (2003) still reflect productivity, but it is unwise to draw conclusions from comparisons with the resistant cysts's abundances.

Eutrophication indicator species

In the northern Gulf of Mexico, a few species are commonly recognized as indicators for eutrophication:

- The autotrophic *Lingulodinium machaerophorum*. A signal of increasing *L. machaerophorum* (often together with overall rising dinocyst concentrations) is referred to as the "Oslofjord Signal" (Dale and Fjellså 1994; Dale et al. 1999; Dale 2009).
- A group of heterotrophic species. This is referred to as the "heterotroph signal". The species are (e.g. Pospelova et al. 2002; Matsuoka et al. 2003; Krepakevich and Pospelova 2010; Pospelova and Kim 2010; Shin et al. 2010, Price et al. 2018)
  -Selenopemphix quanta
  -Polykrikos kofoidii and schwartzi
  -Protoperidinium Americanum
  -Dubridinium spp.
  -Brigantedinium spp.
  Price et al. (2018) recognized two more:
  -Archaeperidinium minutum
  -Quinquecuspis concreta

Since *Protoperidinium americanum, Dubridinium spp, Archaeperidinium minutum* and *Quinquecuspis concreta* were not or hardly recognized in the samples of 80b, I will turn to the other species:

Lingulodinium machaerophorum

- Background value ~50-80 dinocysts per gram sediment
- Displays two main peaks: ~1970-1974 (150) and 1990 (162)
- Trend: high in 70s (around 12%), falls during 80s (lowest point 5,38% in 1986), peak at beginning of 90s, then relatively constant until 2018, sharp rise from there.

Brigantedinium spp.

- Background value up to the 80s ~10-14, background in 90s and up ~20-26.
- Peaks at 1974 (44,4), 1986 (40), 2017 (41,7) and very slightly at 2007 (28,5)
- Overall, Brigantedinium displays a slow rising trend.
- A very brief fall in 2018 (16,8).

Although both the counts (2-8 counts per sample) and relative abundances of *Brigantedinium spp.* are low, *Brigantedinium* was consistently found in the samples, and the risk of missing or incorrect identification of *Brigantedinium spp*. is small. Therefore, it is still useful to consider this species as an indicator for eutrophication, but since a count difference of only one count may result in pronounced differences in relative abundances, only the general trends should be analyzed.

Selenopemphix quanta

S. quanta was counted together with *Properidinium nudum*. While *Selenopemphix quanta* may be regarded as an indicator species for eutrophication, *Propoperidinium nudum* is not. Also, in four samples, none of these species were found. *Selenopemphix quanta*, therefore, does not seem useful in determining eutrophication trends.

Polykrikos schwarzii/kofoidii.

For *Polykrikos,* even fewer counts could be made. Counts did not exceed a maximum of 4, and often (in 9 of the 22 samples counted for dinocysts) there were no counts. *Polykrikos* is therefore also not useful in determining eutrophication trends and will be omitted.

Pollen assemblage

In most samples, arboreal pollen (AP) dominate the pollen assemblage, with percentages of ~36-56%. Most of the arboreal pollen stem from *Quercus*. Other major contributors to the AP fraction (although still far behind Quercus) are *Alnus, Betula, Carpinus, Carya, Castanea, Corylus, Fraxinus, Ilex, Salix, Tilia* and *Ulmus*. Non-arboreal pollen (NAP), not including grasses and ferns, follow the AP fraction closely, with percentages of ~21-44%. It exceeds the AP fraction in samples 32-33, 29-30 and 26-27 cm (1962-1974). The dominant contributors to this fraction are from the *Asteraceae tubuliflorae* and *Chenopodiaceae* groups. Other major contributors *are Artemisia, Brassicaceae, Acacia, Caryophillaceae, Filipendula, Nyssa* and *Rumex*. Grasses, consisting of *Cyperaceae* and *Poaceae*, make up ~2-20% of all pollen. Ferns vary between 6-25%.

Not included in the total pollen fraction are wind-pollinated plants: Bisacchates and other conifers (mostly Taxodium and Juniperus). As these species produce many more pollen compared to species that pollinate by other means, the ratio between species abundances for wind-pollinated species and other species will become skewed. There will appear to be a much higher fraction of wind-pollinated species than there is in reality.

Comparing the percentages of pollen groups and some individual pollen to the surface count of 80b and the other surface samples, we see:

- %AP and %NAP are similar in my counts and Yord IJdema's surface count. %grasses is lower in my counts than in Yord's count (3-9 versus 14,87), while %ferns is higher (10-18 versus 3,35).
- In samples closest to the shore, %AP and %NAP are lower than in deep samples, while %grasses and %ferns are higher. The percentages of the slope samples, consisting of A300, A100 and 80b, are in between these two endmembers.

The Mississippi river transports pollen from its catchment area to the northern Gulf of Mexico. Since this catchment area extends for over 3 million km^2, it is not possible for most pollen to determine where they originate from, and it is therefore also not possible to give precise vegetation reconstructions. Our pollen record may only show the largest changes that affect (most of) the catchment area. Pollen are only a fraction of all plant-derived organic material entering the northern Gulf of Mexico,

but they can indicate what the plant material consists of: grass-derived organic material, tree-derived, et cetera. The type of plant material may influence the isotopes of the incoming carbon: trees (the AP pollen group) are C3-plants, which bear a more depleted isotopic fingerprint than do C4-plants, which belong almost exclusively to the grasses pollen group. A change in the isotopic fingerprint of the incoming carbon may influence our measured $\delta^{13}C$ (see Environmental Reconstruction).

When we assess the pollen record for trends and compare different pollen groups to one another, the most important observations are:

- %grasses and %ferns seem to display a negative relationship: mostly, when one rises, the other falls.
- We see a high fern/low grasses regime before the 50s. In the middle of the 50s, ferns start to fall, and grasses start to rise. At the beginning of the 60s, %ferns is at an all-time low, and %grasses at an all-time high. After this point, however, %grasses decreases again, up towards the present, while %ferns increases.
- %AP and %NAP are more steady.
- A minor trend can be observed from the middle of the 80s onwards, where %AP slowly starts to rise (particularly after 2007), with short fallbacks in 2007 and 2017. %NAP seems to be decreasing. However, the difference in %AP and %NAP between the middle of the 80s and the core top is 10-15% maximum, which, compared to the overall dominance of %AP (~50%) and %NAP (~35%), is small.

A possible interpretation of %grasses/%ferns -and refutation

From the surface samples, we know that samples close to the shore (both the 20-series close to the Atchafalaya mouth as the M-series close to the Mississippi mouth, see their locations in Figure 1) have a high grasses/low ferns fingerprint, while samples taken from deep sediment have a low grasses/high ferns fingerprint. Therefore, we may interpret the %grasses/%ferns ratio as a measure of terrestrial influence. If the ratio is high, the sample resembles samples closer to shore, on the continental shelf. When it is low, the sample resembles deeper sediment off the slope.

If we interpret the %grasses/%ferns ratio this way, it suggests that the sediments at the location of 80b became more shore-like during the 50s. During the 70s, sediments quickly became more deeper marine again. From the 70s/80s boundary onwards, sediments shifted further towards the marine endmember, only at a slower rate than in the 70s, all the way towards the present.

However, this is completely contrary to the other proxies (d13C, %N, C/N, TOC, a*, dinoflagellate assemblages) that all suggest rising nitrogen load, rising productivity and eutrophication, and overall rising terrestrial influence. Since these proxies are better established and all point towards the opposite result, I will not use the %grasses/%ferns ratio as a proxy.

Bisacchates

Bisacchate pollen are windborne, which makes locating their site of origin even more problematic; they could also originate from outside the Mississippi catchment area. Since the concentration of bisacchates is most likely more a reflection of wind patterns than of vegetation changes, it is not considered useful in reconstructing vegetation. The bisacchates' very different mode of production (bisacchates are significantly overproduced compared to other pollen) and transportation also renders comparison to other pollen groups unhelpful.

%N

%N reflects the amount of nutrients in the system. Most importantly, %N rises continuously throughout the core. It only stagnates (at a high level) between ~1995-2007. In the last ~10 years, %N rises again, in two steps (2018 disrupts the rise shortly). This same two-step rise can be seen in $\delta^{13}C$, TOC, and several of the palynological proxies. This rising trend is most likely caused by rising nutrient input via the rivers; we know this is happening from previous research (see Introduction). This may have to do with the difference in what is being measured: the nitrate concentration does not tell us about the actual amount of nutrient input, as that is also dependent on discharge. Also, the Mississippi river, not taken into account, might contribute significantly to the total nutrient input.

TOC

TOC (or % organic carbon) is the percentage of organic material making up the bulk sediment. It varies between 0,82 and 1,43% (core top). This is a normal value range for this area, quite average when compared to TOC in surface samples. Only those samples taken close to the shore and away from the Mississippi mouth (the 20-series and A15) have TOC values a factor 10 smaller. In 80b, TOC rises continuously throughout the core, like %N, also showing the same ups and downs as %N.

The TOC curve could reflect a production, preservation or dilution signal, or a combination of these. When the amount of nutrients rises (%N) it would spark production of organic matter, but this, in turn, might cause hypoxic conditions at the bottom of the water column, enhancing preservation of organic matter. The fact that the graphs of TOC and %N look very similar supports the hypothesis that TOC reflects a production or preservation signal, or a combination of both. Dilution is governed by a third factor, namely clastic input, which might vary independently from nutrient input, decreasing over the core while nutrient input increases. However, it is harder to explain the correspondence of TOC and %N if TOC were to be mainly a dilution signal.

From this information alone, we cannot determine if TOC is a production, preservation or dilution signal. We find further evidence by Principal Component Analysis (see Statistics).

C/N ratio

While both %N and TOC rise, %N rises faster. Their ratio, the C/N ratio, therefore shows a general falling trend throughout the core. C/N falls from 9,4% at the bottom of the core to 7,6% at the top. These values are characteristic of a marine provenance (0-10%, often around 7-8%). As we can see while analyzing TOC and %N separately, the falling trend of C/N is very likely a trend in increasing nutrients, *not* a trend in (relatively) decreasing input of terrestrial organic matter, which has a higher C/N value (>20%) than does marine-produced organic matter. Further evidence is provided by Principal Component Analysis (see Statistics).

δ13C

In $\delta^{13}C$, important observations are:

- The background value, from the bottom of the core to the 50s, is around -22,15.
- A slow rise towards more enriched values initiates in the 60s and continues during the 70s, up to around -21,9.
- This culminates in a last, sharp rise in ~1980. Values are now around half a promille more enriched than background value.
- Values fall back to the more depleted background value in roughly 2000-2010.

Although the isotopic changes in $\delta^{13}C$ are small, we must remember that this was measured on *bulk* $\delta^{13}C$, so that changes of even half a promille points towards serious environmental changes. We find no such dramatic overturn in the dinoflagellate species assemblage (although, of course, other kinds of changes can be observed).

A common way to interpret $\delta^{13}C$ is to attribute depleted values to the fraction of sedimentary organic matter originated from land (the $\delta^{13}C$ fingerprint of C3 land plant material is around -28) and enriched values to the fraction of sedimentary organic matter from local marine production (d13C fingerprint ~-22). This also seems to be the best interpretation for 80b's $\delta^{13}C$ record, for several reasons:

- There is a possibility that the clear-cut relationships between depleted and enriched, terrestrial and marine values is contaminated by the influence of C4 plants, which have a $\delta^{13}C$ fingerprint of ~-15. One such C4 plant is corn, a crop intensively cultivated in the southern Mississippi basin. But if corn was so prevalent, surely some corn pollen (which are very large and clearly recognizable) would have made it into the microscope slides for palynology analysis. None were found. Instead, the pollen assemblage found in the samples consist almost exclusively of C3 plants.

- Yord IJdema found a clear $\delta^{13}C$ transect in surface sediment samples from the area, where coastal samples were more depleted in $\delta^{13}C$ and marine samples more enriched (personal communication, 2021).

- Student Rebecca Puyk (Utrecht University), studying core M100 taken by the same cruise as 80b (closer to the shore), found pulses of depleted $\delta^{13}C$ corresponding to known pulses of terrestrial organic matter input, caused by river floods, especially the 1993 flood (personal communication, 2021).

It is therefore safe to say that depleted values of $\delta^{13}C$ in 80b indicate terrestrial influence on the carbon isotopes found in bulk sediments. This means that enriched (heavier/less negative) values point towards a larger contribution of local marine producers. Clearly, marine (algae) production rose (relative to land carbon input) starting in the 70s, or possibly already in the late 60s.

The major flood of 1993, causing the $\delta^{13}C$ peak in M100, might have started or helped the shift towards more depleted values. The 1993 "pulse" of M100 might here, in a more marine setting, have been smeared out over a longer time span. Even in M100, the "pulse" is smeared out over five years. We might also take into account the standard deviation of around 4 years for the ages around 1993. The ages attributed to the start of the fall in 80b's $\delta^{13}C$ might be offset by several years from its possible true age of 1993.

The last %~10 years $\delta^{13}C$ sees a rise to more enriched values again. This is a two-step rise, with a short fallback in 2018. This same pattern is seen in %C and %N. As is to be expected, primary production follows the amount of nutrients closely.

$\delta^{15}N$

The $\delta^{15}N$ record might be interpreted in two possible ways:

1. Ideally, $\delta^{15}N$ might primarily reflect N acquisition pathways used:
   - $\delta^{15}N$ 0 to -2 ‰ = little fractionation, meaning that N is primarily acquired through N^2 fixation, which entails almost no fractionation.

- $\delta^{15}N$ <-2‰ = more fractionation. N acquisition through NO3 fixation is dominant, using remineralized nutrients and nutrients brought into the system by rivers.
- $\delta^{15}N$ > 0‰ = strong fractionation. Depleted N2 has been released by denitrification, so that the NO3- that is left behind (and measured in bulk d15N) is enriched. This is an indicator of anaerobic respiration, and therefore, of hypoxia.

This way, $\delta^{15}N$ can give us the most direct account of bottom water hypoxia in core 80b compared to all other proxies.

We might use this interpretation if:

- The range of isotopes found in terrestrial N is similar to the range of isotopes in marine sedimentary N, so that isotopic changes in N are most likely not due to changing input of terrestrial N. And/or:
- The trend in $\delta^{15}N$ has similarities with trends productivity indicators (%TOC, %TIC, $\delta^{13}C$), as more productivity leads to more intense hypoxia, but differs significantly due to other factors that influence hypoxia; it is unlikely the relationship between productivity and hypoxia is (close to) 1:1. And/or:
- In periods with increased storm intensity, $\delta^{15}N$ is mostly in the "normal" range of 0-2 as increased ventilation breaks down hypoxia. In periods with reduced storm intensity, $\delta^{15}N$ shows more positive values.

2. $\delta^{15}N$ might primarily reflect N input from land. This is most likely the case if:
    - Terrestrial N has a different isotopic fingerprint from marine sedimentary N. And/or:
    - The trend in $\delta^{15}N$ is similar to trends in %N, land input proxy's (a*, dinos/pollen) and productivity proxy's (%TOC, %TIC, $\delta^{13}C$). And/or:
    - In periods with increased storm intensity, $\delta^{15}N$ shows more positive values, as storms cause floods on land which bring in extra terrestrial N. In periods with reduced storm intensity, $\delta^{15}N$ remains in the "normal" range of 0-2‰.

These three factors (isotopic signatures, similarity in trends, the effect of storms) determine the usefulness of $\delta^{15}N$ as a proxy for hypoxia. Below, I will analyze these three factors.

Isotopic fingerprints of terrestrial and marine sedimentary N

Two studies gave indications for the isotopic N fingerprints of the Mississippi river (isotopic N fingerprints for the Atchafalaya river could not be found):
-Chang et al. (2002), soil-derived Mississippi N isotopes, based on four samples from 1998. Isotopic range 2-12‰
-Panno et al. (2006), Mississippi N isotopes measured on nitrate. Isotopic range 4,8-16,4‰.

Sigman and Karsh (2009) gave values for N signatures in the open ocean, and N signatures caused by ocean denitrification:
-Ocean particulate N (fixed by N2 fixation), isotopic signature ~0‰.
-Dissolved organic nitrogen, isotopic signature ~4‰.
-Denitrification in the water column: 5-30‰.
-Denitrification in the sediment: less than 3‰.

I assume that, if denitrification happens in the northern GoM, it takes place primarily in the sediment. This suggests that incoming terrestrial N will have higher isotopic values than marine sedimentary N

(both with and without sedimentary denitrification). This is also suggested by Childs et al. (2002). They found the highest isotopic N values close to shore, decreasing further out to sea.

Furthermore, Childs (2002) mentions that the denitrification potential in hypoxic zones is lower than expected. Although the current paradigm holds that the hypoxic zone should be an ideal location for denitrification, with its high carbon and nitrate content and low oxygen, denitrification in the GoM's hypoxic zone will probably be limited. Therefore, there is only a small chance that bulk sedimentary $\delta^{15}N$ would be influenced by denitrification, and a larger chance that $\delta^{15}N$ values are influenced by incoming terrestrial N.

So, it is not very likely that $\delta^{15}N$ will reflect hypoxia.

Trends in δ15N and proxies for N availability, land input and productivity

To determine if $\delta^{15}N$ is correlated to land input and productivity proxies, we might perform PCA's and calculate correlation coefficients (Kendalls tau). However, these statistical methods yielded conflicting results. For example, in the PCA's, $\delta^{15}N$ seems to be closely related to a*, but no such correlation can be found in the correlation coefficients. Also, while one PCA implied a positive relationship between $\delta^{15}N$ and $\delta^{13}C$ (on PC1), another, with just one variable less, did not imply such a relationship. Because of these conflicting results, I disregard statistical methods and only compare $\delta^{15}N$ with %N, %TOC, %TIC, $\delta^{13}C$ and a* visually; see Figures 4.3 and 10. Before 1980, $\delta^{15}N$ does not reflect the nutrient- and productivity proxies. The former remains rather stable, while the latter are rising.

Starting around 1980, $\delta^{15}N$ enters a new regime. Now, $\delta^{15}N$ is positive regularly. Also at 1980, in $\delta^{13}C$, a sharp rise occurs, and $\delta^{13}C$ enters a new, high-productivity regime in the 80s and 90s.

In 1995, $\delta^{15}N$ experiences a one-off fallback to <-2. This coincides with the start of the stagnation in TOC, TIC and %N (although they settle at high values). So, in this time period, $\delta^{15}N$ does seem to match the productivity- and nutrient availability proxies.

In the period 2000-recent, $\delta^{15}N$ is almost continuously positive. It only falls back to negative values (but never >-2) around 2010-2014 and 2018-2019. %TOC and %N also show fallbacks in ~2010-2014 and ~2018, just like $\delta^{15}N$. So, in this final period, $\delta^{15}N$ seems to match %N, %TOC and $\delta^{13}C$ quite closely.

The match between $\delta^{15}N$ and a* is less clear. The start of the rise in a*, in ~1993, does not match the transition points of $\delta^{15}N$ (1980 and 2000). They do, however, both show a general rising trend over the last ~30 years. Furthermore, in 2010-2014, when $\delta^{15}N$ returns to negative values, the rise in a* stagnates.

All in all, there seems to be a relatively good match between $\delta^{15}N$, $\delta^{13}C$ %TOC and %N. This suggests that $\delta^{15}N$ in this record reflects the isotopic fingerprint of marine versus terrestrial N, more than it reflects N acquisition pathways.

The effect of storms on $\delta^{15}N$

I used the HURDAT best track database of storm tracks over the last century, provided by NOAA on https://www.nhc.noaa.gov/data/#annual. For every year, I assessed how many tropical storms, hurricanes and major hurricanes had passed in the vicinity of 80b's location. Tropical storms and hurricanes were only assigned a "1" when they passed very close to 80b's location. Major hurricanes were given a 1 when they did not pass 80b's location, but somewhat further away (eastwards until the

mouth of the Mississippi, and the same stretch of kilometers westwards and south), and a special notation when they did pass 80b's location.

Time periods with high frequency of storms:
1978-1989
2002-2008
2017

Calmer periods:
Most of the 50s, 60s and 70s
1990-2002
2009-2016

Apart from 2017, all time periods with high frequency of storms coincided with a positive to almost fully positive regime of $\delta^{15}N$. All calmer periods coincided with periods in which $\delta^{15}N$ was mostly negative, or fell back to negative.

If positive values of $\delta^{15}N$ correspond to periods of hypoxia, then we would expect these values to occur in *calmer* periods, as storms tend to disrupt hypoxia. But instead, we see positive values in periods with high storm activity. This may be because storms, reaching land, also induce more terrestrial input and therefore more terrestrial N, enriching $\delta^{15}N$. So, also here it seems that $\delta^{15}N$ mostly reflects land input, not N acquisition pathway.

Final verdict

From the above, it becomes clear that $\delta^{15}N$ is more likely to reflect terrestrial N input than fractionation/hypoxia. I will not draw further conclusions from the $\delta^{15}N$ proxy, as I cannot completely rule out the possibility that fractionation and hypoxia have influenced the proxy. But what this study *does* indicate, is the possible usefulness of $\delta^{15}N$ as a proxy for terrestrial N input in comparable systems. Further studies may define and constrain the different effects on $\delta^{15}N$ and assess this usefulness.

Colour parameters

The three parameters l*, a* and b* are the means to quantitatively measure colour in sediments. L* reflects the lightness of the sediment (l*=0 is black). The value for a* determines the sediment colour's position on the red-green axis. The higher a* is (more positive), the more red the sediment is. Similarly, b* determines the position on the yellow-blue axis.

a* can be used as a proxy for changes in lithology related to iron intensity (Zeebe and Lourens 2019, Debret et al. 2011). Zeebe and Lourens (2019) found that their a* and iron intensity yielded nearly identical results. As the source of red-colored iron is terrestrial sediment, a* may be used as a proxy for terrestrial clastic input into the system, either by wind or rivers.

Furthermore, l* is usually highly correlated with carbonate content. B*, however, cannot be interpreted in such a straightforward way. Therefore, l* and b* do not yield much information. The information given by l* can be more readily assessed by the TIC measurements, and interpreting b* might take up many more hours without prospect of a clear result. Since a* might be useful as a measure of terrestrial clastic influx in the system, I will only use a* in this study.

a* displays high-frequency fluctuations probably due to standard measuring errors (Figure 3.4). This can be seen on a zoom-in on one of the graphs, were we see the sharp negative excursions are consistently 0,0979 cm apart from each other. The graphs in Figure 3.4 are based on 7054 datapoints. In contrast, in order to statistically compare a* to the results of this study, I took the 47 datapoints

corresponding to the middles of my samples (and even less for comparison with palynological proxy's). As evidenced by the resulting graphs for these 47 datapoints (see a* in Figure 5), the original trends remain preserved. However, there seem to appear some excursions not present in the original dataset, because some of the selected 47 datapoints might be located near the maxima or minima of the high-frequency fluctuations present in the original dataset. Therefore, in visually analyzing the trends, maxima and minima a*, I use the graphs of the original dataset, aided by a trendline. I only use the reduced dataset of 47 datapoints for statistical comparison with the other proxy's. The extreme, almost vertical spikes at the very end of the core are probably due to the measuring device meeting the edge of the core container, and should be ignored.

The most important observations on a* are twofold:

- a* is very constant, until around 1993 (15-16 cm), when it starts to rise (=more red relative to green) and keeps on this rising trend towards the upper end of the core.
- a* rises in three steps: from ~1993-1997 (13,5-16 cm), 2004-2010 (7-10 cm) and 2015 to the top of the core, 2019 (0-4 cm). In between these rising phases, there are two plateaus.

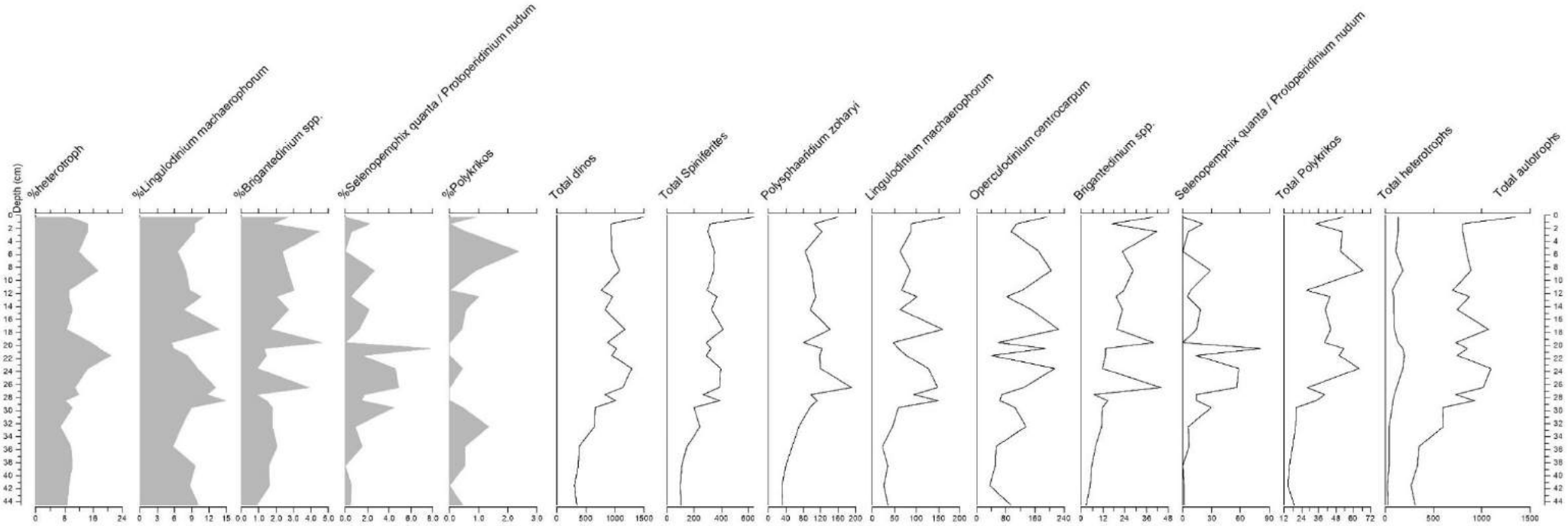

Fig. 3.1 Dinocyst proxies against Depth (cm). All species of relative importance are included.

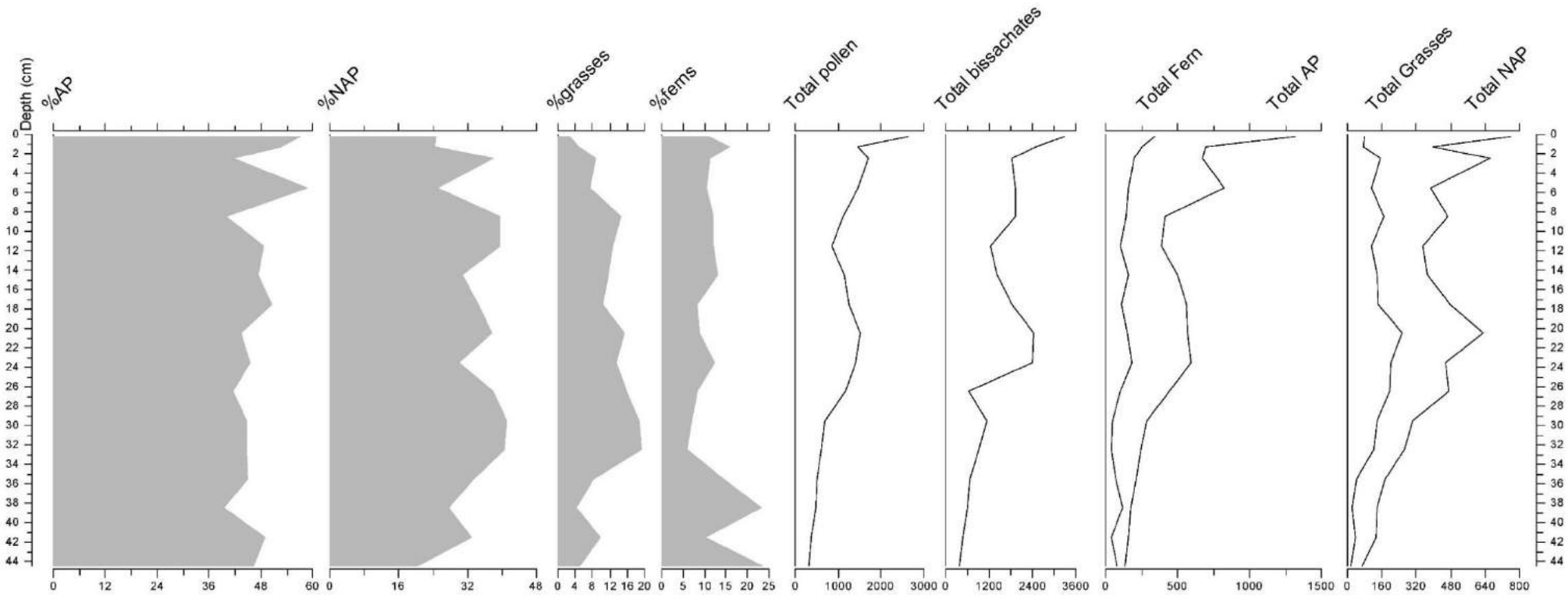

Fig. 3.2 Pollen proxies against Depth (cm).

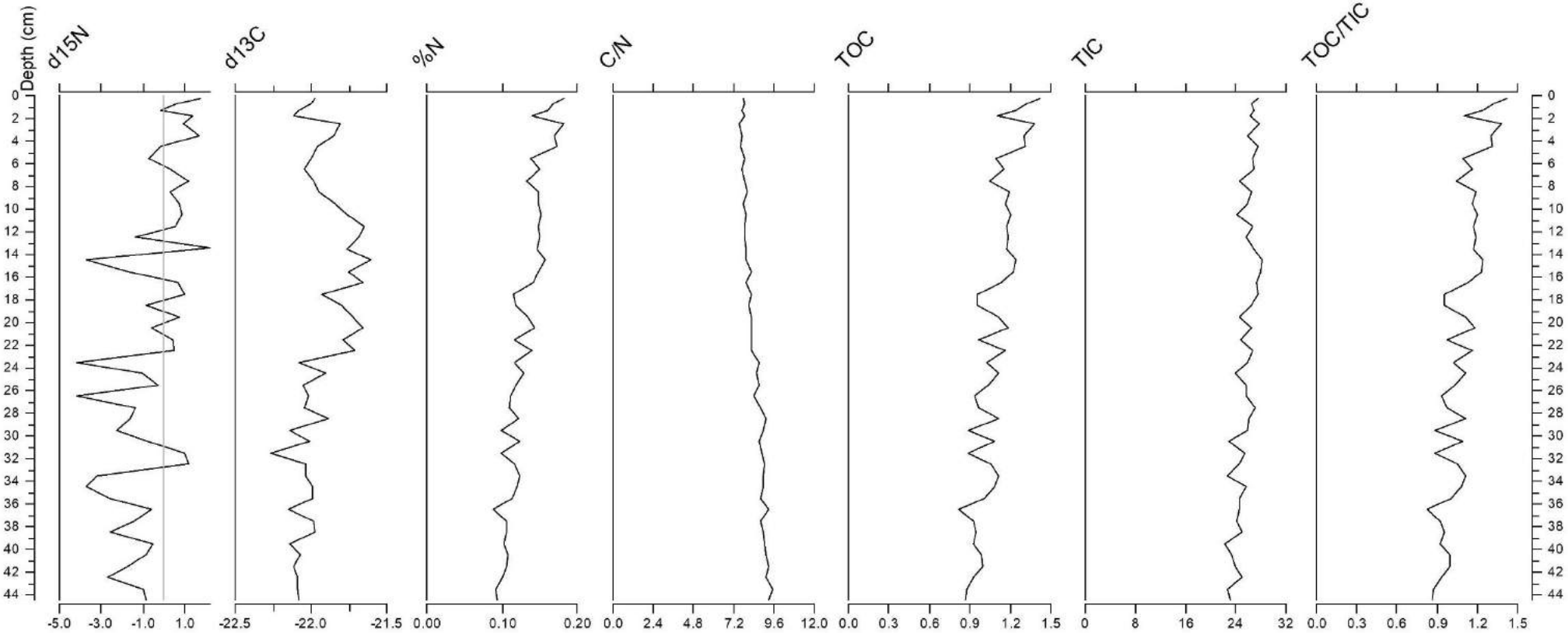

Fig. 3.3 Chemical proxies against Depth (cm).

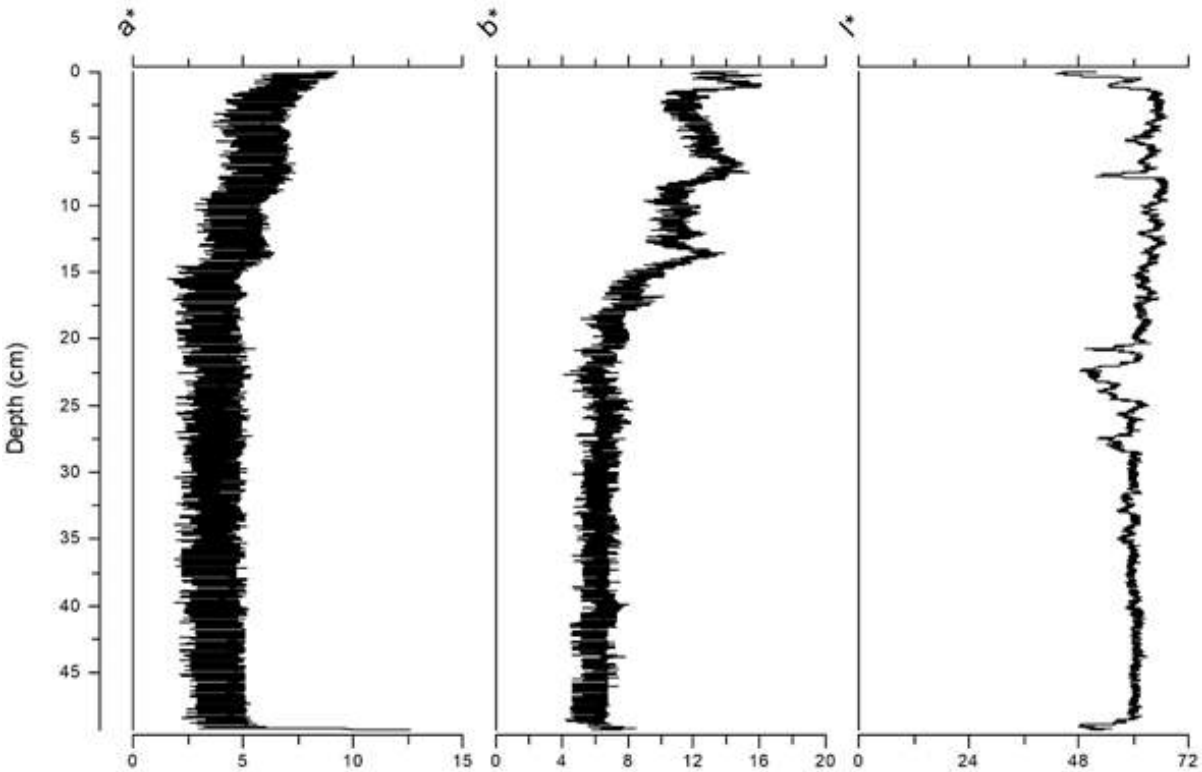

Fig. 3.4 Full records of colour parameters (a* = red/green, b* = blue/yellow, l* = brightness) against Depth (cm). Colour parameters are measured every 0,007 cm.

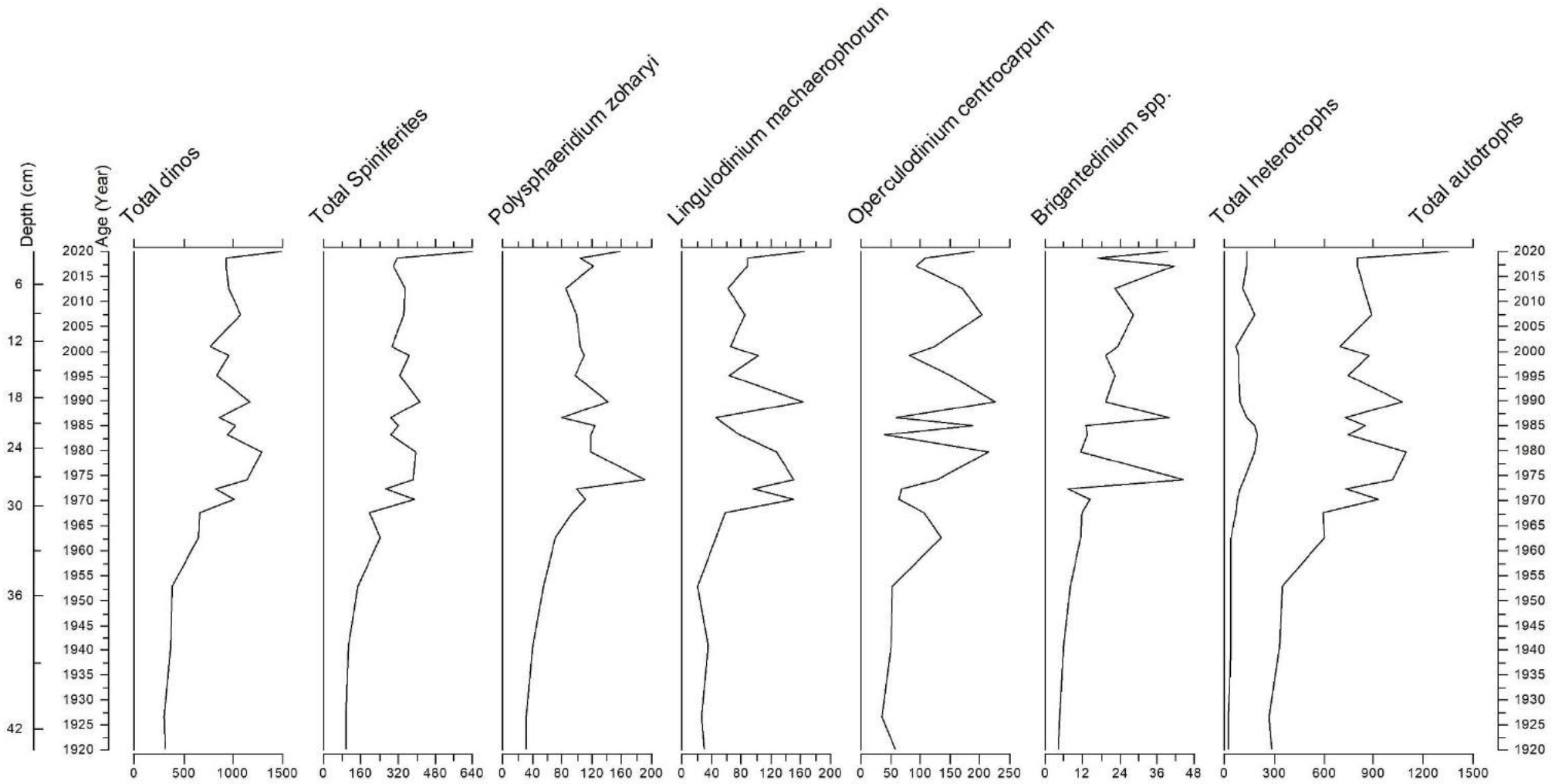

Fig. 4.1 A selection of dinocyst proxies against Age (year).

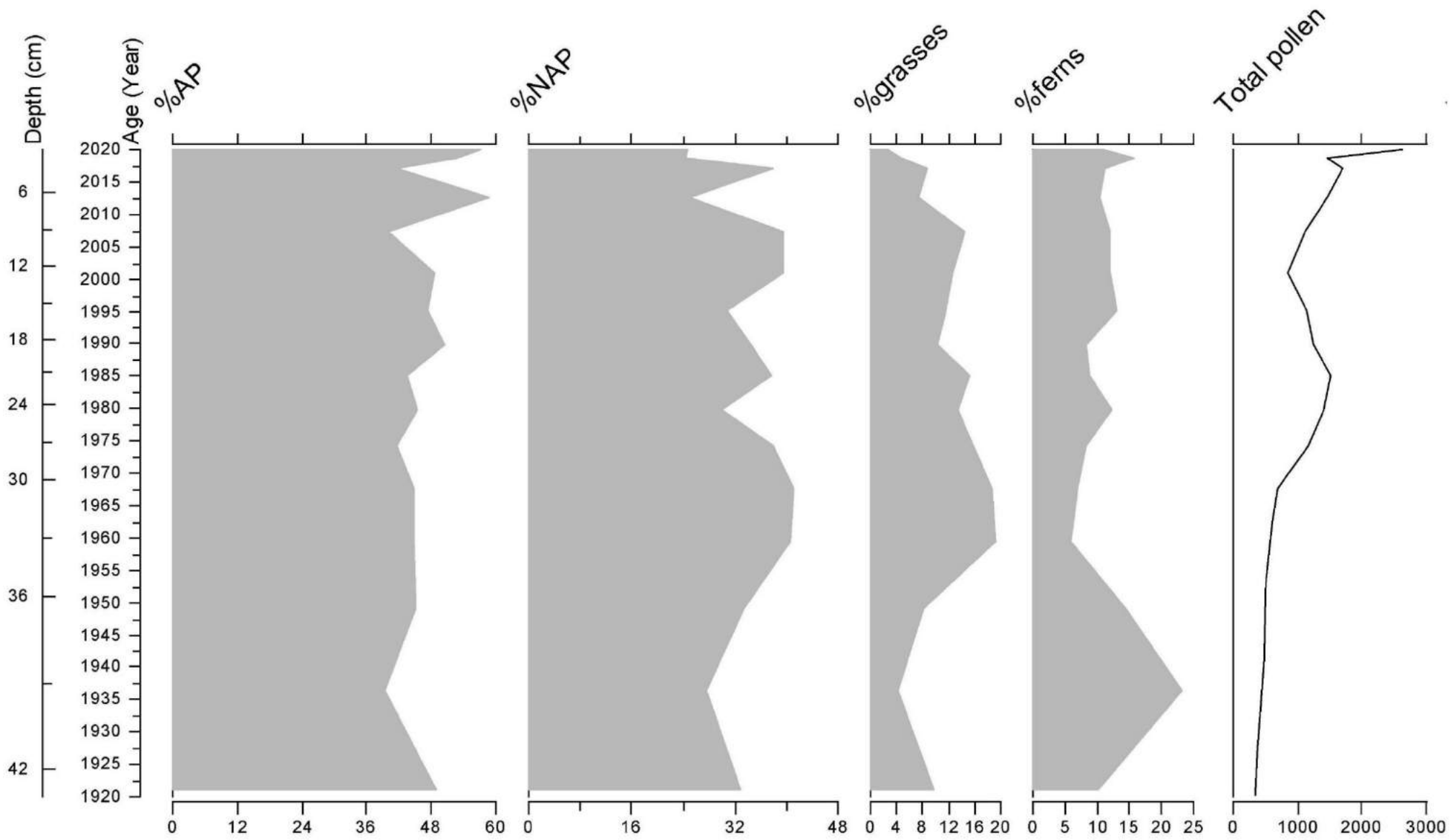

Fig. 4.2 Selection of pollen proxies against Age (year).

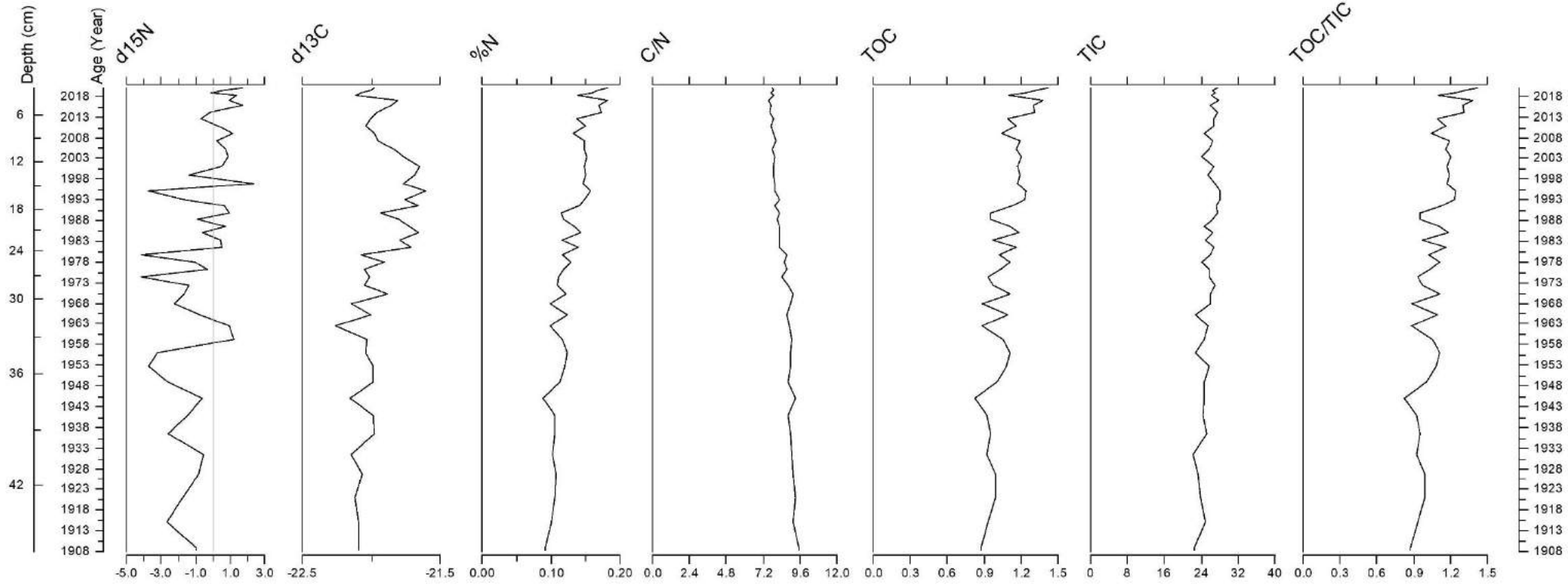

Fig. 4.3 Chemical proxies against Age (year).

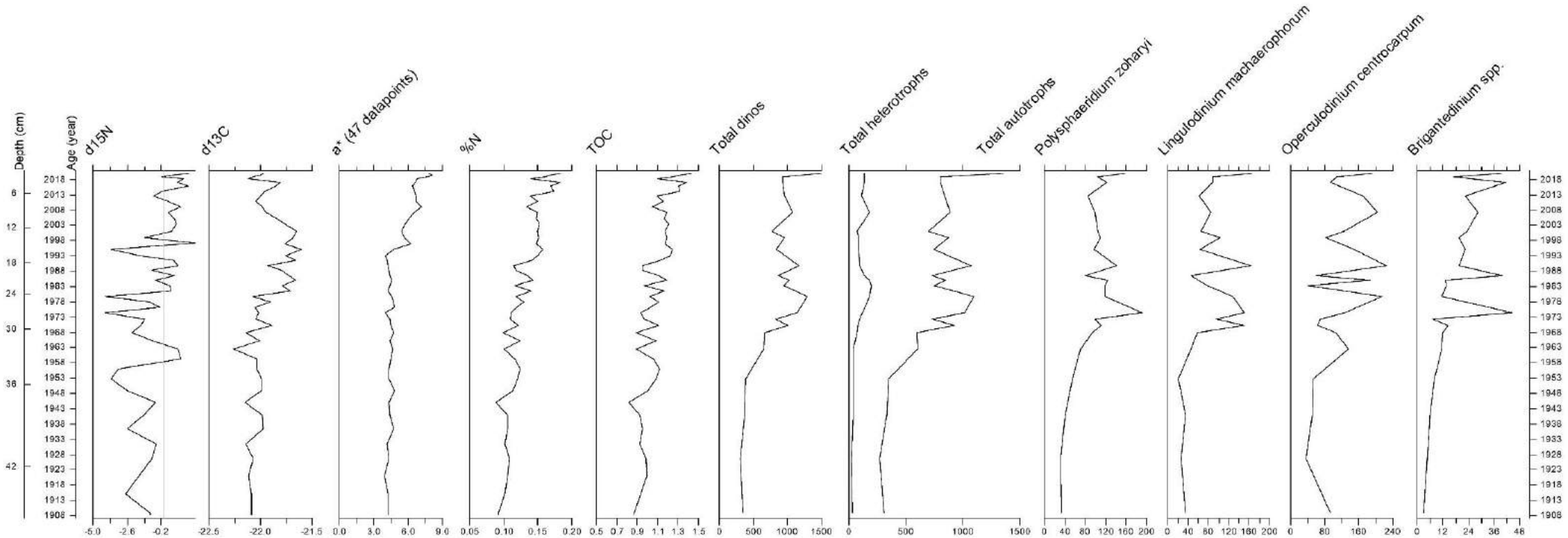

Fig.5 Side-by-side comparison of selected proxies against Age (year).

Statistical Analysis

Relationships with accumulation rate and river N input

First, a PCA was performed using the most important factors for terrestrial influence, nutrient availability, productivity and eutrophication. PC1 seemed to indicate clastic input, so accumulation rate was added to the same PCA (Figure 6). Indeed, accumulation rate is strongly positively correlated with PC1 in Figure 6. However, not accumulation rate, but %N falls exactly on the PC1 axis. PC1 is therefore interpreted as an axis displaying nutrient availability.

%C, TIC, accumulation rate and $\delta^{13}C$ are all strongly positively related to %N (interpreted as the amount of nutrients in the system). This provides further evidence for interpreting higher values in d $\delta^{13}C$ (enrichment) as indicative of relatively more local marine production. Accumulation rate and %N are related (no causal link), as both clastics and nutrients enter the system via river discharge. For %C and TIC, this suggests that these signals are primarily governed by primary production, not dilution. If they were primarily dilution signals, they would show a negative correlation with accumulation rate (and therefore also %N). This positive relationship with accumulation rate is persistent in later PCA's.

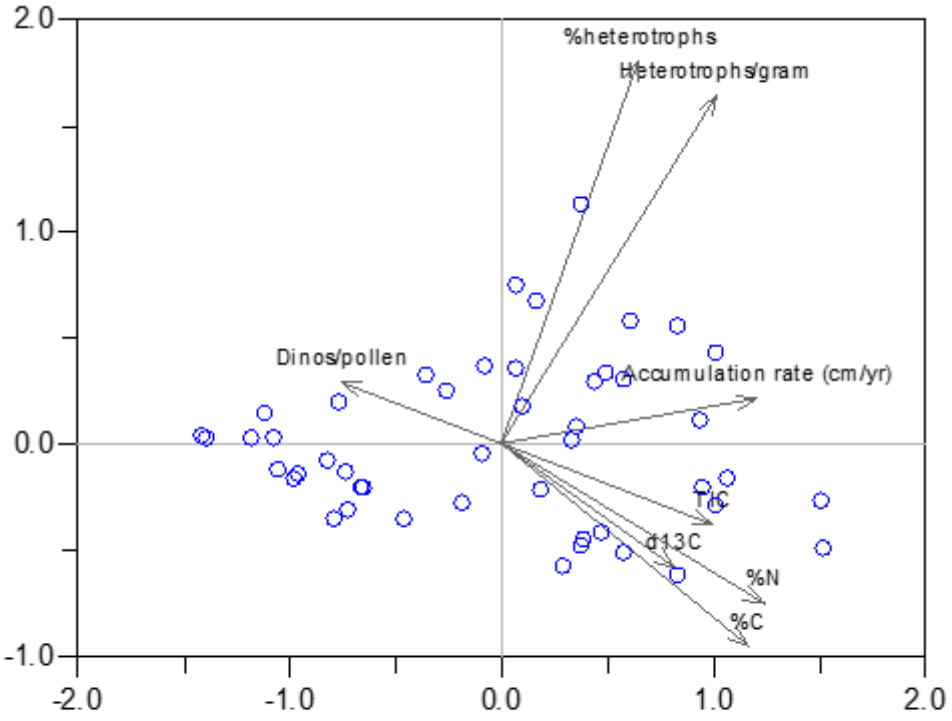

Fig. 6 PCA result of a comparison between several proxies and accumulation rate (axis 1 x axis 2). Blue circles indicate samples.

Relationships between dinocyst species and nutrients- and productivity indicators

The PCA in Figure 6 does not give us a clear axis which we may attribute to productivity and/or eutrophication. If we identify PC1 (in Figure 6) as the productivity axis, all dinocysts have a positive relationship with it, with *Spiniferites* and *Polyspaeridium* having the strongest positive relationship,

Brigantedinium, *Operculodinium* and Heterotrophs/gram slightly weaker and *Lingulodinium* in between.

If we identify PC2 (Figure 6) as the productivity axis, only *Brigantedinium* bears a very slight, positive relationship with it, while *Lingulodinium, Operculodinium* and *Polyspaeridium* display a negative relationship with it. PC3 (in Figure 7.1 and 7.2) cannot be a productivity axis, since we would expect that on such an axis, d13C and %N would both be positive.

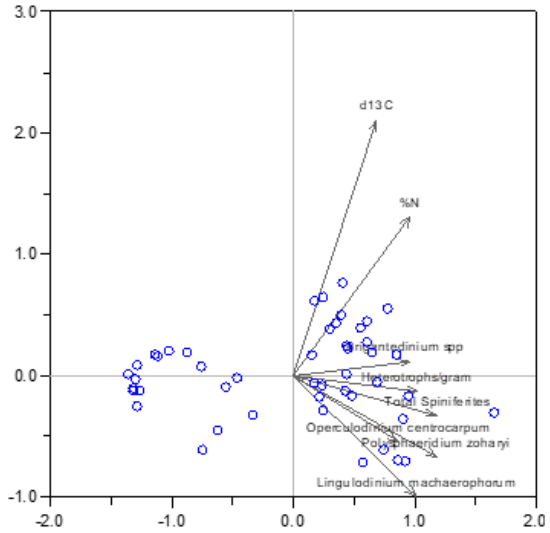

Fig.7.1 PCA result of several dinocyst species compared to nutrient- and productivity proxies (axis 3 x axis 1).

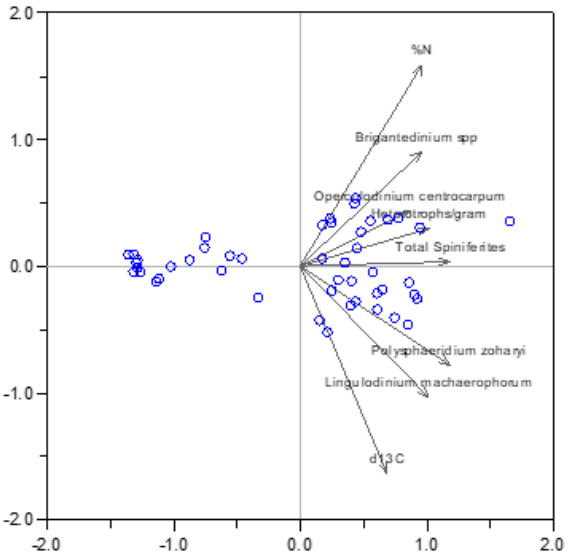

Fig. 7.2 PCA result of several dinocyst species compared to nutrient- and productivity proxies (axis 3 x axis 1).

The first possibility seems more logical than the second. To further investigate this, a second PCA included more productivity proxies in order to increase the weight of productivity in the dataset, so that a productivity axis might come out more clearly. The number of dinocyst proxies was reduced, so as not to use too many proxies for the amount of datapoints, which would make the analysis inaccurate. Therefore, I performed two PCA's, in which I varied the dinocyst proxies that would participate. They are displayed in Figures 8.1 and 8.2.

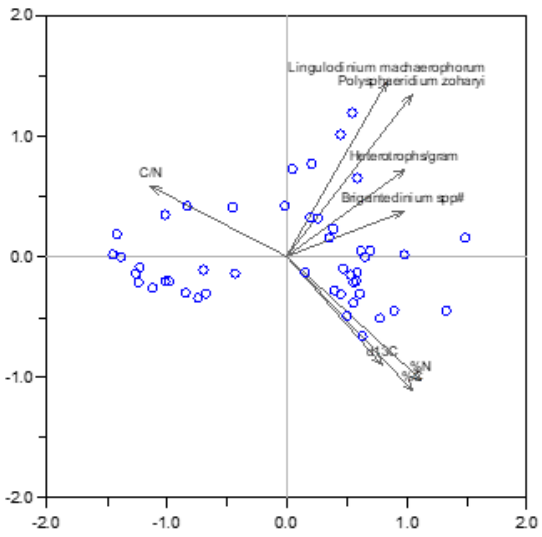

Fig.8.1 PCA result of several other dinocyst species compared to nutrient- and productivity proxies (axis 1 x axis 2).

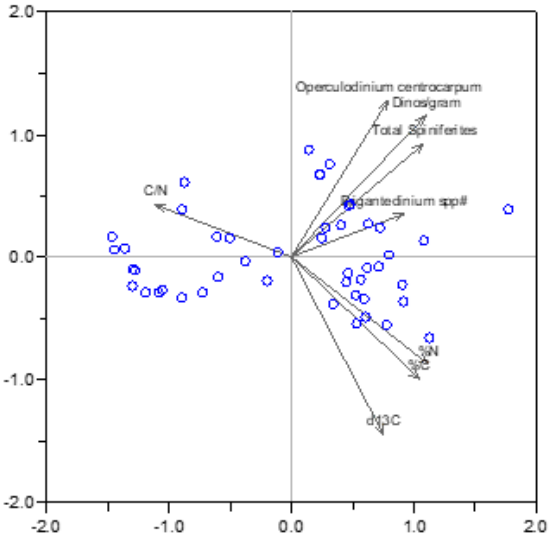

Fig.8.2 PCA result of several other dinocyst species compared to nutrient- and productivity proxies (axis 1 x axis 2).

It seems here that the productivity axis is PC1, or the x-axis in Figure 8.1 and 8.2 (it cannot be PC2, otherwise all dinocyst proxies would correlate negatively with productivity). Indeed, all dinocyst proxies have a positive relationship to productivity. The difference in stronger/weaker positive relationships is too small to pinpoint to specific dinocyst proxies as being better productivity proxies than the others: they may all equally be used as productivity indicators.

When it comes to eutrophication instead of productivity, no chemical proxies can directly be related to that, and no PCA can be done to determine how well the dinocyst proxies might correlate with eutrophication. So, while all dinocyst proxies may be used as productivity indicators, I will follow the literature and use the absolute abundances of *Lingulodinium machaerophorum*, *Brigantedinium spp*. and heterotrophs/gram as indicators of eutrophication, specifically.

In which samples is eutrophication most intense?

To determine this, I use the biplot of the last PCA of the previous section (Figure 8.1), in which PC1 was the axis associated with productivity. I divided the samples visually into three groups based on their scoring on PC1 (Figure 9).

Group 1: High productivity, score >0,7.
Group 2: Medium productivity, score between -0,2 and 0,7.
Group 3: Low productivity, score <-0,2.

Table 3. Scores of all samples on PC1 (Figure 9), where PC1 is linked to productivity.

Name	Depth (cm)	Score01 (Productivity)
IS1	0-0,5	1.49314
IS2	0,5-1	0.983799
IS3	1-1,5	0.541791
IS4	1,5-2	0.391336
IS5	2-3	1.3373
IS6	3-4	0.902087
IS7	4-5	0.778184

IS8	5-6	0.154259
IS9	6-7	0.472431
IS10	7-8	0.361939
IS11	8-9	0.656306
IS12	9-10	0.564592
IS13	10-11	0.562015
IS14	11-12	0.510154
IS15	12-13	0.615072
IS16	13-14	0.457386
IS17	14-15	0.636721
IS18	15-16	0.593334
IS19	16-17	0.693826
IS20	17-18	0.210599
IS21	18-19	0.260384
IS22	19-20	0.406841
IS23	20-21	0.5837
IS24	21-22	0.203518
IS25	22-23	0.620722
IS26	23-24	0.0557483
IS27	24-25	0.595919
IS28	25-26	0.4574
IS29	26-27	0.546074
IS30	27-28	-0.449309
IS31	28-29	-0.0103288
IS32	29-30	-0.824749
IS33	30-31	-0.428138
IS34	31-32	-1.00852
IS35	32-33	-0.690455
IS36	33-34	-0.665203
IS37	34-35	-0.731461
IS38	35-36	-0.838095
IS39	36-37	-1.40754
IS40	37-38	-0.972212
IS41	38-39	-1.00542
IS42	39-40	-1.21804
IS43	40-41	-1.11569
IS44	41-42	-1.22598
IS45	42-43	-1.2442
IS46	43-44	-1.4369
IS47	44-45	-1.37435

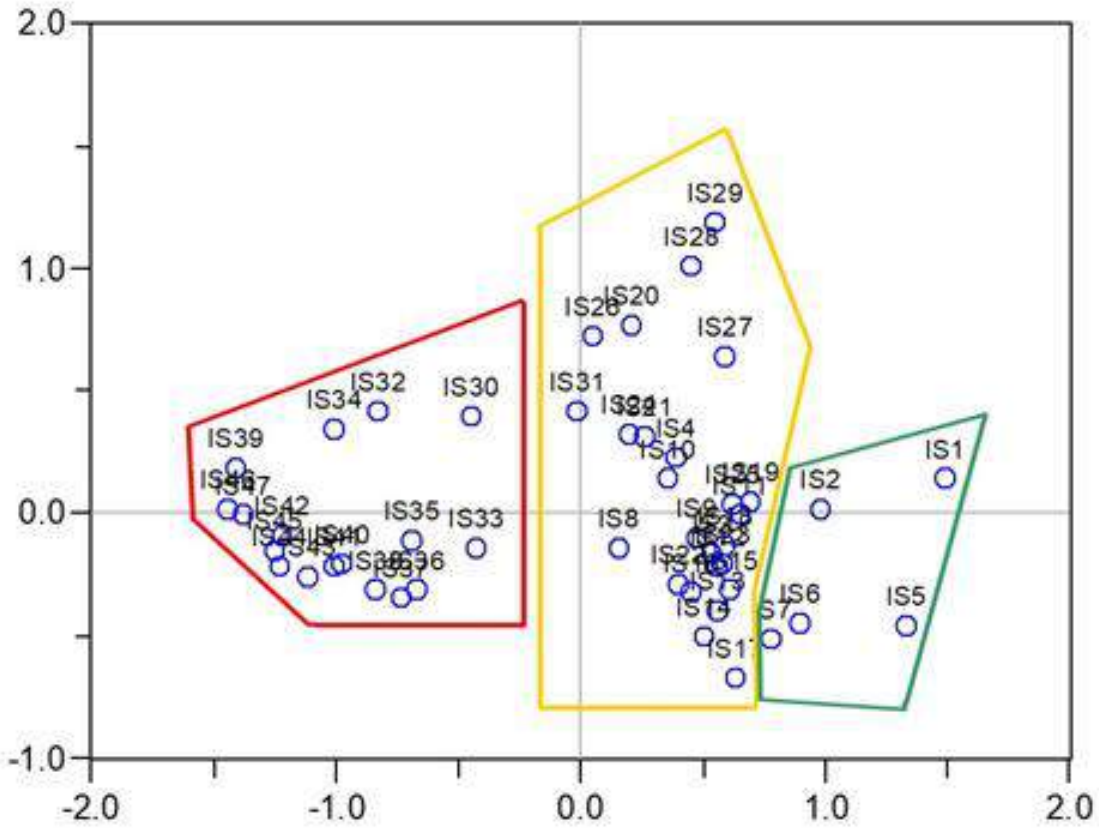

Fig. 9 PCA result only displaying the sample scores on axis 1 (associated with productivity) versus axis 2. They are visually divided into three groups based on their scoring on axis 1 (productivity).

In Table 3 and Figure 9, we can see that there seems to be a transition from low to medium productivity from IS32-IS29 and from medium to high productivity from IS8-IS7. These transitions remain if we place our boundaries for the three groups slightly differently, for example >0,5 or >0,7 for Group 1, or <0 for Group 3. The transition period from low to medium productivity corresponds to ~1961-1969. The transition period from medium to high productivity corresponds to ~2008-2010.

Environmental reconstruction

Pre-1950s

- $\delta^{15}N$ negative.
- All dinocyst species are low and unchanging.

1950s

- $\delta^{15}N$ is low. Starts to rise at the end of the 50s (becomes positive at the very end of the 50s).
- $\delta^{13}C$ is somewhat higher than its background value
- %N and TOC are higher than expected based on their rising trend.
- In the beginning of the 50s, *Lingulodinium* and *Operculodinium aculeatum* start to rise. This results in a total rise in (absolute) autotrophs, but not in heterotrophs.

In the 50s, we see the first signs of enhanced productivity (higher TOC, %N and $\delta^{13}C$). $\delta^{15}N$ remains low. If $\delta^{15}N$ does reflect terrestrial N input, this might suggest these first signs of enhanced productivity are caused by something else, for example the input of another limiting nutrient like phosphorus. Conversely, the $\delta^{15}N$ proxy might not have picked up a slight increase in terrestrial N input. This slight increase in productivity is not enough to cause eutrophication. Although autotrophic species slowly rise, this rise is too slight to seem important. Also, heterotrophs do not rise.

1960s

- Start of (slow) rise in $\delta^{13}C$. Still low.
- $\delta^{15}N$ negative.
- *Operculodinium aculeatum* experiences a low peak, falls back around the 60s-70s boundary. *Lingulodinium* rises slowly. The total amount of autotrophs also rises.
- Heterotrophs begin to rise.
- According to PCA and my classification of samples in three groups, this decade is the transition period from a low to medium productivity regime.

The 60s are comparable to the 50s. $\delta^{13}C$ very slowly rises. There still seems to be no large-scale productivity, but a change is at hand: heterotrophs begin to rise at the end of the decade. The autotrophs continue their rise, and *Operculodinium aculeatum* even peaks. This fits my statistical findings, in which the 60s came out as a transition period from a low to a medium productivity regime.

The beginning of the rise in $\delta^{13}C$ coincides with the construction of a dam in 1964. This dam blocked the rising discharge of the Atchafalaya river by redirecting the water into the Mississippi, so that only 30 percent of the Mississippi discharge would flow through the Atchafalaya. From 1964 onward, the influence of the Mississippi relative to the influence of the Atchfalaya may therefore have risen. This may have influenced the pollen that would end up in the northern GoM's sediment. In the 60s, ferns have a low abundance relative to grasses. But from the beginning of the 70s onwards, ferns become increasingly more abundant relative to grasses. This may reflect a change in the providence of the river-carried pollen, rather than actual vegetation changes.

1970s

- $\delta^{13}C$ slowly rises, with fallbacks. Mostly medium, except for 1972 and 1979, where it is low.
- $\delta^{15}N$ negative.

- *Lingulodinium* and *Brigantedinium* peak (the last one very sharply), with the maximum on ~1974. *Operculodinium* had fallen back in the first years of the decennium, but climbs again towards a peak in 1980. This causes a peak in autotrophs.
- Heterotrophs does not see a distinct peak, but is rising.
- According to PCA and my classification, the system is now in a medium productivity regime, which will remain until 2008-2010.

In the 70s, we see a regime of medium productivity. $\delta^{13}C$, TOC and %N continue their rise, but still do not exhibit exceptionally high values. Both autotrophic (specifically *Lingulodinium)* and heterotrophic dinoflagellates seem to profit from these conditions. Dinoflagellate species that favor eutrophic conditions (*Lingulodinium, Brigantedinium*) peak at mid-century.

$\delta^{15}N$ remains negative. This may mean that this increase in productivity is still not mainly nitrate-driven. Since the heterotrophic abundance is high, this implies that no or very little oxic degradation has occurred during this time period; a possible indication of hypoxia.

1980s

- Beginning of 80s: sharp rise of $\delta^{13}C$, stabilizes at more enriched values.
- At 1980, $\delta^{15}N$ enters a new, routinely positive regime (with fallbacks to negative values)
- Heterotrophs experience a peak at the middle of the decade, then fall back during the later 80s.
- After the high values of the 70s, *Lingulodinium* and *Operculodinium* now fall during this decade.
- *Brigantedinium* starts out low, but peaks very sharply in ~1987.

Much changes at the 70s-80s boundary. Productivity ($\delta^{13}C$) increases sharply, settling at a higher, more enriched value. Now, $\delta^{15}N$ also shows a marked increase. This might suggests that this increase in productivity was mainly driven by increased input of terrestrial nitrogen. The heterotrophs also point towards an increase in productivity. The autotrophic dinoflagellate proxies do not exhibit the increase in productivity that the other proxies show. It may be the case that this productivity is driven by primary producers other than dinoflagellates. These other primary producers might drive the enhanced productivity evidenced in $\delta^{13}C$ and %N.

As evidenced by $\delta^{13}C$ and the PCA productivity seems to settle at a high and relatively stable value around the middle of the 80s, when %N and TOC are also high. We see this stabilization even more clearly in the 90s (see below). This coincides with a period of relatively high heterotrophic abundances. At the end of the decade, the heterotrophic abundance falls somewhat. This coincides with an excursion to lower values in $\delta^{13}C$, %N and TOC. This again shows the interconnectedness of these proxies.

1990s

- %TOC and %N sharply rise from 1993 to 1996, then their rise stagnates. They plateau at a high level (do not fall back).
- $\delta^{15}N$ in new regime. Fallback to somewhat more negative values in 1995, but a large spike around 1996.
- a*, having been very constant, suddenly starts to rise at 1993 until 1996, then plateaus after that.
- Right at the start of the 90s, *Lingulodinium* and *Operculodinium* peak. During the rest of the decade, they fall again.
- *Brigantedinium* is low, but slowly rising (without peaks) in the 90s.
- Heterotrophs are relatively low and unchanging

- 1993: a great flood, which enhanced the measured oxygen minimum zone.
- 1998: a drought, which shrank the measured oxygen minimum zone.

Apart from a peak in autotrophs at the 80s/90s boundary, the autotrophic abundance is relatively low during this decade. The same goes for heterotrophic abundance. However, it must be stated that, although the autotrophic abundance is lower than in the 70s and 80s, it is still quite high. The other proxies ($\delta^{13}C$, %N, TOC) suggest that productivity is still high. Again, productivity here may be primarily driven by other primary producers than autotrophic dinoflagellates.

If $\delta^{13}C$, %N and TOC are high, why is the heterotrophic abundance low? It may have two causes:

1. The initial, higher abundance of heterotrophs has decayed significantly by oxic degradation, as heterotrophs are much more sensitive to that than are autotrophic dinocysts. In this case, high productivity may have combined with oxygenation of the bottom waters. Oxygenation may be caused by increased storm activity. I have gathered rough storm data from the yearly storm track images from the HURDAT best track database. They can be found in the NOAA database archive, https://www.nhc.noaa.gov/data/#annual. I counted the amount of tropical storms, hurricanes and major hurricanes occurring 1. In the area, and 2. Very close to the location of 80b. It seems that the 80s did indeed experience more storms overall than the 70s, 60s and 50s. The possibly resulting breakdown of stratification and bottom water oxygenation may explain the falling abundance of heterotrophic dinocysts in the 80s.

However, the 2000s are also a decade which seems to have experienced a higher amount of storms than usual, but here, heterotrophs *peak*, instead of remaining low. Furthermore, it is unclear if we should take the total amount of storms in the region into account (where, for example, a smaller tropical storm and a hurricane both count as one) or if we should look at the intensity of occurring storms. The 90s, for example, experienced less storms than the 80s overall, but while the 80s did not see a major hurricane in the region, the 90s experienced two, in 1992 and 1995. What affects bottom water oxygenation the most: a handful of smaller, less intense storms, or one major storm? With these considerations in mind, we cannot say anything with certainty about the relationship of these falling heterotrophic abundances and storm activity or -intensity, although a relationship remains a possibility.

2. The initial abundance was already low, and heterotrophs simply did not thrive during this decade. Heterotrophic dinoflagellates may live off a specific diet of certain autotrophic species. If these did not peak (because other organisms drove the enhanced productivity), the heterotrophic abundance also did not peak. In this case, their dietary preference causes them to decline. Another possibility is that heterotrophic dinoflagellates profit from rising (or, more broadly, changing) productivity levels, and not necessarily from high and stable productivity levels. Rising productivity levels may lead to more or stronger eutrophication, which then leads to changes in the heterotrophic abundance. This may be why the heterotrophic abundance rises and peaks during the 70s, when productivity is rising and eutrophication commences, but falls back in the late 80s and remain low throughout the 90s, when productivity has stabilized at a higher value. Without further evidence, this possible relationship between rising/stable productivity, eutrophication and heterotrophic abundance remains speculative.

A definitive answer to this issue may only be acquired with an almost impossibly high resolution record, dated with an equally impossibly precise age model. For now, I will have to let the issue rest. What does seem clear is that heterotrophic abundance, even when used absolutely instead of relatively, may not always be the best indicator for high productivity and eutrophication. It needs to be used in conjunction with other proxies.
The sediments become increasingly red in color from 1993-1996. This is probably due to increased clastic input coupled to a higher nutrient input (as %TOC and %N also rise sharply, and d15N spikes

around 1996). Possibly, river discharge in general rose during these years. This may be coupled to a particularly large 1993 flood occurring at the beginning of the 1993-1996 period of sharply rising a*, TOC and %N. The fact that such a spike seems smeared out over three years may have two causes: 1. a spike may not be picked up as a spike, but a broader peak because of the ~3-year resolution of the record during this time period, and 2. The terrestrial pulse may be smeared out more in the marine setting of 80b. We also see such a peak in $\delta^{15}N$ around 1996. If $\delta^{15}N$ reflects terrestrial N input, this might be the same peak.

We might not see this productivity peak show up in $\delta^{13}C$: as the expected productivity peak of 1993-1996 coincided with a peak in clastic material, more terrestrial carbon might also have been brought into the system. This might have diluted the productivity-related enrichment of carbon, so that the net effect on $\delta^{13}C$ would be close to zero.
The terrestrial "pulse" found by Rebecca Puyk in core M100 around 1993 (see section "$\delta^{13}C$" in Results and Discussion) is quite possibly the same pulse seen here in a*, leading to a pulse in productivity (%N, TOC) that was not picked up by $\delta^{13}C$ because of an increase of terrestrial carbon. Puyk also noticed that this pulse coincided with the major Mississippi flood event of 1993.

The 1998 drought does not seem to have an effect on the proxies.

After 1996, we see that %N, TOC and $\delta^{13}C$ do not rise further, but stabilize at a high value.

2000s

- Grasses decrease, ferns increase
- %N and TOC still stagnate. In 2005-2010, they even reach slightly lower values.
- Now, from ~2000 to 2010, the rise in TIC also stagnates.
- $\delta^{13}C$ falls back to its previous, more depleted values during these ten years.
- $\delta^{15}N$ completely positive.
- a* rises during 2005-2010.
- %AP (C3 plants) rises slightly, while %NAP and %grasses (also some C4 plants) fall.
- *Operculodinium* rises strongly towards a peak in ~2007, while *Lingulodinium* remains fairly low and constant.
- There is a small peak in autotrophs in ~2007.
- Heterotrophs show a sharp peak in ~2007. *Brigantedinium* also shows a moderate peak in ~2007.
- At the very end of this decade (2008-2010), the system transitions from a medium to high productivity regime, according to my PCA and classification of the samples into three groups.
- In 2003 and 2005, two great storms disrupted stratification and caused a smaller than expected measured oxygen minimum zone.
- In 2001, the Action Plan was brought before Congress. We might expect it to be implemented over the course of this decade.

Right at the start of this decade, $\delta^{13}C$ starts to fall, and continues to fall over the decade. Does productivity fall here? Indeed, TOC also seems to fall slightly after 2007, but this fall would be too small to match the marked shift to more depleted $\delta^{13}C$ values. Also, if productivity falls here, this happens despite the fact that the amount of nutrients seems to remain high: $\delta^{15}N$ even enters a fully positive regime in 2000-2010. %N, although it falls back slightly after 2007, still remains very high. And clastic input (which often goes together with nutrient input), indicated by a*, rises from 2005 and 2010.

What has triggered the fall in productivity, if not a lack of N input? Maybe, it is not a fall in productivity

at all; something else other than productivity might have influenced $\delta^{13}C$. Following the interpretation laid out for 1990-2000, the fall in $\delta^{13}C$ might be caused by a large increase in terrestrial, depleted carbon input. From a*, we know clastic input was high during this decade, and increased during 2005-2010. This might have brought terrestrial carbon with it. The increase in clastic input from 2005 to 2010 might also have increased the dilution effect on %N and TOC, causing their fallback of 2005-2010. All the while, productivity itself might not have decreased. This is indicated by the fact that all other proxy's for nutrient input and productivity remain rather high, or even rise. It is also consistent with previous research.

%AP rises during this time period, while %grasses and %NAP fall. The AP group consists mainly of C3 plants, that have a more negative carbon isotope fingerprint than the grasses group, which also contain C4 plants. Although pollen are only a slight fraction of plant material that enters the system, this may be an indication that the source of terrestrial depleted carbon is an overall change in the type of plant material carried to the system: more tree-derived material, instead of grasses, herbs, shrubs and crops.

The signal of the eutrophication proxies is mixed. The heterotrophic abundances are high (including *Brigantedinium*), indicating high productivity and/or preservation by hypoxia. There is a small peak in autotrophic dinoflagellates as well, although *Lingulodinium* (eutrophication indicator) does not seem to contribute much to this small peak.

Since it does not seem that the nutrient input is falling during this decade, the Action Plan, brought to Congress in 2001, does not seem to have immediate effect. This might be because 1. The relevant actors did not follow through with the promises made in the Action Plan, or took too little action, or 2. They did act upon the Action Plan, but it was not enough to reduce nutrient input. One reason for this may be that nitrogen lingers in soils for several years after it is applied to that soil, continuously leaching into ground waters and rivers even if no new nitrogen is applied. This lag can be as large as 30 years (Van Meter et al, 2018).

2010s

- Grasses decrease, ferns increase
- %N and %TOC rise again, in two steps, disrupted by short 2018 fall
- $\delta^{13}C$ rises again, short fallback around 2017.
- $\delta^{15}N$ mostly positive, except for 2010-2014 and ~2018.
- 2010-2014, a* plateaus, or even falls slightly. It rises again from 2014-2019. Maybe, it slightly falls in 2018.
- The beginning of this decade sees a fall in heterotrophs (however, the value it falls back to is still relatively high compared to the beginning of the record). The rest of the decade, it slowly rises.
- *Brigantedinium* peaks sharply in 2017, then falls back shortly, then again rises sharply in 2019. Its short fallback may correspond to the short fallback from high to medium productivity in my PCA around 2018.
- All dinocyst species rise sharply in the last 1-2 years of the record, 2018-2019.

During this decade, the influence of productivity overrides again the presumed dilution effects of terrestrial carbon (on d13C) and clastic input (on %TOC and %N, and also %TIC). Further evidence for this comes from the nutrient- and eutrophication indicators, which remain high. This is despite the fact that a*, reflecting clastic input, also remains high, and rises from 2014-2019. In order to override this, productivity must have been particularly intense. The exception to this is 2018. Here, all productivity- and eutrophication indicators shortly fall back (also *Brigantedinium*). Therefore,

this seems to be an absolute fallback in productivity, not (necessarily) a relative change due to dilution effects.

What may have been the cause? Low river discharge is one possibility: clastic input indicator a* (and b*) and possible N input indicator d15N fall in 2018. However, the fall in a* is only slight. Overall, however, this decade does not see any large-scale reduction of nutrient input, productivity or eutrophication. In fact, this decade (apart from 2018) seems to be the most intense in terms of productivity and eutrophication to date, despite the Action Plan's measures. I have outlined the possible reasons for the ineffectiveness of the Action Plan in the previous section. If the Action Plan is indeed implemented as agreed, and the lag caused by the nutrient legacy in soils is overcome after two or three decades, we may finally see a reduction of nutrient input into the northern Gulf of Mexico. But that is still uncertain. If no strong and effective measures are taken, the trend of rising nutrients, productivity and eutrophication will most likely continue into the future.

Conclusion

History of productivity and eutrophication

- The first signs of enhanced productivity appear in the 1950s. But the rise is slight, and not enough to cause eutrophication.
- Productivity slowly continues to rise into the 60s. In the late 60s, the first signs of slight eutrophication appear.
- A regime of medium productivity ensued in the 70s. The gradual increase in productivity may be because of other factors than nitrogen loading, but this is uncertain.
- Change at the 70s-80s boundary. Productivity increases sharply, now almost certainly because of nitrogen loading.
- Productivity stabilizes at a high value during 80s and 90s. The system probably experienced peaks of eutrophication. More clastic and nutrient input during the middle of the 90s, quite possibly coupled to the 1993 flood.
- Productivity keeps on rising through the 2000s and 2010s, together with clastic input. The clastic input may have diluted productivity proxies. Still, nutrient load and eutrophication show no signs of falling.
- The exception is 2018, where productivity and eutrophication shortly fall (possibly because of low river discharge, but this is uncertain).

History of hypoxia

- There is evidence for hypoxia in the 70s, 80s, 00s and 2010s, at least.
- Relatively low levels of N load and productivity probably caused the absence of signs of hypoxia before the 70s.
- In the 90s and beginning of the 2010s, the absence of signs of hypoxia is most likely caused by other means (storm activity is a possibility), as N load and productivity are high.
- This suggests that widespread hypoxia started in the 70s.

Land vegetation

There is no clear link between the developments in the marine system and land vegetation changes. We cannot say if the changes in the pollen assemblage reflect overall vegetation changes on land, or rather a change in the providence of the pollen, for example caused by the damming of the Atchafalaya in 1964, causing the influence of the Mississippi to have increased since then. This generally caused a relative increase in fern pollen and a decrease in grass pollen.

On the usage of proxies

- The relative abundance of heterotrophic dinoflagellates cannot be used in hypoxic environments, due to the enhanced degradation of heterotrophs in oxic environments. This causes all relative dinocyst abundances to be suspect. In cases like these, it may be better to use absolute abundances of dinocysts for environmental reconstruction, contrary to palynological custom.

  The absolute heterotrophic abundance covaries with $\delta^{13}C$, %N and TOC, so, it seems to be a fairly reliable indicator for productivity. However, this is not always the case, so, it should not be used in isolation.
- In this case, $\delta^{13}C$, TOC and TIC are mainly production signals, not dilution or preservation. However, $\delta^{13}C$, and possibly also %N and TOC, probably suffered dilution effects in the 2010s due to large terrestrial inputs. This goes to show that it should always be carefully assessed what these proxies actually indicate at every point in a core.

- The absolute abundance of autotrophic dinocysts mostly corresponds to productivity (and nitrogen load) proxies, but not always. This is also the case for the abundances of specific autotrophic species. It is probable, for example, that an increase in productivity was mainly caused by other primary producers than autotrophic dinoflagellates. Therefore, the absolute abundance of autotrophs may not be the ideal proxy for productivity, and should always be used together with other proxies.
- $\delta^{15}N$ might be more fit as a proxy for terrestrial N input than for N acquisition pathways/hypoxia. The $\delta^{15}N$ proxy matches the other proxies for terrestrial input quite well.
- The %grasses/%ferns ratio as a proxy for terrestrial/marine influence does not fit the other proxies. Therefore, such a proxy most probably cannot be used in this way. However, there does seem to be a relationship between the relative abundances of grasses- and fern pollen and distance from the shore, which may be worth investigating in future studies.

Overall picture and future outlook

In the 50s, we see the first signs of enhanced productivity. But because of the scarcity of the record here, the enhancement of productivity may have started earlier.

The first signs of eutrophication appear in the late 60s. Only shortly after, in the 70s, we see signs of widespread hypoxia. Since then, N load, productivity, eutrophication and most probably also hypoxia have intensified, showing no signs of fallbacks. During the late 80s and 90s, N load and productivity stabilized, but resumed their rise in the 00s towards the present. The last decade even seems to be the most intense in terms of productivity and eutrophication compared to the rest of the record.

This is despite the efforts of the Mississippi River/Gulf of Mexico Watershed Nutrient Task Force. Their Action Plans of 2001 and 2008 have not been realized, and judging from the records presented in this study, the Action Plans did not even cause a dent in the overall rising trend in N load, productivity and hypoxia.

References

Adhikari, P. L., J. R. White, K. Maiti, N. Nguyen. 2015. "Phosphorus speciation and sedimentary phosphorus release from the Gulf of Mexico sediments: Implication for hypoxia." Estuarine, Coastal and Shelf Science 164, 77-85.

Anderson, D.M., 1998. "Physiology and bloom dynamics of toxic Alexandrium species, with emphasis on life cycle transitions." In *Physiological ecology of harmful algal blooms*, eds. Anderson et al., NATO ASI series. Springer-Verlag, Berlin, Germany, pp. 29–48.

Blum, M. D. and H. H. Roberts, 2012. "The Mississippi Delta region: past, present, and future." *Annual Review of Earth and Planetary Science*, 40, 655–683, https://doi.org/10.1146/annurev-earth-042711-105248

Bravo, I., and R. I. Figueroa, 2014. "Towards an Ecological Understanding of Dinoflagellate Cyst Functions." *Microorganisms* 2(1): 11–32.

Breitburg, D., L. A. Levin, A. Oschlies, M. Grégoire, F. P. Chavez, D. J. Conley, V. Garçon, D. Gilbert, D. Gutiérrez, K. Isensee, G. S. Jacinto, K. E. Limburg, I. Montes, S. W. A. Naqvi, G. C. Pitcher, N. Rabalais, M. R. Roman, K. A. Rose, B. A. Seibel, M. Telszewski, M. Yasuhara, J. Zhang, 2018. "Declining oxygen in the global ocean and coastal waters." *Science* 359: 46.

Buffler, R. T., and D. S. Sawyer, 1985. "Distribution of Crust and Early History, Gulf of Mexico Basin Gulf Coast." *Association of Geological Societies Transactions* 35, 333-344 https://archives-datapages-com.proxy.library.uu.nl/data/gcags/data/035/035001/0333.htm

CENR, 2000. *Integrated Assessment of Hypoxia in the Northern Gulf of Mexico.* National Science and Technology Council Committee on Environment and Natural Resources, Washington, DC.

Chang, C. C. Y., C. Kendall, S. R. Silva, W. A. Battaglin, D. H. Campbell. 2002. "Nitrate stable isotopes: Tools for determining nitrate sources among different land uses in the Mississippi River Basin." *Canadian Journal of Fisheries and Aquatic Sciences* 59(12): 1874-1885. DOI:10.1139/f02-153

Childs, C. R., N. N. Rabalais, R. E. Turner, L. M. Proctor. 2002. "Sediment denitrification in the Gulf of Mexico zone of hypoxia." Marine Ecology Progress Series 240, 285-290.

Coleman, J. M., H. H. Roberts, and G. W. Stone, 1998. "Mississippi River Delta: An Overview". Journal of Coastal Research 14, 699–716.

Couvillion, B. R., H. Beck, D. Schoolmaster, and M. M. Fischer, 2017.: "Land area change in coastal Louisiana (1932 to 2016)." *U.S. Geological Survey Scientific Investigations Map 3381*, U.S. Geological Survey, Reston, VA.

Dale, B., 1996. "Dinoflagellate cyst ecology: Modeling and geological applications." In *Palynology: Principles and Applications*, ed. J. Jansonius and D.C. McGregor, 1249–1275. Salt Lake city: AASP Foundation.

Dale, B. 2001. "Marine dinoflagellate cysts as indicators of eutrophication and industrial pollution: a discussion." The Science of the Total Environment 264, 235-240.

Dale, B. 2009. "Eutrophication signals in the sedimentary record of dinoflagellate cysts in coastal waters." *Journal of Sea Research* 61 (1-2): 103–113. https://doi.org/10.1016/j.seares.2008.06.007.

Dale, B., and A. Fjellså. 1994. "Dinoflagellate cysts as productivity indicators: State of the art, potential and limits". In *Carbon cycling in the glacial ocean: Constraints in the ocean's role in global change,* ed. R. Zahn, 521–537. Berlin: Springer. https://doi.org/10.1007/978-3- 642-78737-9_22

Dale, B., A. Thorsen, and A. Fjellså. 1999. "Dinoflagellate cysts as indicators of cultural eutrophication in the Oslofjord, Norway." *Estuarine, Coastal and Shelf Science* 48 (3): 371–382. https://doi. org/10.1006/ecss.1999.0427.

Dale, V. H., C. L. Kling, J. L. Meyer, J. Sanders, H. Stallworth, T. Armitage, D. Wangsness, T. Bianchi, A. Blumberg, W. Boynton, D. J. Conley, W. Crumpton, M. David, D. Gilbert, R. W. Howarth, R. Lowarance, K. Mankin, J. Opaluch, H. Paerl, K. Reckhow, A. N. Sharpley, T. W. Simpson, C. S. Snyder, D. Wright, 2000. *Hypoxia in the Northern Gulf of Mexico*, edited by B. N. Anderson, R. W. Howarth and L. W. Walker. New York: Springer.

Davis, C., 1948. “Gymnodinium breve: a cause of discolored water and animal mortality in the Gulf of Mexico.” *Botanical Gazette* 109, 358–360.

Debret, M., D. Sebag, M. Desmet, W. Balsam, Y. Copard, et al.. 2011. “Spectrocolorimetric interpretation of sedimentary dynamics: The new ”Q7/4 diagram”.” Earth-Science Reviews, Elsevier, 109 (1-2), pp.1-19.

Draut, A. E., G. C. Kineke, D. W. Velasco, M. A. Allison, and R. J. Prime, 2005. “Influence of the Atchfalaya River on recent evolution of the chenier-plain inner continental shelf, northern Gulf of Mexico.” *Continental Shelf Research* 25: 91-112.

Edwards, L.E. and D.A. Willard, 2001. “Dinoflagellate cysts and pollen from sediment samples, Mississippi Sound and Gulf of Mexico.” In *Paleontology and Geology of Mississippi Sound sediments,* ed. G.S. Gohn, 01–415. Jackson County: U.S. Geological Survey Open-File Report.

Ewing, T. E., 2009. “The ups and downs of the Sabine Uplift and the northern Gulf of Mexico Basin: Jurassic basement blocks, Cretaceous thermal uplifts, and Cenozoic flexure.” *Gulf Coast Association of Geological Societies Transactions*, 59, 253-269.

Faust, M. J., 1990. “Seismic stratigraphy of the mid-Cretaceous unconformity (MCU) in the central Gulf of Mexico basin.” *Geophysics* 55(7), 806-948.

Fennel, K. and A. Laurent. 2018. “N and P as ultimate and proximate limiting nutrients in the northern Gulf of Mexico: implications for hypoxia reduction strategies.” Biogeosciences, 15, 3121–3131.

Galloway, W. E., 2008. “Depositional Evolution of the Gulf of Mexico Sedimentary Basin. *In Sedimentary Basins of the World, Vol 5,* ed. K.J. Hsü . The Netherlands: Elsevier, pp. 505 – 549. ISBN: 978-0-444-50425-8

Galloway, W. E., T. L. Whiteaker, and P. Ganey-Curry., 2011. “History of Cenozoic North American drainage basin evolution, sediment yield, and accumulation in the Gulf of Mexico basin.” *Geosphere* 7(4): 938–973.

Garcés, E., M. Masó, J. Camp, 2002. “Role of temporary cysts in the population dynamics of Alexandrium taylori (Dinophyceae).” *Journal of Plankton Research* 24, 681–686.

Gómez, F., 2012. "A checklist and classification of living dinoflagellates (Dinoflagellata, Alveolata)". *CICIMAR Océanides* 27 (1): 65–140.

Hense, I., 2010. “Approaches to model the life cycle of harmful algae.” *Journal of Marine Systems* 83, 108–114.

Itakura, S., I. Imai, K. Itoh, 1997. ““Seed bank” of coastal planktonic diatoms in bottom sediments of Hiroshima Bay, Seto Inland Sea, Japan.” *Marine Biology* 128, 497–508.

Justić, D., N. N. Rabalais, and R. E. Turner. 1995. “Stoichiometric nutrient balance and origin of coastal eutrophication.” *Marine Pollution Bulletin* 30: 41– 46.

Krepakevich, A., and V. Pospelova. 2010. “Tracing the influence of sewage discharge on coastal bays of Southern Vancouver Island (BC, Canada) using sedimentary records of phytoplankton.” *Continental Shelf Research* 30 (18): 1924–1940. https://doi.org/10.1016/j.csr.2010.09.002

Limoges, A., L. Londeix, A. de Vernal. 2013. “Organic-walled dinoflagellate cyst distribution in the Gulf of Mexico.” Marine Micropaleontology 102, 51-68, https://doi.org/10.1016/j.marmicro.2013.06.002.

Limoges, A., A. de Vernal, N. Van Nieuwenhove. 2014. “Long-term hydrological changes in the northeastern Gulf of Mexico (ODP-625B) during the Holocene and late Pleistocene inferred from organic-walled dinoflagellate cysts.” Palaeogeography, Palaeoclimatology, Palaeoecology 414, 178-191, https://doi.org/10.1016/j.palaeo.2014.08.019.

Limoges, A., A. de Vernal, and A.-C. Ruiz-Fernández, 2015. “Investigating the impact of land use and the potential for harmful algal blooms in a tropical lagoon of the Gulf of Mexico.” *Estuarine, Coastal and Shelf Science* 167B: 549–559.

Limoges, A., L. Londeix, K. N. Mertens, A. Rochon, V. Pospelova, T. Cuéllar, A. de Vernal. 2018. “Identification key for Pliocene and Quaternary Spiniferites taxa bearing intergonal processes based on observations from estuarine and coastal environments.” Palynology 42(1), 72–88 https://doi.org/10.1080/01916122.2018.1465733

Lundholm, N., S. Ribeiro, T. J. Andersen, T. A. Koch, A. Godhe, F. Ekelund, M. Ellegaard, 2011. "Buried alive-germination of up to a century-old marine protist resting stages". *Phycologia* 50 (6), 629–640.

Matsuoka, K., 1999. "Eutrophication process recorded in dinoflagellate cyst assemblages—A case of Yokohama Port, Tokyo Bay, Japan". *The Science of the Total Environment* 231 (1): 17–35. https://doi. org/10.1016/S0048-9697(99)00087-X

Matsuoka, K., L.B. Joyce, Y. Kotani, and Y. Matsuyama, 2003. "Modern dinoflagellate cysts in hypertrophic coastal waters of Tokyo, Japan." *Journal of Plankton Research* 25 (12): 1461–1470. https://doi.org/ 10.1093/plankt/fbg111.

Mississippi River/Gulf of Mexico Watershed Nutrient Task Force, 2001. *Action Plan for Reducing, Mitigating, and Controlling Hypoxia in the Northern Gulf of Mexico.* Washington, DC.

Mississippi River/Gulf of Mexico Watershed Nutrient Task Force, 2008. *Gulf Hypoxia Action Plan 2008 for Reducing, Mitigating, and Controlling Hypoxia in the Northern Gulf of Mexico and Improving Water Quality in the Mississippi River Basin.* Washington, DC.

Moar, N. T. and J. M. Wilmshurst. 2003. "A key to the pollen of New Zealand Cyperaceae." New Zealand Journal of Botany 41(2), 325-334, DOI:10.1080/0028825X.2003.9512852.

Panno, S. V., K. C. Hackley, W. R. Kelly, H. Hwang. 2006. "Isotopic Evidence of Nitrate Sources and Denitrification in the Mississippi River, Illinois." Journal of Environmental Quality 35, 495-504.

Pospelova, V., G. L. Chmura, W.S. Boothman, and J.S. Latimer. 2002. "Dinoflagellate cyst records and human disturbance in two neighboring estuaries, New Bedford Harbor and Apponagansett Bay, Massachusetts (USA)." The *Science of the Total Environment* 298 (1-3): 81–102. https://doi.org/10.1016/S0048-9697(02)00195-X

Pospelova, V., and S. J. Kim. 2010. "Dinoflagellate cysts in recent estuarine sediments from aquaculture sites of southern South Korea." *Marine Micropaleontology* 76 (1-2): 37–51. https://doi.org/10.1016/j.marmicro.2010.04.003.

Pospelova, V., K. A. F. Zonneveld, M. Heikkilä, M. Bringue, A. M. Price, S. Esenkulova, K. Matsuoka. 2018. "Seasonal, annual, and inter-annual Spiniferites cyst production: a review of sediment trap studies." Palynology 42(1), 162-181, https://doi.org/10.1080/01916122.2018.1465738

Price, A.M., K.N. Mertens, V. Pospelova, T.F. Pedersen, and R.S. Ganeshram. 2013. "Late Quaternary climatic and oceanographic changes in the Northeast Pacific as recorded by dinoflagellate cysts from Guaymas Basin, Gulf of California (Mexico)." *Paleoceanography* 28 (1): 200–212. https://doi.org/10.1002/palo. 20019

Price, A.M., M.R.S. Coffin, V. Pospelova, J.S. Latimer, and G.L. Chmura. 2017. "Effect of nutrient pollution on dinoflagellate cyst assemblages across estuaries of the NW Atlantic. *Marine Pollution Bulletin* 121 (1-2): 339–351. https://doi.org/10.1016/j.marpolbul. 2017.06.024.

Price, A. M, M. M. Baustian, R. E. Turner, N. N. Rabalais, G. L. Chmura, 2018. "Dinoflagellate Cysts Track Eutrophication in the Northern Gulf of Mexico." *Estuaries and Coasts* 41:1322–1336 https://doi.org/10.1007/s12237-017-0351-x

Rabalais, N. N., E. Turner, D. Scavia, 2002. "Beyond Science into Policy: Gulf of Mexico Hypoxia and the Mississippi River." *BioScience* 52:2, 129-142.

Radi, T., V. Pospelova, A. de Vernal, and J.V. Barrie, 2007. "Dinoflagellate cysts as indicators of water quality and productivity in British Columbia estuarine environments." *Marine Micropaleontology* 62 (4): 269–297. https://doi.org/10.1016/j.marmicro.2006.09.002.

Reichart, G. and H. Brinkhuis. 2003. "Late Quaternary Protoperidinium cysts as indicators of paleoproductivity in the northern Arabian Sea." Marine Micropaleontology 49, 303-315.

Ribeiro, S., T. Berge, N. Lundholm, T. Andersen, F. Abrantes, M. Ellegaard, 2011. "Phytoplankton growth after a century of dormancy illuminates past resilience to catastrophic darkness." *Nature Communications* 2 (311). http://dx.doi.org/10.1038/ ncomms1314.

Scavia, D., I. Bertani, D. R. Obenour, R. E. Turner, D. R. Forrest, A. Katin. 2017. "Ensemble modeling informs hypoxia management in the northern Gulf of Mexico." PNAS 114(33), 8823-8828.

Sigman, D. and K. Karsh. 2009. “Ocean Process Tracers: Nitrogen Isotopes in the Ocean.” In *Encyclopedia of Ocean Science.* Amsterdam: Elsevier.

Stern, R.J., and W. R. Dickinson, 2010. “The Gulf of Mexico is a Jurassic backarc basin.” *Geosphere* 6 (6), 739–754.

Stets, E. G., V. J. Kelly, and C. G. Crawford. 2015. “Regional and temporal differences in nitrate trends discerned from long-term water quality monitoring data.” *Journal of the American Water Resources Association.* 51: 1394– 1407. https://doi-org.proxy.library.uu.nl/10.1111/1752-1688.12321

Steidinger, K.A., 2009. “Historical perspective on Karenia brevis red tide research in the Gulf of Mexico.” *Harmful Algae* 8, 549–561.

Turner, R. E., and N. N. Rabalais. 1991. “Changes in Mississippi River water quality this century and implications for coastal food webs.” *Bioscience* 41: 140– 147. https://doi-org.proxy.library.uu.nl/10.2307/1311453

Turner, R. E., N. N. Rabalais, R. B. Alexander, G. McIsaac, R. W. Howarth, 2007. “Characterization of Nutrient, Organic Carbon, and Sediment Loads and Concentrations from the Mississippi River into the Northern Gulf of Mexico.” *Estuaries and Coasts* 30(5), 773–790.

Turner, R. E. and N. N. Rabalais. 2013. “Nitrogen and phosphorus phytoplankton growth limitation in the northern Gulf of Mexico.” Aquatic Microbial Ecology 68, 159–169.

Van Dolah, F.M., 2000. “Marine algal toxins: origins, health effects, and their increased occurrence.” *Environmental Health Perspectives* 108, 133–141.

Van Soelen, E.E., E.I. Lammertsma, H. Cremer, T.H. Donders, F. Sangiorgi, G.R. Brooks, R.A. Larson, J.S. Sinninghe Damsté, F. Wagner-Cremer, and G.J. Reichart, 2010. “Late Holocene sea-level rise in Tampa Bay: Integrated reconstruction using biomarkers, pollen, organic-walled dinoflagellate cysts, and diatoms.” *Estuarine, Coastal and Shelf Science* 86 (2): 216–224. https://doi.org/10. 1016/j.ecss.2009.11.010.

de Vernal, A., M. Henry, J. Matthiessen, P. Mudie, A. Rochon, K.P. Boessenkool, F. Eynaud, K. Grøsfield, J. Guior, D. Hamel, R. Harland, M.J. Head, M. Kunz-Pirrung, E. Levac, V. Loucheur, O. Peyron, V. Pospelova, T. Radi, J.-L. Turon, and E. Voronina, 2001. “Dinoflagellate cyst assemblages as tracers of sea-surface conditions in the northern North Atlantic, Arctic and sub-Arctic seas: The new ‘n = 677’ data base and its application for quantitative palaeoceanographic reconstruction.” *Journal of Quaternary Science 16* (7): 681–698. https://doi.org/10.1002/jqs.659.

Van Meter, K. J., P. Van Cappellen, N. B. Basu, 2018. “Legacy nitrogen may prevent achievement of water quality goals in the Gulf of Mexico.” *Science* 10.1126.

Verleye, T. J., K. N. Mertens, S. Louwye, H. W. Arz. 2009. “Holocene salinity changes in the southwestern Black Sea: a reconstruction based on dinoflagellate cysts.” Palynology 33(1), 77-10.

Versteegh, G. J. M., K. A. F. Zonneveld, G. J. de Lange. 2010. “Selective aerobic and anaerobic degradation of lipids and palynomorphs in the Eastern Mediterranean since the onset of sapropel S1 deposition.” Marine Geology 278, 177-192.

Versteegh, G.J.M., P. Blokker, K. A. Bogus, I. C. Harding, J. Lewis, S. Oltmanns, A. Rochon, K. A. F. Zonneveld, 2012. “Infra red spectroscopy, flash pyrolysis, thermally assisted hydrolysis and methylation (THM) in the presence of tetramethylammonium hydroxide (TMAH) of cultured and sediment-derived Lingulodinium polyedrum (Dinoflagellata) cyst walls.” *Organic Geochemistry* 43, 92–102.

Wrenn, J.H., 1988. “Differentiating species of the dinoflagellate cyst genus Nematosphaeropsis.” *Palynology* 12 (1): 129–150. https://doi.org/10.1080/01916122.1988.9989340.

Zeebe, R. E. and L. J. Lourens. 2019. “Solar System chaos and the Paleocene–Eocene boundary age constrained by geology and astronomy.” Science 365, 926–929.

Zonneveld, K. A. F., F. Bockelmann, U. Holzwarth. 2007. “Selective preservation of organic-walled dinoflagellate cysts as a tool to quantify past net primary production and bottom water oxygen concentrations.” Marine Geology 237, 109–126.

Zonneveld, K. A. F. and V. Pospelova. 2015. “A determination key for modern dinoflagellate cysts.” Palynology 39(3), 387-409.

Appendix 1

Cruise Report of cruise 64PE467, 2020

Cruise Report 64PE467
GoM2020

28/01/2020 – 22/02/2020
Nassau, Bahamas – Nassau, Bahamas

chief scientist: Francien Peterse

co-chief scientist: Rick Hennekam

Table of contents

1. Introduction

This GoM2020 cruise is a follow up on NICO expedition leg 7 in March/April 2018 (GoMex), during which sediment samples were collected along a land-sea transect from the Atchafalaya River mouth. Due to delays in the harbor, a long transit, and a change of weather once sampling had started, only part of the scientific program could be carried out. The current cruise thus provided a chance to complete and further extend the program based on initial results derived from material collected during the GoMex expedition. Furthermore, the cruise fits within Research Theme 2 'Land-Ocean transfer' of the Netherlands Earth System Science Center (NESSC), which just started its second phase. Several of the scientific participants are involved in this program as a PhD student or supervisor.

The main focus of the cruise is to investigate the fate of terrestrial organic carbon (OC), in this case discharged by the Atchafalaya/Mississippi Rivers, in the marine realm. The Mississippi/Atchafalaya River system is one of the largest on the North-American continent, and discharges on average 436.000 tons of sediment to the Gulf of Mexico per day. Upon burial in marine sediments, the associated organic carbon (OC) may serve as a long-term sink for photosynthetically fixed CO_2 depending on the composition and properties of this OC, which are generally not well characterized. Besides sediment, the Atchafalaya and Mississippi Rivers transport nutrients to the ocean, where they are used by primary producers. Increasing agricultural activity and associated fertilizer use in the drainage basin have led to a severe enrichment in particularly nitrogen and phosphorus of fresh and marine waters. The high input of nutrients triggers (harmful) algal blooms, and results in the seasonal development of an oxygen deficient zone (ODZ) in the Gulf of Mexico, which is now the second largest human-induced ODZ in the world. Despite attempts to reduce impacts, ecosystem functioning does not always recover, due to its 'memory', where its present state depends on its long-term history, which is often unknown. The second focus of this cruise is on the occurrence of harmful algal blooms in relation to ODZ development. In addition, the seasonally anoxic conditions influence biogeochemical cycles of nutrients and essential trace metals, which is the third focus of the cruise. The sediments from the land-sea transects will furthermore be studied for the microbial community composition to further investigate the occurrence and properties of the recently described bacterial clade of Woeseiales that is presumably feeding on terrestrial OC. Finally, the relation between CO_3^{2-} content in the bottom water and that in benthic foraminifera will be studied to investigate the development of a proxy for pCO_2.

2. Team members

2.1 Scientific participants

Table 1. Scientific participants, their expertise, and main task on board.

Name and affiliation	Expertise	Main task
Francien Peterse (chief scientist), Utrecht University	Organic Geochemistry	Sediment slicing, multibeam, piston core
Rick Hennekam (co-chief scientist), Royal NIOZ	Paleoceanography	Multibeam, piston core, SPM collection
Francesca Sangiorgi, Utrecht University	Palynology	Sediment slicing
Yord IJedema, Utrecht University and NESSC PhD	Organic Geochemistry/ Palynology	Did not sail – hospitalized in Nassau
Wesley Plugge, Utrecht University	MSc student Marine Sciences	Sediment slicing
Zeynep Erdem, Royal NIOZ	Paleoceanography	O_2 micro-profiling, resin embedding, multibeam, piston core
Laura Pacho Sampedro, Royal NIOZ and NESSC PhD	Benthic foraminifera	Sediment slicing
Alena di Primio, Royal NIOZ	Microbiology	Sediment slicing
Kristin Ungerhofer, Royal NIOZ	Geochemistry	Pore water sampling, incubations
Torbjörn Törnqvist, Tulane University	Quaternary Geology	Sediment slicing

2.2 Crew

Table 2. Crew members.

Name	Task
Bert Puijman	Master
Len Bliemer	Chief Officer
Kelly Kat	Second Officer
Bert Hogewerf	Chief Engineer
Freddy Hiemstra	Second Engineer
Sven Wolffers	ETO
Cor Stevens	Bosun
Jacco Heneweer	AB1
Peter van Maurik	AB2
Martin de Vries	AB3
Barry Boersen	Marine technician
Hendrikjan Lokhorst	Cool
Vitali Maksimovs	Steward

Figure 1. All participants of the GoM2020 expedition. From left to right, top middle: Len Biemer, Jacco Heneweer, Sven Wolffers. From left to right, standing: Francien Peterse, Bert Puijman, Cor Stevens, Wesley Plugge, Laura Pacho Sampedro, Alena di Primio, Peter van Maurik, Barry Boersma, Torbjörn Törnqvist, Hendrikjan Lokhorst, Kelly Kat. From left to right, sitting: Kristin Ungerhofer, Rick Hennekam, Francesca Sangiorgi, Bert Hogewerf, Vitali Maksimovs, Zeynep Erdem, Freddy Hiemstra, Martin de Vries.

3. Scientific program

3.1 Transit Nassau – Gulf of Mexico

Scientists boarded RV Pelagia on Tuesday 28 or Wednesday 29 January. Departure was extended due to a last minute change of the cook and subsequent awaiting of the arrival of the new cook on Thursday 30 January. In the mean time, one of the scientific participants, Yord IJedema, was sent to the hospital to check on an infection on his hand. The infection turned out to be serious and Yord was admitted to the hospital immediately. It was clear that he could not join the cruise, and instead would need a 5-day antibiotics treatment before returning to the Netherlands. Departure was on Friday 31 January at 11.00. During our transit to the first sampling station test the CTD; on Wednesday 5 February the CTD was deployed at 500m water depth, and later at 300m.

3.2 Mississippi/Atchafalaya River plume sampling

Thursday February 6

- Station 1 – 20f (20m water depth)

This station is located furthest west in the Mississippi/Atchafalaya River plume. The CTD was deployed at 8.00 to obtain a water column profile. The low salinity (30.9) confirms a fresh water influence at this site. Two bottles were closed at 20m depth for water sampling (microbiology/Alena) and the calibration of the O_2 sensors for microprofiling. After that, the multicorer (MC) was deployed. The first trial with 4 weights did not yield enough sediment. The second trial with 8 weights still yielded too little material (less than 20 cm). For the third trial, the full set of 20 weights was used, after which we recovered about 20cm material. Finally, the MC was sent down for a fourth time with full weights and only 8 core liners. The recovery was slightly better, although only liners at one side contained sediment. The sediment is very sandy. The distribution of the cores at each station is given in Table 6.

- Station 2 – 20e (20m water depth)

We arrived to our second station of the day around 13:00. First, the CTD was deployed. The salinity was higher (32.3) compared to the first station, but still showing a fresh water surface layer. No water was collected at this site. The MC was deployed 3 times in total. For the first deployment, the full set of full weights with 8 liners was used, but the recovery was less than 20 cm. We disposed the sediment, but kept one liner for the collection of a surface sediment sample. The recovery of the second deployment was similar to the first. For the third deployment only 6 liners were used. The sediments consisted of a thin sandy layer with stiff and sticky grey silty mud below.

- Station 3 – 20d (20m water depth)

We arrived to the station around 17:15. The CTD was deployed to confirm the fresh water influence of the river plume (surface water salinity = 30.8). One bottle was closed at 20m to collect water for microbiology slurries (Alena). The MC was deployed at 17:30. During the first deployment with full weights and 8 liners only one side recovered sediment (4 liners). The second deployment with again 8 liners brought

back ~25cm of sediments in 7 of the liners, whereas one was empty. The sediments are sandy on top, but finer downcore.

Figure 2. Waiting for the MC to surface.

Friday February 7

- Station 4 – 20c (20m water depth)

The day started with a CTD cast at 08:00, showing a salinity of 26.9. Bottles were closed for SPM sampling at 20m, 12m, and 5m (porewater/Kristin). The MC was deployed twice with full weight and 8 liners. Both deployments brought back about 30cm of sediments, although one liner was empty during the first, and 2 liners were empty during the second deployment. The sediments consist of sticky, grey clays.

- Station 5 – 20b (20m water depth)

The CTD was deployed around 13:15. Even though we were supposedly closer to the mouth of the Atchafalaya River, the salinity was 30.7. No water was collected here. The MC was deployed twice with full weights and 8 liners each time. Sediment consists of heavy, sticky grey clays.

3.3 Atchafalaya River land-sea transect sampling

Saturday February 8

- Station 6 – A15 (17m water depth)

This is the most eastern station of the Atchafalaya River plume, and the most landward station of the Atchafalaya land-sea transect. However, due to the very shallow slope, the mouth (and thus land) is still >50km away from our sampling location. We started the day with the deployment of the CTD at 08:00. The salinity was 29.3. Bottles were closed at 17m (4x), 13m (1x), 5m (1x) for SPM collection and incubation setup

(porewater/Kristin), and microbiology slurries (Alena). The MC was deployed 4 times in total. The first two deployments were with full weights and 8 liners. The last 2 times only had 4 liners to collect sediments for incubations (Kristin). The sediment cores are about 30cm and comprise of consolidated grey mud.

- Station 7 – A600 (622m water depth)

The coordinates of the planned station were on a pipeline and at a water depth of 900m. We performed a multibeam survey to select a more suitable place for sampling around a water depth of 600m. The CTD was deployed at 18:30 and indicated that the salinity of the surface water was 36.2. One bottles was closed at 618m to collect water for microbiology slurries (Alena). The MC was deployed once with 16 weights and 12 liners. The MC recovered about 45cm sediment, but one side was better than the other. The top ~10 cm was brown in color and rich in foraminifera. The sediment becomes grey below that.

Sunday February 9

- Station 8 - A3200 (3124m water depth)

A multibeam survey was performed to determine a sampling location. The station is located in the basin of the Gulf, (hopefully) out of reach from the slope and slope-associated sediment transport and reworking processes. The CTD was deployed at 12:00. Surface salinity was 36.3. Two bottles were closed at the bottom for microbiology slurries (Alena).
After that, the MC was deployed around 14.00 with 12 liners and 16 weights. One liner was lost during the recovery. The liners contained ~30cm sediments and at least 10-15cm overlying water. In the mean time, the piston core (PC) was prepared with a 12m liner and deployed at 16.55. The PC was back on deck at 19:20 with a recovery of 9.32m. No trigger core was sampled, but the core catcher material was collected and stored with the core material.

Monday February 10

- Station 9 – Pigmy Basin (2260m water depth)

We started the morning with a multibeam survey to determine the shape and location of the Pigmy Basin, and our sampling location. We decided to sample close to previous core locations; south of DSDP Site 619 and east of MD02-2553.
The CTD was deployed at 9.30, and two bottles were closed at the bottom (not used). Subsequently, the MC was deployed with 12 weights and 12 liners around 11:20. The recovery was very nice, with ~45cm of muddy sediments and about 15cm overlying water. We then deployed the PC with an 18m liner. The PC was back on deck at 15:25 and had a final length of 13.47m. We did not keep the trip core, but the core catcher material was stored with the core sections at 4°C. We spent the whole evening after dinner labeling for porewater samples.

Tuesday February 11

- Station 10 – A300 (275m water depth)

The original coordinates appeared to be a location at 200m water depth, so we transited towards a depth of 300m. We left the multibeam pinging and collecting data during transit, but this data has not been registered as a cast in Casino. The CTD was

deployed at 8:45 and in total 5 bottles were closed at 270m (2x), 180m (1x), 70m (1x), and 10m (1x) for SPM collection (porewater/Kristin). The salinity of the sea surface water was 36.2. The MC was deployed at 09:15 with 12 weights and 12 core liners and yielded good recovery; all liners were filled with ~45cm muddy sediments.

- Station 11 – A100 (100m water depth)

On our transit to this station a multibeam survey was performed to determine the final sample location, as the initial coordinates were located on one of the many oil pipelines in the area. The final location is ~1nM towards the SE. The CTD was deployed at 13.00 (salinity 36.3) and bottles were closed at 104m (2x), 75m (1x) and 10m (1x) for SPM analysis (Kristin). The MC was deployed at 13.30 with 12 weights and 12 liners, which resulted in good recovery (~40cm sediment). The MC was deployed a second time with only 4 liners to collect sediment for foraminifera sampling (Frans Jorissen). Subsequently, a PC was prepared with a 6m liner at 15.00, which yielded 3.65cm of sediments (Fig. 3).

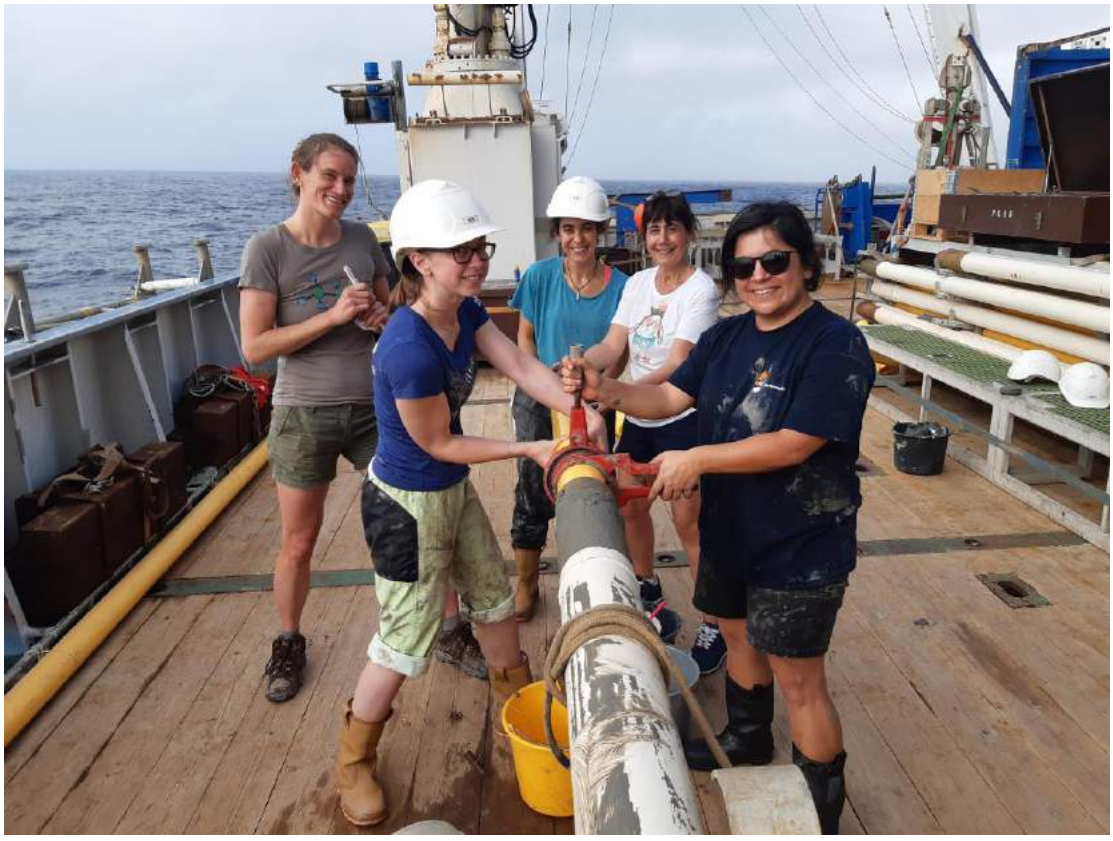

Figure 3. Processing of the piston core at station 11.

Wednesday February 12

- Station 12 – A30 (30m water depth)

The CTD was deployed at 8.00. The salinity of the surface water was 30.0, indicating a fresh water influence at this site. Bottles were closed at 28m (2x), 16m (1x), and 6m (1x) for SPM collection (Kristin). However, filtration of the water had to be stopped early due to the arrival at the second station of this day. The MC was deployed at 8.25 with 16 weights and 12 liners. It recovered ~30cm sediment, but one liner emptied on the way up.

- Station 13 – A50 (48m water depth)

We reached the station at 10.40, after which the CTD was deployed. Surface water salinity was 31.9. Water was collected at 46m (2x), 14m (1x), and 5.5m (1x) for SPM filtration (Kristin). The MC was deployed at 11.00 with 16 weights and 12 liners. All came back with ~40cm sediment.

- Station 14 – 80b (80m water depth)

This station was added to the original program, and was specifically picked to collect a piston core from the shallow shelf area that is influenced by seasonal hypoxia. Once in the area a multibeam survey was performed to select the final location. At 16.15 the CTD was deployed, indicating a surface water salinity of 36.0. The MC was subsequently deployed at 16.30 with 16 weights and 12 liners. All liners were filled with ~45cm sediment. Preparation of a PC deployment with a 12m liner started at 17.00. The PC was back on deck at 17.50, after which we started our transit to the Mississippi River mouth to sample the land-sea transect there (scheduled 19 hours). The piston core was cut after dinner and yielded 9.64m sediments. The cut between sections #2 and #3 showed red mottles (Fig. 4), potentially indicating input from the Red River, a tributary of the Atchafalaya River (pers. comm. Torbjörn). With the recovery of this piston core the sampling of the Atchafalaya River land-sea transect was completed.

Figure 4. Red mottles between sections #2 and #3 of the piston core at station 14 (80b)

3.4 Mississippi River land-sea transect sampling

Thursday February 13

- Station 15 – M15 (15m water depth)

We arrived at the first station of the Mississippi River transect at 13.40. Deployment of the CTD indicated that the surface water salinity was 32, which was higher than we expected for a location so close to the river mouth. The seawater was relatively clear, whereas we could see murkier waters a bit further towards the river. Hence, we decided to move further into the river plume. We followed surface water salinity with the aquaflow during the short transit (not recorded). Although salinity reached ~24 during transiting, the CTD at the final location (Station 15b, deployment at 14.20) indicated a surface water salinity of 31.5. Water was collected for SPM filtering (porewater/Kristin) at 14.5m (2x), 10m (1x), and 5m (1x). The MC was deployed at 14.45 with 16 weights and 12 liners. There was good recovery with nicely visible brown and black layers of mud and sand (Fig. 5). The MC was deployed a second time at 15.15 to collect sediments for incubations (Kristin), but liners were too full. The third deployment was successful. Three of the cores were sampled for Frans Jorissen.

Figure 5. Sediment layers at station 15 (M15).

- Station 16 – M300 (300m water depth)

The CTD was deployed at 18.45 and showed a surface salinity of 24.1. Bottles were closed at 300m (2x), 130m (1x), 60m (1x), and 7m (1x) for SPM collection (Kristin). The MC was next on the program, and went down with 16 weights and 12 liners. The liners came on deck with ~35cm sediment containing many forams.

Friday February 14

- Station 17 – M600 (600m water depth)

This station is located on the slope and was reached early in the morning. The CTD was deployed at 8.00. Surface water salinity was 34.1. One bottle was closed at 607m water depth for microbiology surries (Alena). The MC was deployed at 9.00 with 16 weights and 12 liners. It came back on deck with ~45cm muddy sediments.

- Station 18 – M200 (200m water depth)

The station is located near transition of the shelf to the slope, so we performed a short multibeam survey to check the sea floor at the sampling site. The sea floor appeared regular, so the sampling location was approved. The CTD was deployed at 13.05, indicating a sea surface salinity of 31.3. Water was collected at 186m (2x), 90m (1x), 50m (1x), and 9m (1x) for SPM (Kristin). After that, the MC was deployed with 16 weights and 12 liners. The recovery was (too) good, with only 10cm overlying water. We let some sediment escape at the bottom of the tube while taking them from the MC.

Saturday February 15

- Station 19 – M100 (100m water depth)

We started with a multibeam survey to make sure that the station was located on the shelf, and not the shelf break or on the slope, as we planned to take a piston core here. At 8.00 the CTD could be deployed. Sea surface salinity was 25.8 and water was collected for SPM (Kristin) at 95m (2x), 50m (1x), 20m (1x) and 6m (1x). The MC was then deployed at 8.20, with 16 weights and 12 liners, and came back with 5-10cm water overlying muddy sediments. The piston core was prepared with a 12m liner, which recovered 9.83m sediments upon deployment. Processing was done at 10.40.

- Station 20 – M50 (50m water depth)

The CTD was deployed at 13.30, and recorded sea surface salinity of 21.2. Water bottles were closed at 42m, 15m, and 7m for SPM (Kristin). We decreased the weights of the MC before deployment, as the liners came back very full at the previous station. It went down with 12 weights and 12 liners, which yielded 35-40cm of clayey sediments.

Sunday February 16

- Station 21 – Hypoxia Monitoring Site (20m water depth)

*D*ue to our smooth cruise so far we had time left to plan an additional sample site. We chose a location close to a buoy with equipment monitoring the oxygen conditions on the shelf, described in the literature and at www.gulfhypoxia.net. The CTD was deployed at 8.00 showing that sea surface salinity was 26.6. The MC was deployed at 8.20 with 12 weights and 12 liners, but came back with only 10cm of sediments. Weights were increased to the maximum of 20 for the second deployment, which still yielded only 20-25cm of sediment. We kept 5 cores from this cast. A third deployment with 20 weights and 8 liners gave better results, although 2 liners were lost on the sea floor. We kept the 6 remaining cores.

3.5 Transit Gulf of Mexico – Nassau

The transit back to Nassau started after retrieving the liners from the last MC deployment at Station 21. During transit, we repacked the frozen cores from the liners into aluminum bags. Sediment incubations set up at station 15 (M15) were still ongoing, but terminated and sampled in the morning of Thursday 20 February. Arrival back in Nassau was on Thursday in the afternoon.

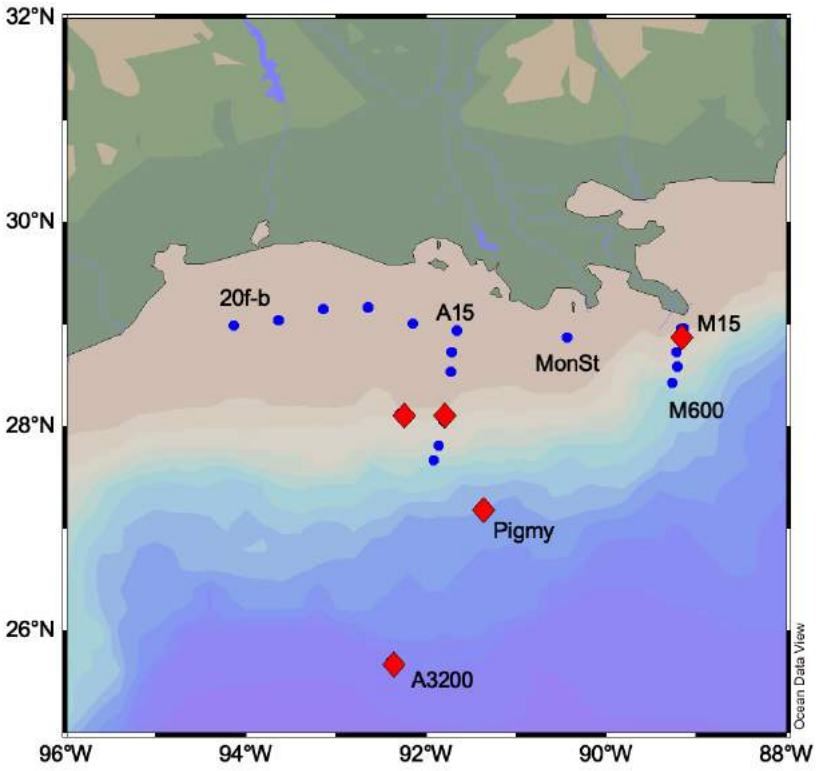

Figure 6. Map indicating the sample locations of 64PE467. Red diamonds indicate stations where a piston core was collected.

3.6 Casino events for 64PE467

Table 3. Casino events for 64PE467.

Date	Time (UTC)	Lattitude	Longitude	Phase name	Device name	Action code	Cast	Echo sounder depth (m)
31/01/2020	16:15:40	25.079152	-77.334351	TRANSIT1				7.6
06/02/2020	12:56:06	28.98346	-94.134995	STATION1				18.7
06/02/2020	13:08:11	28.98363	-94.13512		CTD with samples	Begin	1_1	18.6
06/02/2020	13:11:22	28.98359	-94.135018		CTD with samples	Bottom	1_1	18.5
06/02/2020	13:14:41	28.983613	-94.135073		CTD with samples	End	1_1	18.8
06/02/2020	13:25:58	28.983611	-94.135097		Multi Corer	Bottom	1_2	19.2
06/02/2020	13:34:26	28.983602	-94.135059		Multi Corer	Bottom	1_3	18.7
06/02/2020	13:42:26	28.983692	-94.134641		Multi Corer	Bottom	1_4	19.0
06/02/2020	14:05:34	28.983704	-94.134496		Multi Corer	Bottom	1_5	18.9
06/02/2020	14:09:48	28.983691	-94.134515	TRANSIT2				19.1

06/02/2020	17:27:33	29.032553	-93.641746	STATION2				22.9
06/02/2020	18:09:27	29.034794	-93.640397		CTD	Begin	2_1	22.5
06/02/2020	18:12:09	29.034809	-93.640329		CTD	Bottom	2_1	22.3
06/02/2020	18:14:00	29.034795	-93.640142		CTD	End	2_1	22.8
06/02/2020	18:50:49	29.035022	-93.64063		Multi Corer	Bottom	2_1	22.3
06/02/2020	19:01:27	29.03557	-93.640723		Multi Corer	Bottom	2_2	22.8
06/02/2020	19:15:47	29.035601	-93.640238		Multi Corer	Bottom	2_3	23.3
06/02/2020	19:23:19	29.03676	-93.638708	TRANSIT3				22.7
06/02/2020	22:18:34	29.144951	-93.138873	STATION3				20.4
06/02/2020	22:22:42	29.144944	-93.13921		CTD with samples	Begin	3_1	20.4
06/02/2020	22:23:38	29.144938	-93.139104		CTD with samples	Bottom	3_1	19.8
06/02/2020	22:27:19	29.144912	-93.139168		CTD with samples	End	3_1	20.3
06/02/2020	22:37:26	29.144899	-93.13908		Multi Corer	Bottom	3_2	20.5
06/02/2020	22:47:14	29.144822	-93.138958		Multi Corer	Bottom	3_3	20.5
06/02/2020	23:30:35	29.146059	-93.136228	TRANSIT4				20.3
07/02/2020	12:55:01	29.162113	-92.643925	STATION4				21.2
07/02/2020	13:02:43	29.162058	-92.644007		CTD with samples	Begin	4_1	20.9
07/02/2020	13:05:19	29.162067	-92.644006		CTD with samples	Bottom	4_1	21.2
07/02/2020	13:14:21	29.162131	-92.643991		CTD with samples	End	4_1	21.4
07/02/2020	13:24:46	29.162043	-92.644045		Multi Corer	Bottom	4_2	21.0
07/02/2020	13:50:46	29.162088	-92.644082		Multi Corer	Bottom	4_3	21.2
07/02/2020	13:54:57	29.162087	-92.644118	TRANSIT5				21.0
07/02/2020	17:49:35	29.002203	-92.147546	STATION5				23.1
07/02/2020	18:18:06	29.001708	-92.147314		CTD	Begin	5_1	22.8
07/02/2020	18:20:28	29.001652	-92.147349		CTD	Bottom	5_1	23.2
07/02/2020	18:22:45	29.001656	-92.147377		CTD	End	5_1	23.1
07/02/2020	18:32:33	29.001634	-92.147335		Multi Corer	Bottom	5_2	22.7
07/02/2020	18:56:29	29.001662	-92.147357		Multi Corer	Bottom	5_3	23.4
07/02/2020	19:04:01	29.001214	-92.147138	TRANSIT6				22.9
08/02/2020	12:56:59	28.939483	-91.659258	STATION6				18.1
08/02/2020	13:00:03	28.93955	-91.659235		CTD with samples	Begin	6_1	17.9
08/02/2020	13:02:25	28.939512	-91.659154		CTD with samples	Bottom	6_1	18.1
08/02/2020	13:09:53	28.939361	-91.659187		CTD with samples	End	6_1	18.9
08/02/2020	13:28:01	28.939414	-91.659292		Multi Corer	Bottom	6_2	18.0
08/02/2020	13:53:59	28.939398	-91.659284		Multi Corer	Bottom	6_3	17.9
08/02/2020	14:16:53	28.939517	-91.659167		Multi Corer	Bottom	6_4	18.0
08/02/2020	14:37:18	28.939564	-91.659218		Multi Corer	Bottom	6_5	18.4
08/02/2020	14:43:18	28.93819	-91.659296	TRANSIT7				18.4
08/02/2020	23:29:09	27.664868	-91.920246	STATION7				622.4

08/02/2020	23:36:08	27.664813	-91.920286		CTD with samples	Begin	7_1	623.0
08/02/2020	23:49:35	27.66483	-91.920265		CTD with samples	Bottom	7_1	622.2
09/02/2020	00:07:57	27.664781	-91.920484		CTD with samples	End	7_1	623.5
09/02/2020	00:25:29	27.664838	-91.920472		Multi Corer	Bottom	7_2	618.1
09/02/2020	01:01:29	27.664733	-91.920409	TRANSIT8				619.1
09/02/2020	15:22:44	25.743483	-92.362486	STATION8				3078.4
09/02/2020	15:23:06	25.742868	-92.362631		Multibeam	Begin	8_1	3086.8
09/02/2020	16:00:27	25.684753	-92.379813		Multibeam	Course Change	8_1	3121.1
09/02/2020	16:18:31	25.68905	-92.414307		Multibeam	End	8_1	3140.9
09/02/2020	16:54:04	25.699483	-92.382733		CTD with samples	Begin	8_2	3108.9
09/02/2020	17:49:49	25.699373	-92.382843		CTD with samples	Bottom	8_2	3109.6
09/02/2020	18:46:28	25.699463	-92.383019		CTD with samples	End	8_2	3110.4
09/02/2020	19:51:57	25.699542	-92.382708		Multi Corer	Bottom	8_3	3114.2
09/02/2020	22:51:04	25.699583	-92.382719		Pistoncorer	Bottom	8_4	3119.5
10/02/2020	00:28:05	25.699978	-92.382675	TRANSIT9				3108.9
10/02/2020	12:24:57	27.153381	-91.43323	STATION9				2105.8
10/02/2020	12:25:12	27.153734	-91.433002		Multibeam	Begin	9_1	2093.6
10/02/2020	13:52:18	27.258588	-91.368186		Multibeam	End	9_1	1682.0
10/02/2020	14:36:37	27.187274	-91.409876		CTD with samples	Begin	9_2	2259.0
10/02/2020	15:24:00	27.187227	-91.409709		CTD with samples	Bottom	9_2	2259.8
10/02/2020	16:09:04	27.187442	-91.409497		CTD with samples	End	9_2	2259.4
10/02/2020	17:11:48	27.187243	-91.409436		Multi Corer	Bottom	9_3	2260.5
10/02/2020	19:37:51	27.187356	-91.409364		Pistoncorer	Bottom	9_4	2259.8
10/02/2020	21:57:15	27.173385	-91.402324	TRANSIT10				2150.0
11/02/2020	13:43:46	27.812155	-91.86238	STATION10				272.4
11/02/2020	13:45:44	27.811997	-91.86258		CTD with samples	Begin	10_1	273.1
11/02/2020	13:52:11	27.812095	-91.862506		CTD with samples	Bottom	10_1	272.4
11/02/2020	14:07:32	27.812056	-91.862555		CTD with samples	End	10_1	272.2
11/02/2020	14:19:40	27.811738	-91.862451		Multi Corer	Bottom	10_2	272.9
11/02/2020	14:47:45	27.811856	-91.86239	TRANSIT11				272.9
11/02/2020	16:16:48	27.987077	-91.844027	STATION11				130.7
11/02/2020	16:17:27	27.988377	-91.843855		Multibeam	Begin	11_1	130.5
11/02/2020	17:02:54	28.062022	-91.805775		Multibeam	Course Change	11_1	103.9
11/02/2020	17:27:21	28.036456	-91.817278		Multibeam	Course Change	11_1	111.4
11/02/2020	17:56:54	28.067437	-91.806139		Multibeam	End	11_1	102.2
11/02/2020	18:16:58	28.051985	-91.812419		CTD	Begin	11_2	106.9
11/02/2020	18:20:33	28.051979	-91.812245		CTD	Bottom	11_2	106.5
11/02/2020	18:30:04	28.05171	-91.811923		CTD	End	11_2	109.0
11/02/2020	18:39:51	28.051783	-91.812187		Multi Corer	Bottom	11_3	106.9

11/02/2020	19:12:58	28.051899	-91.812076		Multi Corer	Bottom	11_4	106.7
11/02/2020	20:35:27	28.052017	-91.812017		Pistoncorer	Bottom	11_5	107.5
12/02/2020	13:00:38	28.729517	-91.715239	STATION12				30.4
12/02/2020	13:06:20	28.729657	-91.715287		CTD with samples	Begin	12_1	30.1
12/02/2020	13:10:34	28.729673	-91.715262		CTD with samples	Bottom	12_1	30.2
12/02/2020	13:19:46	28.729679	-91.71514		CTD with samples	End	12_1	30.2
12/02/2020	13:28:10	28.729809	-91.715108		Multi Corer	Bottom	12_2	30.3
12/02/2020	13:46:54	28.729851	-91.715108	TRANSIT12				30.0
12/02/2020	15:31:10	28.529605	-91.731011	STATION13				49.1
12/02/2020	15:40:24	28.529482	-91.73083		CTD with samples	Begin	13_1	48.3
12/02/2020	15:45:08	28.529488	-91.730806		CTD with samples	Bottom	13_1	48.3
12/02/2020	15:53:57	28.52933	-91.730662		CTD with samples	End	13_1	48.5
12/02/2020	16:03:50	28.529283	-91.730765		Multi Corer	Bottom	13_2	48.7
12/02/2020	16:22:51	28.529638	-91.730973	TRANSIT13				48.3
12/02/2020	20:59:24	28.129277	-92.272754	STATION14				85.1
12/02/2020	20:59:38	28.129081	-92.27334		Multibeam	Begin	14_1	85.5
12/02/2020	21:11:05	28.121991	-92.29496		Multibeam	End	14_1	87.9
12/02/2020	21:20:10	28.120308	-92.294757		CTD with samples	Begin	14_2	88.6
12/02/2020	21:22:50	28.120388	-92.294802		CTD with samples	Bottom	14_2	87.9
12/02/2020	21:28:56	28.120245	-92.294815		CTD with samples	End	14_2	88.1
12/02/2020	21:39:07	28.120202	-92.294697		Multi Corer	Bottom	14_3	87.9
12/02/2020	22:27:05	28.120224	-92.294809		Pistoncorer	Bottom	14_4	88.3
12/02/2020	22:53:56	28.121767	-92.293574	TRANSIT14				87.5
13/02/2020	18:32:29	28.957267	-89.17411	STATION15				18.3
13/02/2020	18:43:00	28.957445	-89.174067		CTD	Begin	15_1	18.0
13/02/2020	18:44:43	28.957465	-89.174055		CTD	Bottom	15_1	17.9
13/02/2020	18:46:39	28.957433	-89.173991		CTD	End	15_1	17.5
13/02/2020	18:55:09	28.959033	-89.170889	TRANSIT15				15.6
13/02/2020	19:19:59	28.960855	-89.142511	STATION15B				16.2
13/02/2020	19:26:14	28.960791	-89.142773		CTD	Begin	15B_1	16.5
13/02/2020	19:28:28	28.960765	-89.142858		CTD	Bottom	15B_1	16.7
13/02/2020	19:34:43	28.960778	-89.143043		CTD	End	15B_1	17.1
13/02/2020	19:43:11	28.960635	-89.143184		Multi Corer	Bottom	15B_2	17.8
13/02/2020	20:19:19	28.960601	-89.143445		Multi Corer	Bottom	15B_3	17.1
13/02/2020	20:27:20	28.960447	-89.14358		Multi Corer	Bottom	15B_4	17.4
13/02/2020	20:31:56	28.960562	-89.143489	TRANSIT16				17.4
13/02/2020	23:28:49	28.585667	-89.2132	STATION16				303.7
13/02/2020	23:52:15	28.58571	-89.213129		CTD with samples	Begin	16_1	303.7
13/02/2020	23:58:03	28.585634	-89.213185		CTD with samples	Bottom	16_1	303.7

14/02/2020	00:14:42	28.58558	-89.213215		CTD with samples	End	16_1	304.5
14/02/2020	00:26:24	28.585626	-89.213143		Multi Corer	Bottom	16_2	303.4
14/02/2020	00:37:24	28.585665	-89.212913	TRANSIT17				303.5
14/02/2020	12:59:13	28.421622	-89.267285	STATION17				611.1
14/02/2020	13:06:04	28.421927	-89.267345		CTD with samples	Begin	17_1	620.9
14/02/2020	13:18:39	28.422033	-89.26743		CTD with samples	Bottom	17_1	619.3
14/02/2020	13:32:27	28.422211	-89.267591		CTD with samples	End	17_1	617.0
14/02/2020	13:54:29	28.422159	-89.267463		Multi Corer	Bottom	17_2	619.5
14/02/2020	15:53:09	28.569583	-89.247525	TRANSIT18				291.1
14/02/2020	18:13:57	28.723668	-89.21557	STATION18				194.8
14/02/2020	18:24:40	28.723537	-89.216395		CTD	Begin	18_1	193.4
14/02/2020	18:24:56	28.723558	-89.216354		CTD	Bottom	18_1	193.2
14/02/2020	18:36:50	28.723301	-89.216233		CTD	End	18_1	193.6
14/02/2020	18:49:00	28.723044	-89.216328		Multi Corer	Bottom	18_2	193.6
14/02/2020	19:18:15	28.72142	-89.216139	TRANSIT19				194.8
15/02/2020	10:12:54	28.86559	-89.189873	STATION19				102.5
15/02/2020	10:13:12	28.866065	-89.18966		Multibeam	Begin	19_1	101.3
15/02/2020	12:45:51	28.876079	-89.188395		Multibeam	End	19_1	94.7
15/02/2020	12:59:52	28.872928	-89.183531		CTD with samples	Begin	19_2	97.6
15/02/2020	13:05:11	28.873	-89.183691		CTD with samples	Bottom	19_2	97.8
15/02/2020	13:18:32	28.872914	-89.183816		CTD with samples	End	19_2	97.9
15/02/2020	13:26:40	28.872768	-89.183739		Multi Corer	Bottom	19_3	97.6
15/02/2020	14:21:33	28.873081	-89.183621		Pistoncorer	Bottom	19_4	97.2
15/02/2020	15:40:33	28.87319	-89.183424	TRANSIT20				97.3
15/02/2020	17:26:58	28.931818	-89.173344	STATION20				45.2
15/02/2020	18:28:03	28.931506	-89.173122		CTD	Begin	20_1	45.4
15/02/2020	18:29:29	28.931492	-89.173106		CTD	Bottom	20_1	45.6
15/02/2020	18:38:07	28.931446	-89.173059		CTD	End	20_1	45.4
15/02/2020	18:47:14	28.931506	-89.173065		Multi Corer	Bottom	20_2	45.6
15/02/2020	19:15:13	28.931617	-89.173047	TRANSIT21				45.6
16/02/2020	12:56:41	28.868236	-90.433298	STATION21				20.9
16/02/2020	13:04:23	28.86802	-90.433321		CTD with samples	Begin	21_1	20.6
16/02/2020	13:07:14	28.867966	-90.43335		CTD with samples	Bottom	21_1	21.2
16/02/2020	13:10:29	28.867973	-90.433374		CTD with samples	End	21_1	20.8
16/02/2020	13:22:21	28.867867	-90.433279		Multi Corer	Bottom	21_2	20.8
16/02/2020	13:31:40	28.867837	-90.433246		Multi Corer	Bottom	21_3	21.3
16/02/2020	13:51:13	28.867869	-90.432729		Multi Corer	Bottom	21_4	21.0
16/02/2020	13:54:47	28.867849	-90.432709	TURNING1				20.5
20/02/2020	19:03:49	25.079146	-77.334335	CALL1				7.2

4. Methods and scientific approach

4.1 Multibeam echosounder (Zeynep Erdem)

At each piston core station, the seafloor was mapped using a Kongsberg EM 302 multibeam echosounder that is installed on R/V Pelagia. The system has a 30 kHz echo sounder with a one degree opening angle for the transmitter and a two degree angle for the receiver. Depending on available time, the sea floor at the intended sampling location was mapped by sailing 1-3 transects at 4 -5 knots with multibeam logging. The flattest surface without features was then selected as the coring location. Similarly, multibeam logging was used to determine the exact location of the Pigmy Basin (Station 9; Fig. 7).

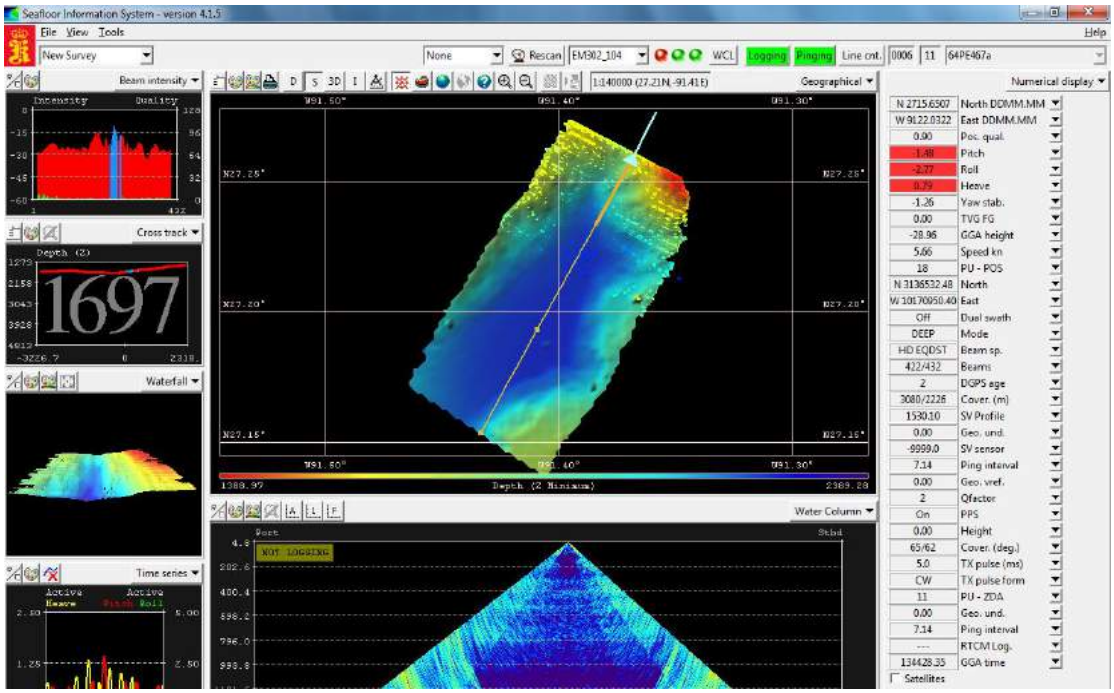

Figure 7. Example of multibeam surveying (screen shot of results at Pigmy Basin, Station 9). Multibeam data will be post-processed prior to final release after the cruise.

4.2 Water column (CTD)

4.2.1 Physical properties and sampling

The CTD (conductivity-temperature-depth)/rosette is equipped with sensors that measure physical parameters provide information on water depth and the conductivity, temperature, salinity, density, fluorescence (a measure for Chl a concentration), beam transmission and turbidity (a measure for suspended particle density) and dissolved O_2. These sensor data are provided real-time as the CTD/rosette unit is lowered through the water column. Based on the “down-cast” (surface-to-deep) data and specific sample requirements, bottles were closed at selected depths during the ensuing “up-cast” (deep-to-surface). To minimize disturbance of the water column structure, the CTD/rosette was held at its greatest

depth (about 2-5 m above the seafloor to avoid disturbance and resuspension) for at least one minute. The CTD/rosette was held for 1 minute at each sampling depth before the appropriate bottle(s) was/were closed.

The salinity data given by the CTD clearly show the presence of a fresh water layer indicating the influence of the Atchafalaya and Mississippi Rivers at the sampling stations (Fig. 8).

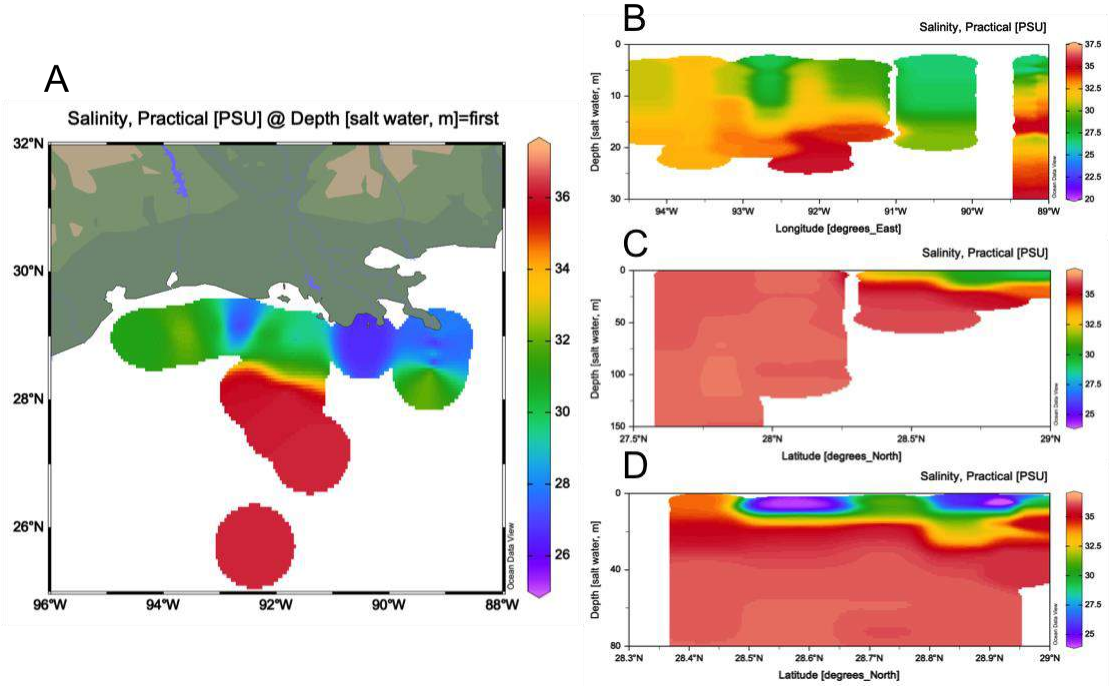

Figure 8. CTD salinity data for A) surface waters, and depth profiles for B) the river plume transect C) the Atchafalaya River transect, and D) the Mississippi River transect.

4.2.2 Seawater sampling and filtration of suspended particulate matter (SPM) (Kristin Ungerhofer)

Seawater for the preparation of microbiology slurries or SPM filtration was collected with the CTD from 3 to 4 depths at selected stations (Table 4). The water for nutrient and trace metal analysis was collected from the CTD with N_2 overpressure and samples according to Table 5.

For the recovery of SPM from the water column, seawater collected with the CTD was filtered over 0.2 µm polyethersulfone (PES) filter membranes (47 mm) in Advantec PE filter holders. The filter holders were connected to the corresponding CTD bottles and N_2 overpressure (~ 0.2 bar) was applied to push the seawater through the filter membranes into jerry cans. A 5 L beaker was used to measure the amount of water passing each filter.

Table 4. Stations with water sample collection

	Microbiology	SPM/Nutrients/ Incubations
St. 1 (20f)	20m	
St. 3 (20d)	20m	
St. 4 (20c)		20m, 12m, 5m
St. 6 (A15)	17m	17m, 13m, 5m
St. 7 (A600)	618m	
St. 8 (A3200)	3124m	
St. 10 (A300)		270m, 180m, 70m, 10m
St. 11 (A100)		104m, 75m, 10m
St. 12 (A30)		28m, 16m, 6m
St. 13 (A50)		46m, 14m, 5.5m
St. 15 (M15)		14.5m, 10m, 5m
St. 16 (M300)		300m, 130m, 60m, 7m
St. 17 (M600)	607m	
St. 18 (M200)		186m, 90m, 50m, 9m
St. 19 (M100)		95m, 50m, 20m, 6m
St. 20 (M50)		42m, 15m, 7m

Table 5. CTD sampling scheme for nutrient and trace metal composition

Nr.	Analyte	Vol. [mL]	Vial	Treatment	Code	Storage
1	NH4, NO3, NO2	5 mL	Pony vial	None	NH4	- 20 °C
2	PO4, Si, metals	5 mL	Pony vial	Acidified 10 µL 5N HCl per mL	PO4, ICP	4 °C

Filtration was stopped when either the CTD bottle was empty or the time schedule required termination of filtration. To avoid the contact with O_2, the tubing at the top and the bottom of each filter holder was connected to form a loop immediately after disconnection. The filter holders were then transferred into an anoxic glove bag. Inside the glove bag, filters were carefully removed from the holders and placed into tightly sealing Whatman petri dishes. Before packing them in N_2-purged Al-laminate bags, each filter was photographed. The packed samples were stored at -80°C for transport. Figure 9 shows an overview of collected SPM.

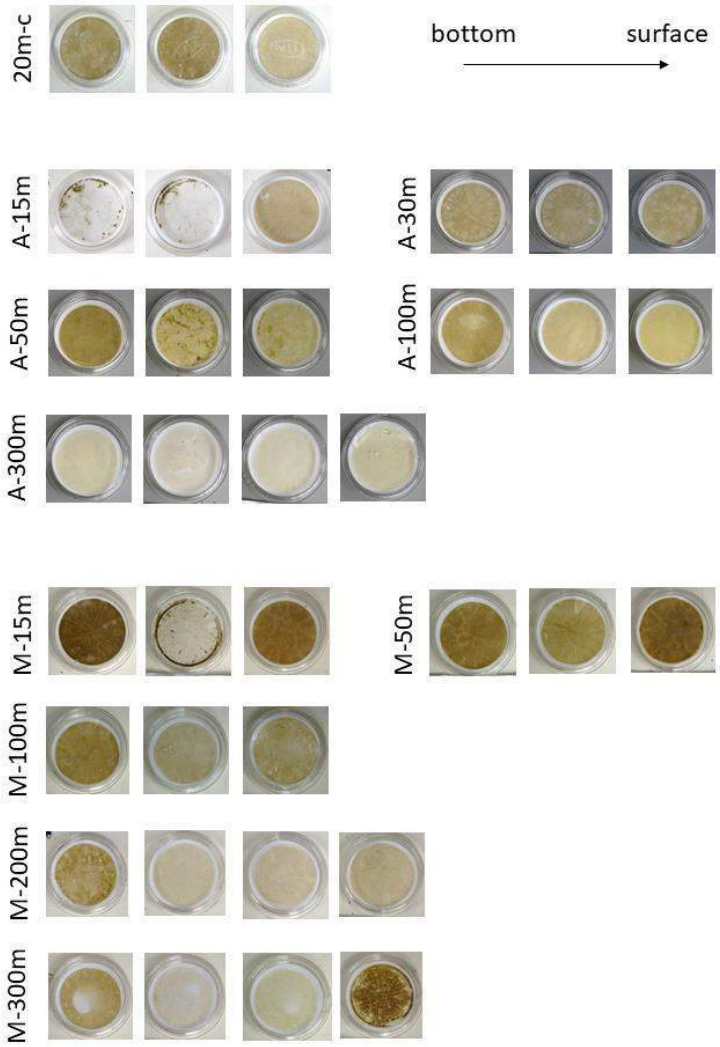

Figure 9. Overview of collected SPM

The filter holders and tubing were acid-washed after each station. After rinsing all parts with milliQ, they were placed in 0.1 M HCl overnight and rinsed several times with milliQ on the following day.

4.3 Multicores

We recovered multicores at all 21 stations with an Oktopus multicoring apparatus (www.oktopus-mari-tech.de) during this GoM2020 expedition. The multicores have a diameter of approximately 10 cm. The weighting system of the multicorer is adjusted at each site to achieve optimum sediment recovery. In general, 12 cores are recovered per cast, however, we sometimes opted for 8 or 6 cores to optimize sediment recovery (i.e. get deeper cores, as we already maximized the weight on top of the corer). Each core contains in general ~25-50 cm of sediment plus overlying water, but for stations 1 and 2 this was a bit less (~15 cm) because the sediment was stiff/sandy. After core collection, the multicores were either stored (XRF and Frozen) or sampled in appropriate resolution (all other cores) following the scheme in Table 6.

Table 6. Muticore sampling plan.

	Biomarkers	Palynology	Dinoflagellates	Microbiology	Benthic forams	s.l. isotopes	XRF	Frozen	Spare (0-2cm)	Oxic	Anoxic	O_2/Resin	Incubation	F.J. (Benthic foram assemlages)
St. 1 (20f)	x	x	x	2x	2x	x	x	x						
St. 2 (20e)	x	x	x	x	2x	x	x	x						
St. 3 (20d)	x	x	x	2x	2x	x	x	x	x					
St. 4 (20c)	x	x	x	x	x	x	x	x	x	x	x	x		
St. 5 (20b)	x	x	x	x	x	x	x	x	2x					
St. 6 (A15)	x	x	x	2x	2x	x	x	x	x	x	x	x	4x	3x
St. 7 (A600)	x	x	x	2x	2x	x	x	x	x					
St. 8 (A3200)	x	x	x	2x	2x		2x	x	x					
St. 9 (Pigmy)	x	x	x	2x	2x		2x	x	x					
St. 10 (A300)	x	x	x	x	x	x	x	x	x	x	x	x		
St. 11 (A100)	x	x	x	x	x	x	x	x	2x	x	x	x		3x
St. 12 (A30)	x	x	x	x	x	x	x	x		x	x	x		
St. 13 (A50)	x	x	x	x	x	x	x	x	x	x	x	x		
St. 14 (80b)	x	x	x	x	x	x	2x							
St. 15 (M15)	x	x	x	2x	2x	x	2x	x	x	x	x	x	3x	3x
St. 16 (M300)	x	x	x	x	x	x	x	x	x	x	x	x		
St. 17 (M600)	x	x	x	2x	2x	x	x	x	x			x (no resin)		
St. 18 (M200)	x	x	x	x	x	x	x	x	x	x	x	x		
St. 19 (M100)	x	x	x	2x	x	x	x	x		x	x	x		
St. 20 (M50)	x	x	x	x	x	x	x	x	x	x	x	x		
St. 21 (MonSt)	x	2x	x	x	x	x	2x	x				x		

4.3.1 Palynology and dinoflagellate subsampling (Francesca Sangiorgi)

Samples for palynology will be processed with the standard palynological technique in use at the GEO laboratory (Utrecht University). Dinoflagellate cysts, pollen and spores and other palynomorphs will be counted. Palynomorph assemblages will be used to (qualitatively) reconstruct salinity (freshwater input), nutrients availability and productivity, upper water stratification and sea surface temperature. Pollen and spore results will help to reconstruct vegetation changes on land and river input.
One core from each location in stations 1 to 20 was sampled according to the following protocol:

- 0-2 cm depth sampled every 0.5 cm
- 2 cm to bottom sampled every cm

The multicorer was deployed twice in Station 21 (bonus station, close to water monitoring facilities). One core from the second deployment was sampled every 0.5 cm throughout in order to achieve a high temporal resolution (previous publications in the region - e.g., Rabalais et al. (2002) - mentioned sediment accumulation rates of ~ 0.5 to 1 cm/y). We noticed that cores retrieved during the first deployment contained a different (muddier) top layer ~ 3.5 cm thick. One core from the first deployment was hence subsequently sampled every 0.5 cm in the upper 3.5 cm only.

A sediment slice, 2 cm-thick, was sampled in one core from each of the 21 stations. These sediments will be used to extract dinoflagellate cysts with intact cellular content (living dormant stage). These cysts will be cultivated in laboratory in special growth media to induce hatching of the cysts.

References:

Rabalais, N.N., Turner, R.E., Scavia, D. 2002. Beyond Science into Policy: Gulf of Mexico Hypoxia and the Mississippi River. BioScience 52, 129 – 142.

Figure 10. The multicore slicing team at work.

4.3.2 Lipid biomarkers (Francien Peterse)

Lipid biomarkers will primarily be used to study the fate of terrestrial organic carbon (OC) in the marine realm. The presence of specific biomarkers in each of the sediments along the land-sea transects, as well as in the river plume, should provide insights in the composition of the OC and thereby the contribution and properties of terrestrial OC. The same dataset can also be used to assess how the terrestrial climate signal carried by certain biomarkers is transferred to continental margin sediments, to reconstruct fresh water discharge, vegetation change, and to reconstruct sea surface temperatures. Subsequently, biomarker distributions in the piston cores will be analyzed to study how processes identified in the modern system operated in the paleo-domain.
Samples were collected following the same protocol as used for palynology in order to enable direct comparison between these two approaches. In short, one core from every station was sampled in the following resolution:

- 0-2 cm depth sampled every 0.5 cm
- 2 cm to bottom sampled every cm

Only the core from Station 21 (bonus station, close to water monitoring facilities) was sampled at a 0.5 cm resolution throughout the core in order to achieve a high temporal resolution and to facilitate comparison with instrumental data.

4.3.3 Short-lived isotopes (Rebekka Larson, Gregg Brooks)

The potentially harmful impact of catastrophic events of both natural (e.g. tropical cyclones) and anthropogenic origin (e.g. land-use change, Deepwater Horizon blowout) to the sedimentary system will be reconstructed using short-lived radioisotope measurements ("isotopes" on sampling bags). Specifically, the high-resolution age control will allow to investigate the variability in timing and frequency of such events in the past. For this, we will use several short-lived radioisotopes, such as $^{210}Pb_{xs}$ (~120 year time scale), $^{234}Th_{xs}$ (monthly time scale), and $^{137}C_s$ (pinpoint peak height of nuclear bomb testing in the 1960's and other thermonuclear incidents, e.g. the 1986 Chernobyl event). Hence, combined with high sampling resolution, these radioisotopes allow high-temporal resolution age control for multiple time-scales over the past ~120 years. Clearly, the sampling resolution is of pivotal importance for this method and during the GoM2020 cruise we therefore sampled at high 2-mm resolution to 2 cm depth, then with 5-mm intervals to 10 cm depth, and the rest of the core in 10-mm resolution. This sampling scheme provides the necessary high temporal resolution for further radioisotope analyses that will be carried out by colleagues (i.e. Rebekka Larson, Gregg Brooks) from Eckerd College (St. Petersburg, United States).

4.3.4 Microbiology (Alena di Primio)

Sediment samples collected for microbiological analyses will be used to evaluate the relation between the bacterial community composition within the seafloor surface (top 2 cm of the sediments) and the nutritional input from the land and sea, the seafloor depth and distance from land. Further we aim at cultivating and later isolating microbial strains, with a special focus on the bacterial clade Woeseiales.

We expect to find differences in community composition along a depth and nutrient gradients, with different lineages of Woeseiales representing the different environments (i.e. Coastal-A15 vs deep sea-A3200, high nutrient input-A15 vs medium input-20d vs low input-20f), and we hope to be able to expand the number of Woeseiales strains to work with, as it currently consists of one single strain only.
One core per station was allocated for the microbiology work. The top 2 cm of the core were sliced with a 1 cm resolution and slices were then stored at -80 °C. For 6 stations the entire core was sliced (top 2 cm in 1 cm resolution, rest in 2 cm resolution). These stations were 20f, 20d, A15, A600, A3200, and M600, M15 and the pigmy basin. At the same time an extra core was used to prepare a slurry using the water and the top 2 cm of the core and filling 0.5 L polycarbonate flasks to 500 ml with bottom water collected with the CTD. Slurries were stored at 4 °C.
One single water sample was taken at station 20c without addition of sediments, as the water color and turbidity suggested a high organic matter content which could result in a largely different pelagic community and hence be interesting to utilize as nutrient source for benthic organisms.
DNA will be directly extracted from frozen sediment samples and 16S amplicons generated by polymerase chain reaction (PCR) from the DNA extracts will be sequenced to get an overview of the composition of bacterial communities inhabiting the sediments. This can later be compared with biomarkers and palynological indicators to reveal potential degraders of terrestrial organic matter, with a special focus on members of the Woeseiales clade. Then, microscopic cell counts and quantitative PCR will be used to evaluate the absolute abundance of lineages that appear to respond to the amount of total terrestrial organic matter in the sediments.
The slurries will be used to enrich and cultivate new bacterial strains, specifically new members of Woeseiales. These samples will be treated in several ways:

1. Adding single sand grains to agar plates to pick new colonies for isolation.
2. Detaching bacterial cells from sand grains using sonication to inoculate culturing plates containing different carbon sources and gelling agents.
3. Inoculation of subsamples in different liquid media ranging from typical media (e.g. Marine broth, LB) to more defined media with following isolation of growing bacteria.
4. Isolation of the most abundant bacterial species by extinction by dilution methods
5. Growth of biofilms on glass slides or copper surfaces to investigate specific requirements for surface attachment.

4.3.5 Benthic foraminifera (Laura Pacho Sampedro, Zeynep Erdem)

The aim of this sampling is to establish a calibration between the CO_3^{2-} in the water and that in benthic foraminifera in the sediment. For that purpose, a rose Bengal (rB) - Ethanol solution (2 g rose Bengal in 1 L Ethanol) was prepared in a 2.5L bottle with a volumetric bottleneck dispenser (adding 5g of rB). The bottle was stabilized on the desk next to the slicer and the volume was arranged according to the volume of the sample. The alcohol concentration in the blend was then 60% at maximum depending

on the amount of pore water from the sediment. After preservation, the sample was shaken for at least one minute to ensure complete mixing (Lutze et al., 1964; Murray, 2006).

The MC tube has an internal diameter of 9.4 cm and a surface area of 70 cm^2.
The first 4 slices were 0.5cm thick; sample volume = 35cm^3 - approximately 55mL solution was added. Slices between 2-10cm had a volume of 70cm^3, to which around 100mL solution was added. The bottles were shaken for at least 1 minute after which they were stored at room temperature according to Schonfeld (2012).

At several stations an additional sample was collected. The top 2cm sediments were treated following the same protocol from stations 20f; 20e; 20d; 20c; A600; A3200; Pigmy Basin; M15; M600; M100.

At stations A15, M15 and A100, three cores were sliced for benthic foraminifera community composition analysis by Frans Jorissen. Sediment slices with the following resolution were treated with the same staining method described above: Core 1: 0-7cm with 0.7cm resolution, core 2 and 3: 0-2.1cm with 0.7cm resolution.

Sampling of bottom water from the MC:
With the aim of determining the CO_3^{2-} composition of the bottom water, 5mL overlying water was collected from the sediment-core while still in the MC frame. The vials for DIC and Alkalinity were poisoned with 15µL of $HgCl_2$. The vials were stored at 4 °C, ready to measure as soon as the ship arrives at NIOZ.

References:
Lutze, G F., Altenbach, A. Technik und Signifikanz der Lebendfarbung benthischer Foraminiferen mit Bengalrot. Geol Jb, 1991, A128: 251-265
Murray, J.W. Ecology and Applications of Benthic Foraminifera, Uni. of Southampton, Cambridge Uni Press, 2006, 426 pp.
Schonfeld, 2012. History and development of methods in recent benthic foraminifera studies Journal of Micropaleontology, 31: 53-72.

4.3.6 Anoxic multicore slicing and porewater subsampling (Kristin Ungerhofer)

One multicore per selected station (Table 7) was sliced and sampled in a N_2-filled glove bag, for sediment and pore water analysis (Fig. 11). After the MC was back on deck, a bottom water sample was taken from each core immediately upon recovery. In a temperature-controlled lab container, brought to the respective bottom water temperature of each station, the cores were measured and then put into a N_2-filled glovebag.

Table 7. Stations selected for anoxic porewater subsampling, CTD sampling and SPM filtration.

Atchafalya transect	Mississippi transect	River plume transect
A-15m	M-15m	20m-c
A-30m	M-50m	
A-50m	M-100m	
A-100m	M-200m	
A-300m	M-300m	

The sediment texture allowed for sampling with a plastic spoon at all stations. Samples, taken at the vertical resolution shown in Table 8, were put into 50 mL Falcon tubes, taken out of the glovebag and centrifuged for 20 minutes at 3500 rpm.

In a separate N_2-filled glovebag, the pore water of each sample was filtered over a 0.45 µm PES filter and subsamples were taken for the species listed in Table 9. DIC and HS samples were always taken first. Subsamples were stored according to Table 9.

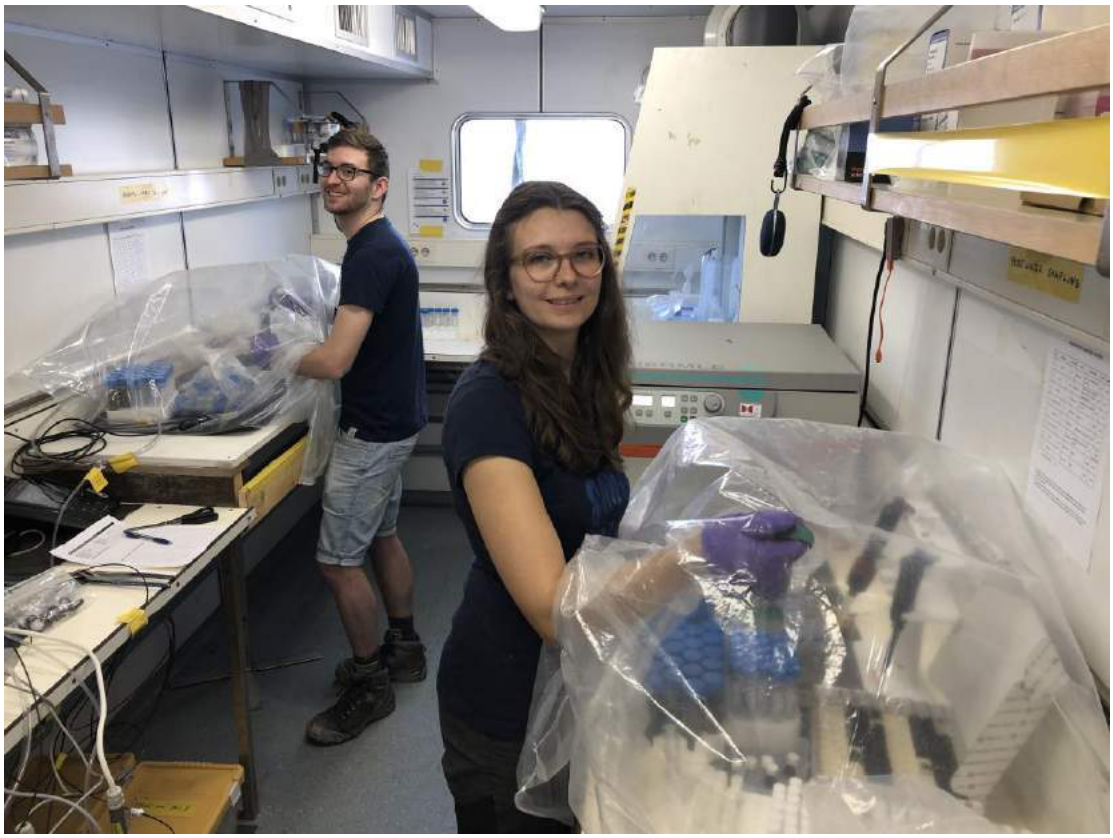

Figure 11. Anoxic slicing and sample processing.

Table 8. Core sectioning scheme.

Sample Nr.	Depth range [cm]	Thickness [cm]	Sample Nr.	Depth range [cm]	Thickness [cm]
1	0.0 - 0.5	0.5	14	12 - 14	2
2	0.5 - 1.0	0.5	15	14 - 16	2
3	1.0 - 1.5	0.5	16	16 - 18	2
4	1.5 - 2.0	0.5	17	18 - 20	2
5	2 - 3	1	18	20 - 24	2
6	3 - 4	1	19	24 - 28	4
7	4 - 5	1	20	28 - 32	4
8	5 - 6	1	21	32 - 36	4
9	6 - 7	1	22	36 - 40	4
10	7 - 8	1	23	40 - 44	4
11	8 - 9	1	24	44 - 48	4
12	9 -10	1	25	48 - 52	4
13	10 - 12	1			

Table 9. Pore water sampling scheme and storage.

Nr.	Analyte	Vol. [mL]	Vial	Treatment	Code	Storage
1	H2S	0.5	Glass vial	2 mL 12.5 mM NaOH, 1% ZnAc	HS	- 20 °C
2	DIC	0.5	Glass vial	Poisoned 15 µL HgCl2, diluted 4.5 mL 41g/L degassed NaCl	DIC	4 °C
3	PO4, Si	1	Pony vial	Acidified 10 µL 5N HCl per mL	PO4	4 °C
4	NH4, NO3, NO2	1	Pony vial	None	NH4	- 20 °C
5	Alkalinity	1	Pony vial	Poisoned 15 µL HgCl2	Alk	4 °C
6	S, Fe, Mn, metals	2	Nalgene 4 mL	Acidified 10 µL 5N HCl per mL	ICP	4 °C
7	SO4	0.5	Pony vial	None	SO4	- 20 °C
	Total volume [mL]	6.5				

4.3.7 Oxic multicore slicing (Kristin Ungerhofer)

At selected stations (see Table 7) an additional multicore was sliced at the resolution depicted in table 8 in the wet lab, using the hydraulic push-up pole. One aliquot of each sample was transferred into a pre-weighed plastic vial and will be used for determining porosity. The remaining sediment was transferred into plastic bags. Both samples were stored at -20 °C.

4.3.8 Multicore incubations for benthic flux measurements (Kristin Ungerhofer)

At the two shallowest stations of the Atchafalaya (A-15 m) and Mississippi (M-15 m) transects, dedicated multicores were taken for on-board incubations at in situ temperatures in the laboratory container. Immediately after recovery, these cores were placed on rubber stoppers and capped at the top with special Perspex lids with sampling ports (that were sealed with small rubber stoppers). The cores were then transported to the lab container, where the incubation setup was prepared (Fig. 12).

Oxygen was measured in a non-intrusive, optical way by using PreSens oxygen-sensitive fluorescent dye spots (SP-PSt3-NAU-D5-YOP) glued into the inside of the multicores (~ 15 cm from the top) and polymer optical fiber cables attached to the outside of the core to transfer the signal from the spot to the meter (PreSens OXY-4).

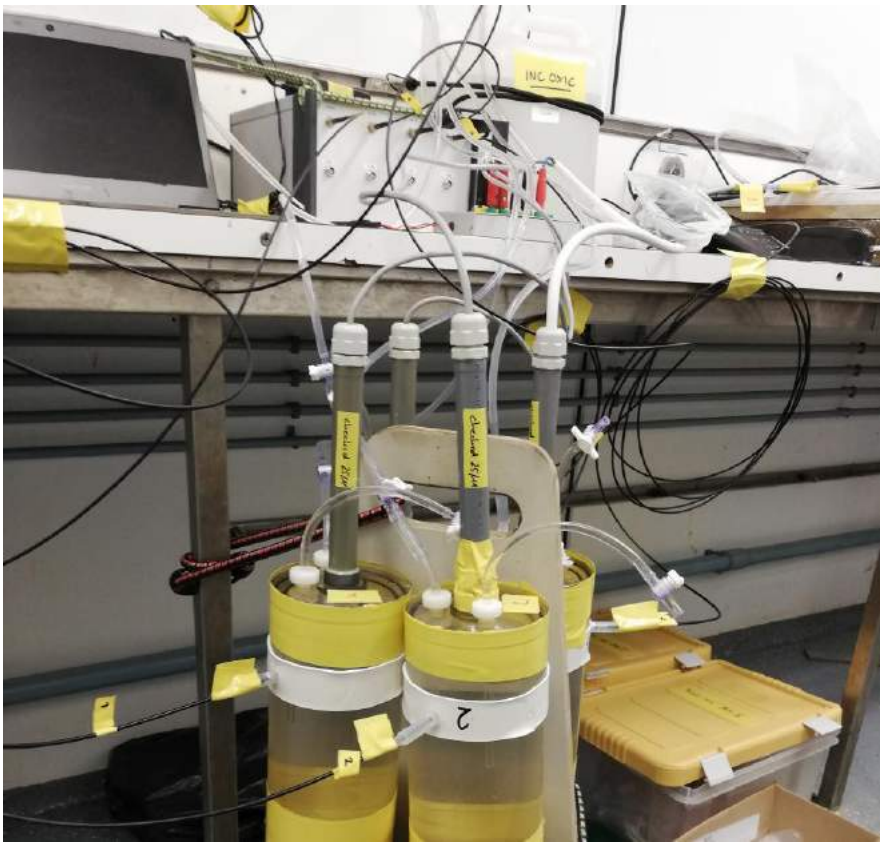

Figure 12. Multicore incubation setup

The lids contained three ports. One for the stir motor, one for sample taking, and one to connect to the vessel with bottom water from the station (collected previously from the deepest CTD/rosette bottle). In this setup, water from the vessel is immediately replaced any water removed during sampling. Oxygen was monitored continuously (with values recorded every 5 seconds), and over the course of the incubation experiment (duration 4 to 6 days) 9 to 26 discrete 25 mL samples were taken for chemical analyses. The sample was filtered (47 mm 0.2 µm PES and Nylon syringe filters) into an acid-clean 15 mL Nalgene bottle, and immediately sub-sampled according to Table 10.

Table 10. Incubation sampling scheme.

Nr.	Analyte	Vol. [mL]	Vial	Treatment	Code	Storage
1	H2S	2	Glass vial	2 mL 12.5 mM NaOH, 1% ZnAc	HS	- 20 °C
2	DIC	5	Glass vial	Poisoned 15 µL HgCl2	DIC	4 °C
3	PO4, Si	3	Pony vial	Acidified 10 µL 5N HCl per mL	PO4	4 °C
4	NH4, NO3, NO2	3	Pony vial	None	NH4	- 20 °C
5	Alkalinity	2	Pony vial	Poisoned 15 µL HgCl2	Alk	4 °C
6	S, Fe, Mn, metals	9	Nalgene 15 mL	Acidified 10 µL 5N HCl per mL	ICP	4 °C
7	SO4	0.5	Pony vial	None	SO4	- 20 °C
8	N gases*	-	Exetainer	Poisoned 25 µL ZnCl2	N	4 °C
	Total volume [mL]	24.5				

The aim of the incubations was to measure benthic fluxes of nutrients and trace metals under different redox conditions. For this purpose, 2 multicores were incubated without modification of the O_2 concentration in the overlying water and 2 others were incubated after their overlying water was purged with N_2. After 4 days, the experiment was stopped. One oxic core was sieved over a 1 mm mesh size sieve to collect fauna; the top 10 cm of one anoxic core was quickly sliced under oxic conditions on the hydraulic push-up pole to sample for foraminifera (as described in section 4.3.5); the top 10 cm of the second anoxic core were sliced inside the N_2-filled glove bag and porewater was subsampled as described in section 4.3.6 and a mini-core for resin embedding was taken as described in section 4.3.10.

At station M-15m this setup had to be modified due to the loss of an oxygen sensor spot. Here, 3 cores were incubated without modification of the O_2 concentration in the overlying water for the first 4 days, after which the overlying water of two cores was purged with N_2. The third core had reached anoxia within 4 days without artificial deoxygenation. The experiment was continued for 3 more days and the cores were processed as described before, with the exception of an additional O_2 microprofile for one of them.

4.3.9 O_2 micro-profiling (Zeynep Erdem)

At selected stations, a multicore was taken from the MC cast and immediately transferred to an on-board lab (room temperature) for O_2 micro-profiling using a UniSense OX-50 micro-electrode connected to a UniSense picoammeter PA2000 (Fig. 13). Where needed, the sediment was raised to appropriate working height using a disc in the bottom of the core. With the aid of a high-power flashlight, the tip of the micro-electrode was placed at the sediment-water interface, after which it was raised 0.5 – 1 cm. From there, measurements started: the stable reading was noted and the needle tip was lowered 0.25 – 1 mm for the next reading, the resolution increasing around the sediment-water interface. The OX-50 micro-electrode was calibrated at three temperatures (5, 13 and 22 °C) using O_2-saturated (20 min bubbling with air and then at least 1 day gently stirred to avoid oversaturation) and oxygen-free (5 g/L Na sulfite) seawater. The readings in O_2-saturated water at the three temperatures showed a linear decrease of signal with decreasing T, this was used to calculate reading for O_2-saturated water at bottom water temperature for that specific site as obtained from the CTD data. The micro-profiling took no more than 10 minutes, during which temperature changes in the bottom water and sediment were likely minimal. All O_2 profiles are in Appendix 2.

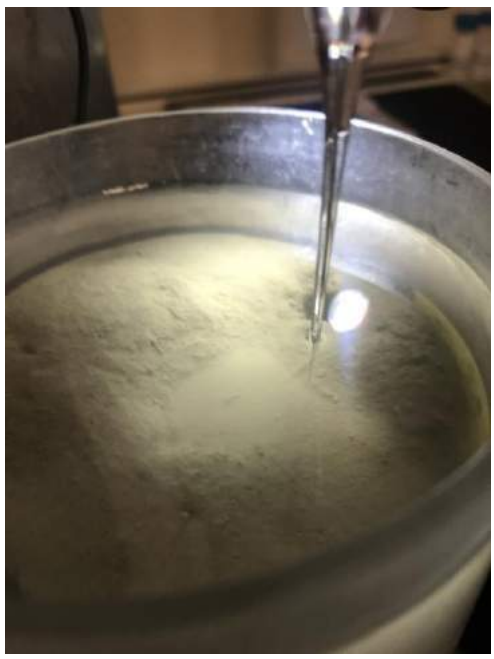

Figure 13. Micro-electrode used for O_2 profiling

4.3.10 Resin embedding (Rick Hennekam, Zeynep Erdem, Kristin Ungerhofer)

Following the O_2 micro-profiling, the core is used to get a surface sediment mini-core for resin embedding. For this purpose, a 50 mL centrifuge tube, a cut-off 15 mL centrifuge tube with a pre-drilled cap and nylon mesh and a squeeze bottle with Acetone were prepared.

The core was mounted on the hydraulic push-up pole and the 15 mL centrifuge tube was carefully inserted into the sediment as far as possible (threaded end first). While the centrifuge tube remained stuck in the sediment, samples were taken around it, until it was possible to cover the bottom end with a spatula and remove the mini-core from the sediment. The pre-drilled cap with the nylon mesh was used to quickly close the tube. The mini-core was then placed into the 50 mL centrifuge tube, which was filled with Acetone and stored upright at -20°C for transport.

4.3.11 Frozen cores for photography and on-shore processing (Zeynep Erdem)

At each station, one core was capped and frozen upright with overlying water at -20 °C for at least 24 h. Hereafter, hot water was poured over the core liner until the frozen sediment core could be pushed from the liner intact. The outside of the frozen core was quickly rinsed with cold water to remove smeared material and expose fresh material. This core was immediately photographed (Appendix 3). Afterwards, the core was quickly packed in an Al-laminate bag and returned to storage at -20 °C for later analysis by Peter Kraal (Royal NIOZ).

4.3.12 XRF core scanning (Rick Hennekam)

One core from each station, with overlying water completely filling the core liner to avoid disturbance of the sediment surface, was capped with plastic red caps, labeled and stored upright at 4 °C. These cores will be analyzed for their bulk geochemical composition using X-Ray Fluorescence (XRF) core scanning (an Avaatech scanner with Rh-tube). First, the core sections will be opened, described, and linescanned (providing a detailed picture with a resolution of 70 µm per pixel). Then, the sediment sections will be covered with a thin (4 µm) Ultralene foil and carefully aligned in the core scanner to make sure the measurement triangle lands on a flat surface. Subsequently, the geochemical composition will be determined by XRF-scanning on the core surface, allowing to reconstruct paleo-environmental conditions (such a redox conditions), but also allowing to easily transfer age model information between cores by aligning geochemical signals. All core material will probably be measured with a 1-cm resolution and where appropriate the resolution will be increased to 1-mm resolution in an additional measurement series. As redox conditions may have fluctuated in the core material, it is suggested to use the method as described in Hennekam et al. 2019 (“Trace metal analysis of sediment cores using a novel X-ray fluorescence core scanning method”), to target variability of redox-sensitive trace metals.

4.4 Piston Cores (Rick Hennekam)

Five piston cores were recovered for the purpose of multiproxy applications and paleo-reconstructions in this delta region. The cores were recovered from stations 8, 9, 11, 14, and 19. The length of the core liner was varied between 6 meters (station 11), 12 meters (stations 8, 14, 19), and 18 meters (station 9), as the chances of bending the piston core tube ("bananas") in consolidated sediments is higher with a longer tube. On deck, the core was split to 1 m sections, with an exception for 1 section for station 19 (95 cm to avoid the part where the liners are glued together) and top sections. Then, the core section were stored in 4°C storage together with the core catcher material in bags. Some trip cores were recovered, but because they were generally poorly recovered relative to the multicores at the same site we decided not to store them. Further processing, such as XRF-core-scanning and biomarker sampling, will be organized once the samples arrive at the NIOZ. At NIOZ, the core sections will first be opened, photographed in high resolution with the XRF core scanner ("linescanning"), and described. For further details on the piston cores are in Table 11.

Table 11. Piston core locations and recovered length.

Station	Date	Long.	Lat.	Water depth (m)	Core Name	Core length (cm)	Sections	Trip core	Core catcher
St. 8 (A3200)	9-2-2020	25.699583	-92.382719	3125	64PE467-8PC	9.32	10	no	yes
St. 9 (Pigmy)	10-2-2020	27.187356	-91.409364	2260	64PE467-9PC	13.47	14	no	yes
St. 11 (A100)	11-2-2020	28.052017	-91.812017	105	64PE467-11PC	3.67	4	no	yes
St. 14 (80b)	12-2-2020	28.120224	-92.294809	80	64PE467-14PC	9.64	10	no	yes
St. 19 (M100)	15-2-2020	28.873081	-89.183621	98	64PE467-19PC	9.83	10	no	yes

Figure 14. Sections of the piston core collected from the Pigmy Basin (Station 9).

APPENDIX 1. Multibeam screenshots

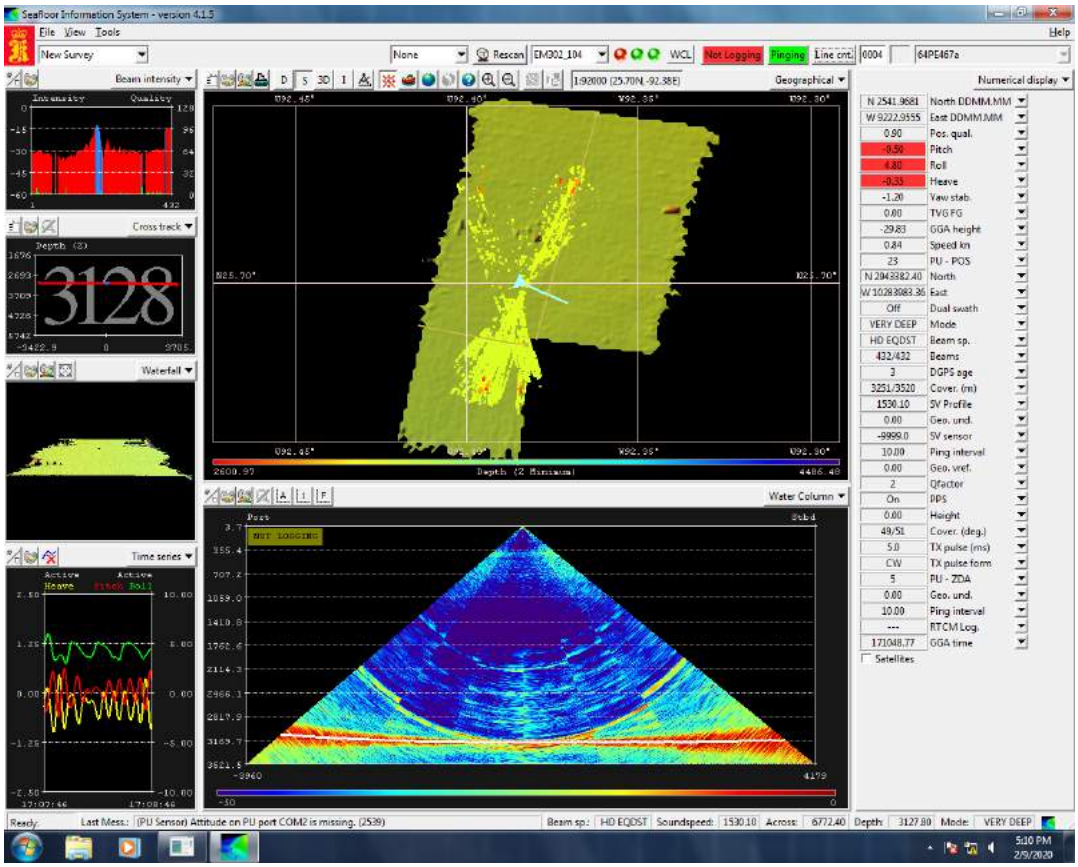

Station 8 – A3200

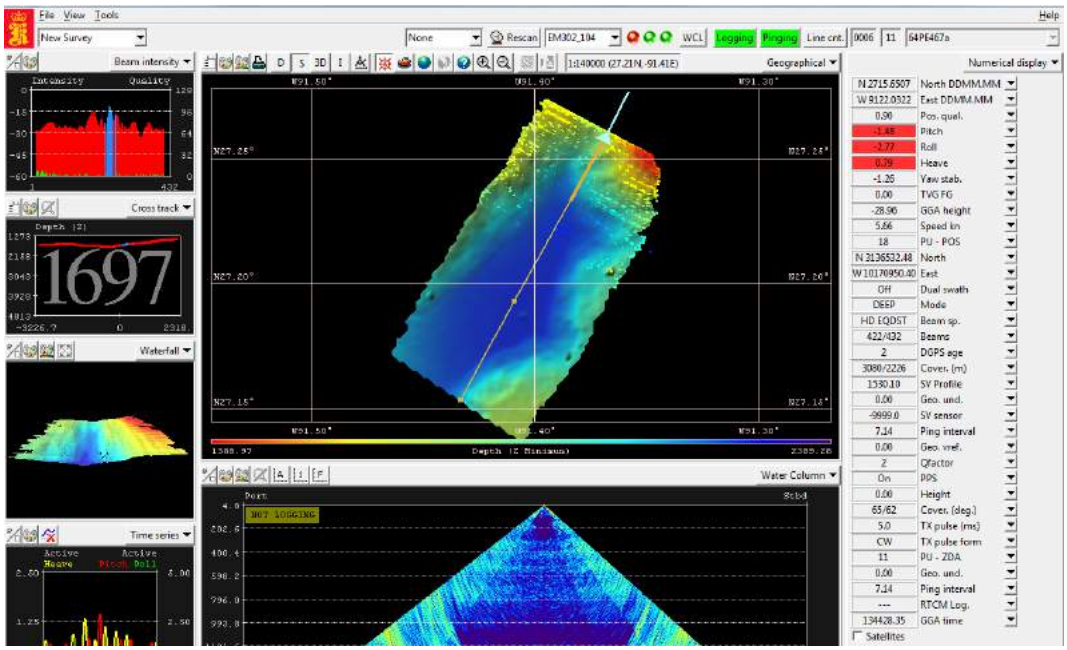

Station 9 – Pigmy Basin

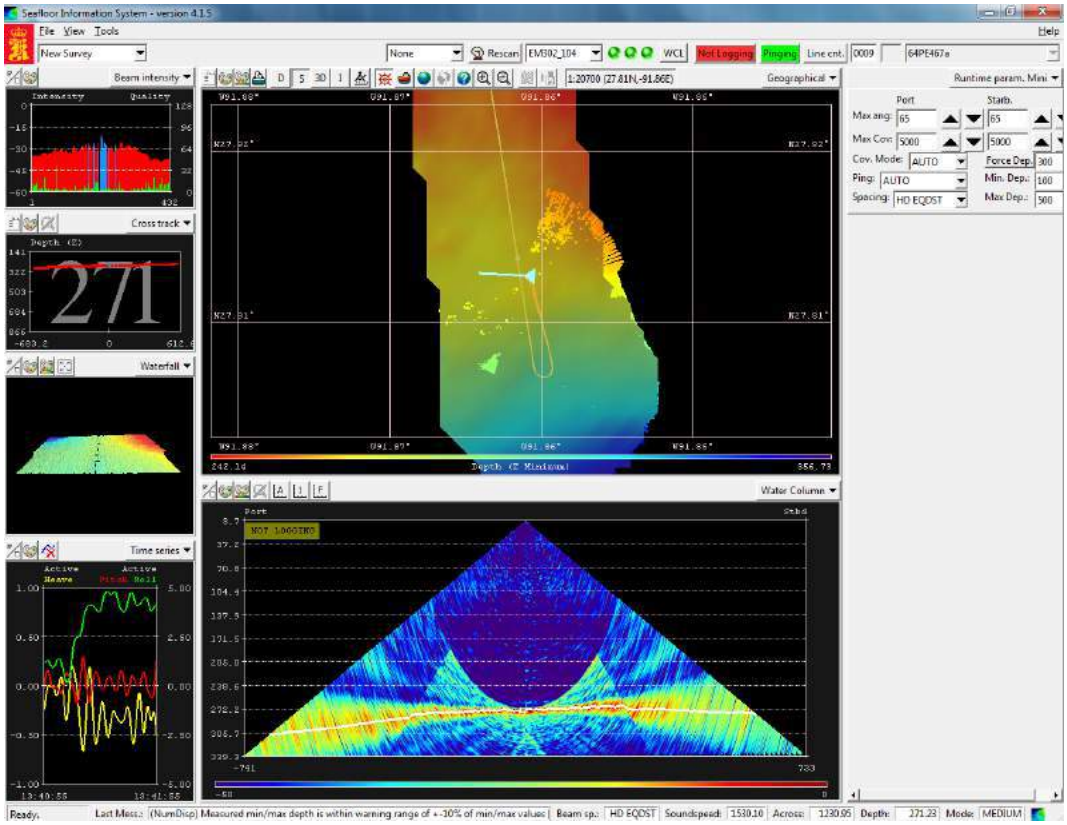

Station 10 – A300

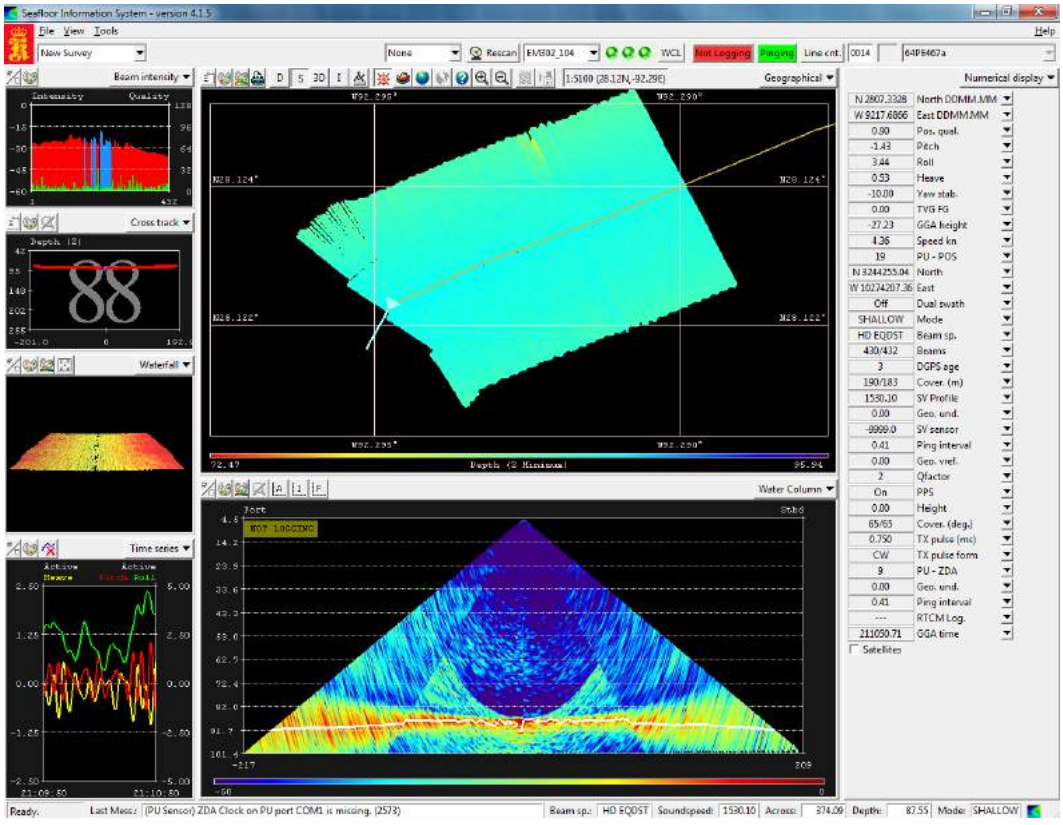

Station 14 – 80b

APPENDIX 2. O_2 micro-profiles

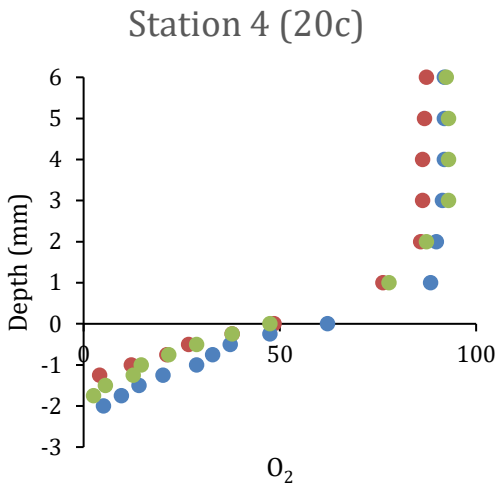

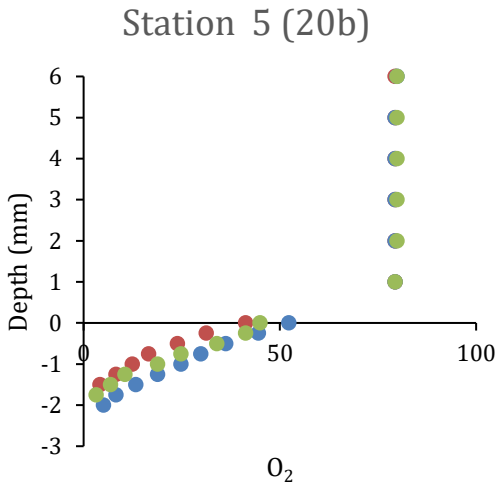

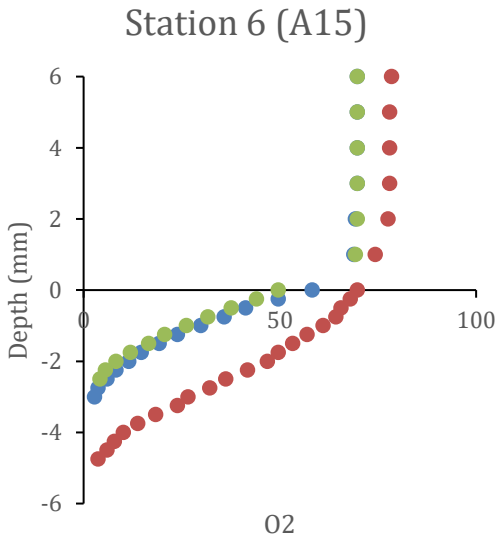

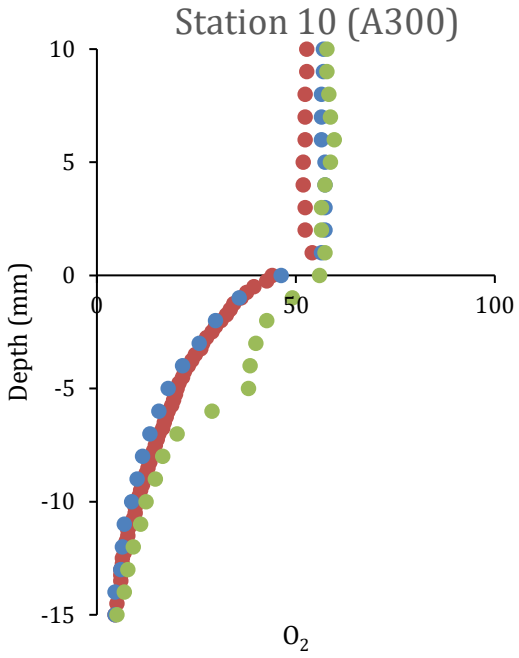
Station 10 (A300)
10
5
0
-5
-10
-15
0
50
100
Depth (mm)
O2

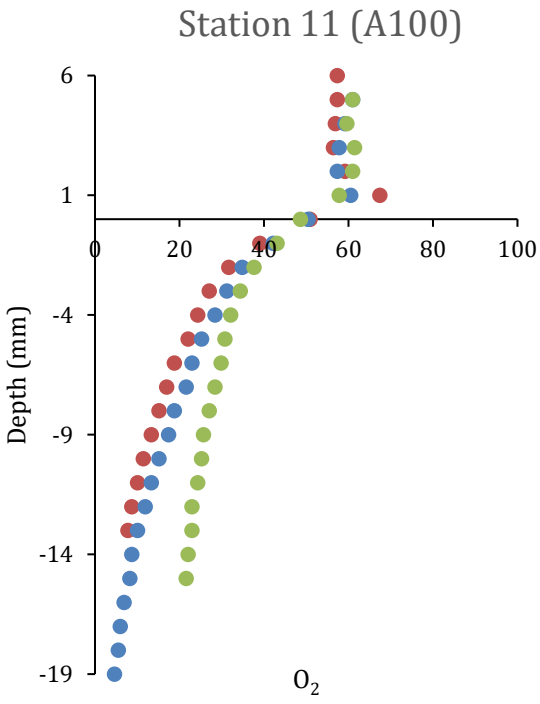
Station 11 (A100)
6
1
-4
-9
-14
-19
0
20
40
60
80
100
Depth (mm)
O2

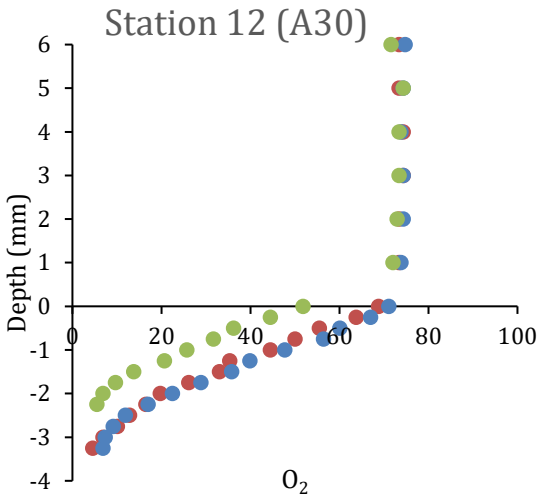
Station 12 (A30)
Depth (mm)
6
5
4
3
2
1
0
-1
-2
-3
-4
0
20
40
60
80
100
O2

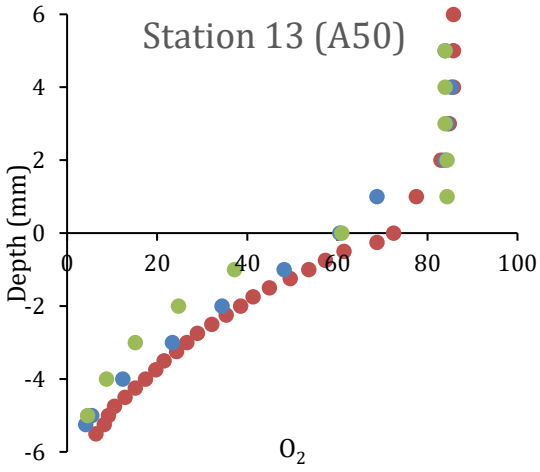
Station 13 (A50)
Depth (mm)
6
4
2
0
-2
-4
-6
0
20
40
60
80
100
O2

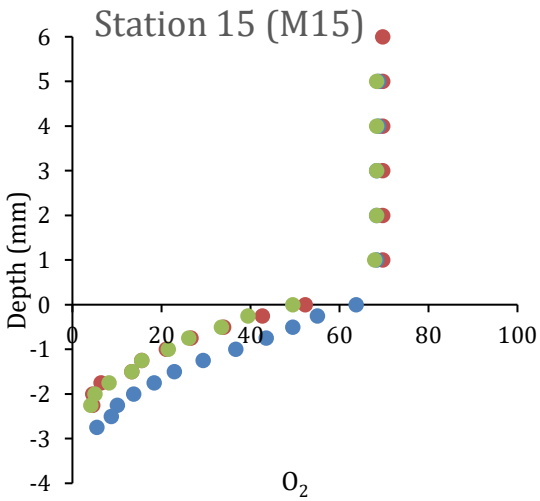
Station 15 (M15)
Depth (mm)
6
5
4
3
2
1
0
-1
-2
-3
-4
0
20
40
60
80
100
O2

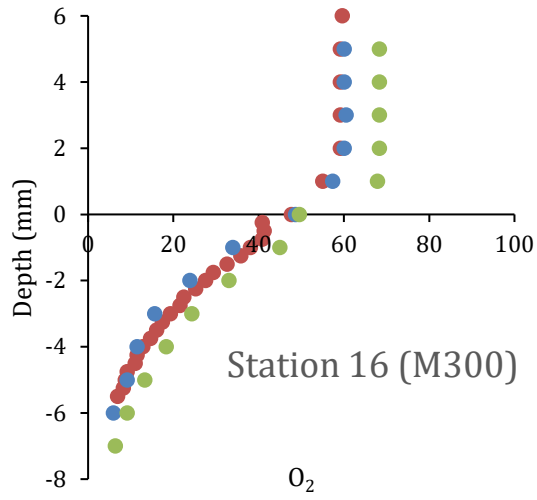
Depth (mm)
6
4
2
0
-2
-4
-6
-8
0
20
40
60
80
100
Station 16 (M300)
O_2

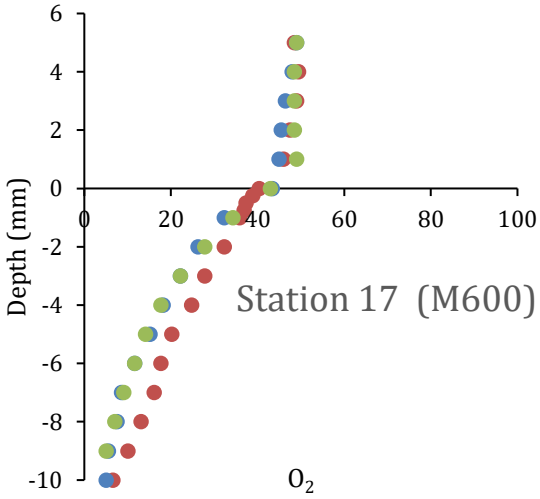
Depth (mm)
6
4
2
0
-2
-4
-6
-8
-10
0
20
40
60
80
100
Station 17 (M600)
O_2

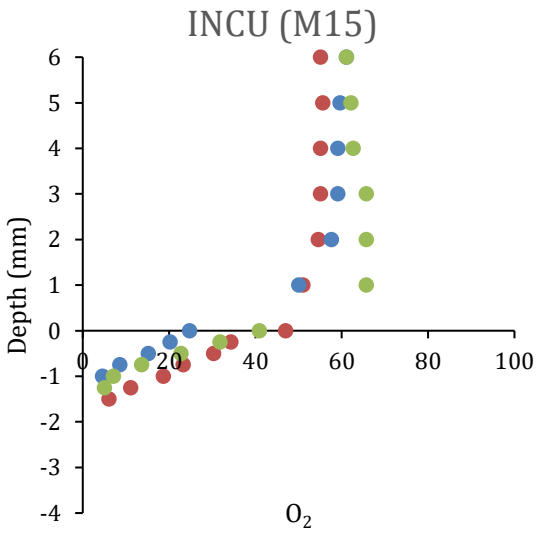
INCU (M15)
Depth (mm)
6
5
4
3
2
1
0
-1
-2
-3
-4
0
20
40
60
80
100
O_2

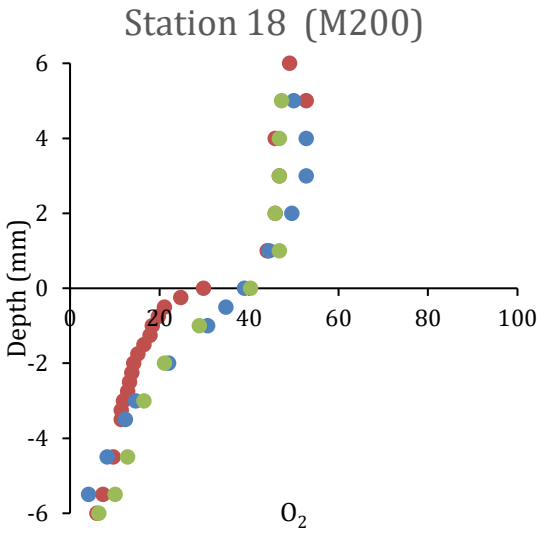
Station 18 (M200)
Depth (mm)
6
4
2
0
-2
-4
-6
0
20
40
60
80
100
O2

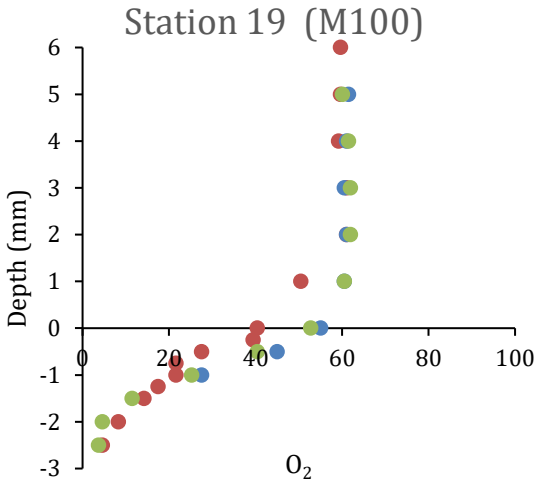
Station 19 (M100)
Depth (mm)
6
5
4
3
2
1
0
-1
-2
-3
0
20
40
60
80
100
O2

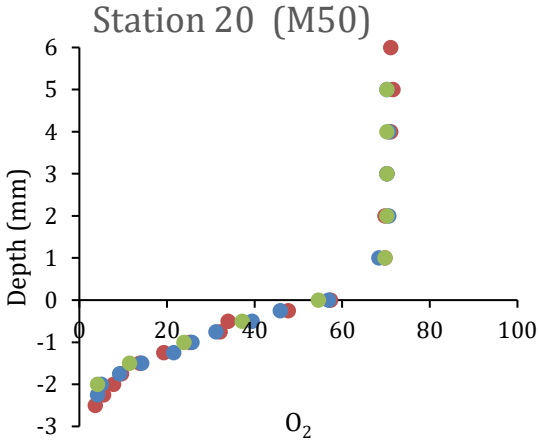
Station 20 (M50)
Depth (mm)
6
5
4
3
2
1
0
-1
-2
-3
0
20
40
60
80
100
O2

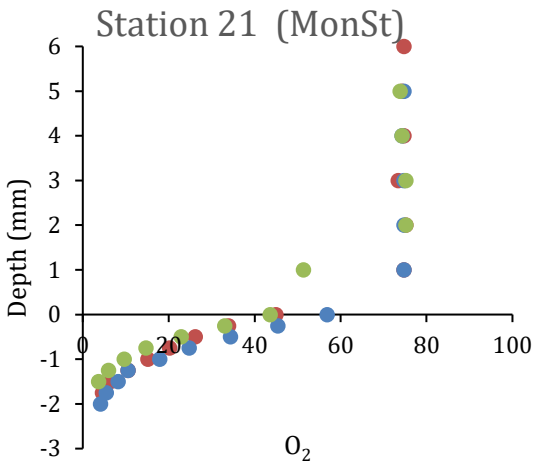
Station 21 (MonSt)
Depth (mm)
6
5
4
3
2
1
0
-1
-2
-3
0
20
40
60
80
100
O_2

APPENDIX 3. Core photos

Appendix 2

Utrecht University Manual for rock sampling, making slides, and palynological techniques

Universiteit Utrecht

Faculty of Geoscience

Manual Palynological Techniques for rock sample processing

Geolab

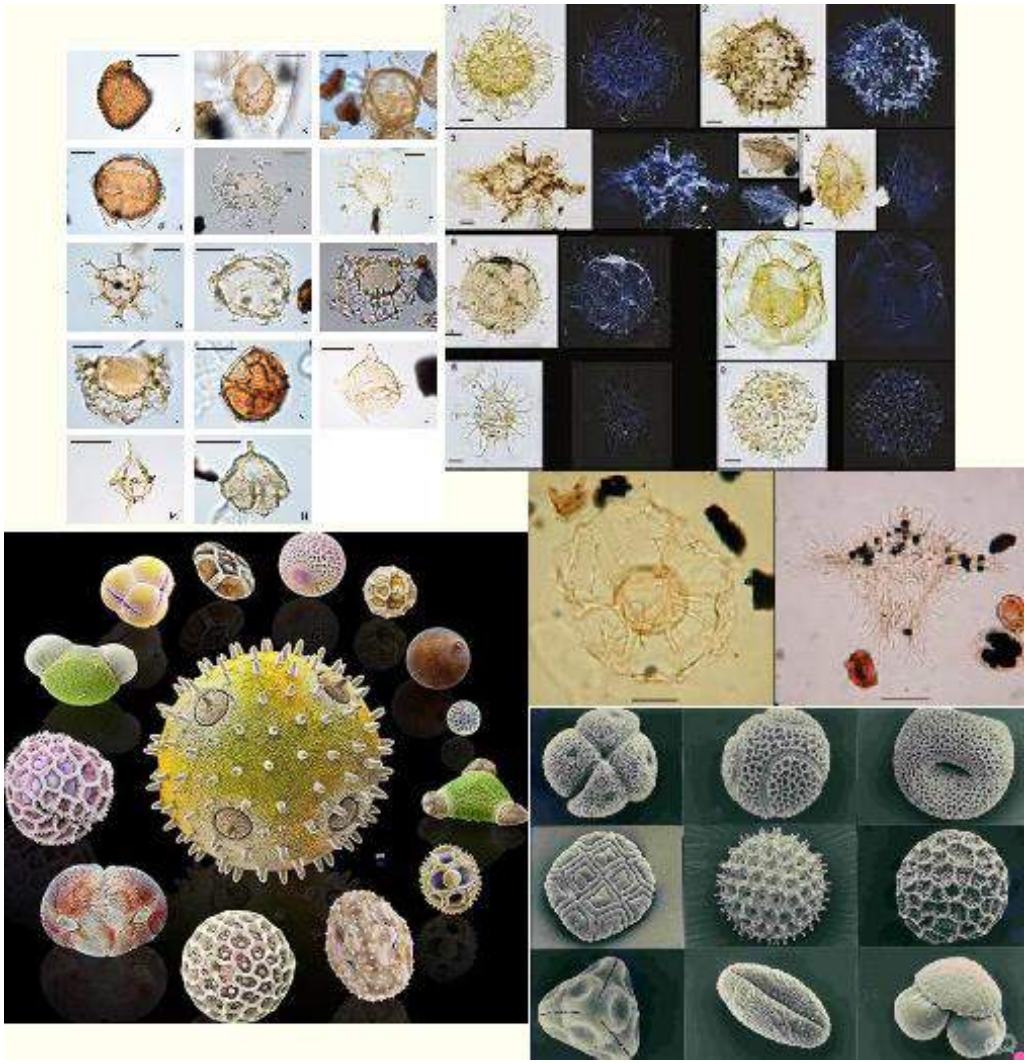

Faculty: Geosciences
Department: GeoLab
Address: Vening Meineszgebouw B
Princetonlaan 8, 3584CB Utrecht

Author: Natasja Welters
Revised by:
Date: 2020
Version: 1

lab: 5.15, 5.26 and HF-lab
Floor/room: 5.15, 5.26 and 5.34
Supervisors: Natasja Welters & Giovanni Dammers

Table of Contents

1 Introduction to Palynological techniques for rock sample processing

A short course in processing rock samples to obtain a residue of organic material for palynological research.

Aim: To provide processing methods which render organic association reflecting the original matter composition (as much as possible).

1.1 Palynological processing is isolating organic material from sediment.
Palynological processing is finding solutions for problems.

Palynological research on rock samples, coals, cuttings and sidewall cores with a transmitted light microscope can unfortunately only be done on material of which all organic material is isolated from the original components from the sediment.
Removal of the unwanted components implies finding solutions for the different problems which occur reaching that goal.

PROBLEM	SOLUTION
Contamination of the sample	Rinsing
Carbonates	Removal with the help of HCl
Silicates	Removal with the help of HF
Small particles	Sieving 10 µm
Large particles	Sieving 250 µm
Residual silicates and other minerals	Heavy liquid separation
Amorphous Organic Debris	Oxidation and/or reduction
Carbonized palynomorphs	Oxidation

All over the world palynological processing of sedimentary rock samples is based on more or less similar principles which should isolate the desired organic material (crushing, HCl, HF, sieving, heavy liquid, bleaching), by removing the undesired components.
This is finally resulting in slide preparations with a realistic reflection of the original organic matter composition and suitable for research with a transmitted light microscope.

Technical aspects of this palynological process depend on the local laboratory conditions and the person who process the samples.

1.2 Palynological processing is accepting compromises

1.2.1 Compromises

A palynological preparation method is aimed at recovering all palynomorphs from a rock sample at the highest possible concentration. Unfortunately nearly all operations directed at reaching this goal are potentially destructive for palynomorphs. Hence, the assemblage you will finally find in your preparation slide might differ considerably from the original assemblage in the rock sample.
Care must be taken not to damage the microfossils and not to loss palynomorphs selectively by overdoing the procedures or maltreatment.

In all laboratories maximum care must be taken during rock sample processing in order:

- To avoid damage to material.
- To avoid selective loss of material.
- To avoid contamination between samples.

Avoiding contamination in a laboratory is only possible if processing occurs in a specific way:

- Organized.
- Disciplined.
- Very clean.

1.2.2 Damaging valuable material might occur:

- As a result of centrifugal force when centrifuging.
- While using ultrasonic waves.
- By using oxidizing and/or reducing agents walls of palynomorphs will be affected and color changes might occur.

1.2.3 Selective loss of valuable material might occur:

- While decanting because small and/or light material might be lost.
- While sieving (10-20 µm) all small pollen, spores, angiosperms, dinoflagellates and acritarch smaller than the sieve mesh disappear in the sink.
- While sieving (250 µm) megaspores, large sheets (such as cuticles) and valuable palynofacies are separated from the original association (but can be captured).
- By using oxidizing and/or reducing agents vulnerable palynomorphs might disappear.

In order to obtain the best results in processing in a relative fast way, sometimes decisions has to be made in spite of the above mentioned possible damaging and loss.

Processing is making decisions.
Processing is accepting compromises.

1.3 Small explanation about the process

1.3.1 Contamination of the sample

- Contamination on the sample can occur during sampling at outcrops.
- Minor contamination can be scraped off with a potato knife and cleaned with pressed-air (if that is available).
- Severe contamination should be rinsed away with water or even put in an ultrasonic bath for a while.

1.3.2 Crush

- The time needed to dissolve the carbonates can take days or weeks if the rock sample is put entirely in the HCl.
- To limit the time needed to dissolve the carbonates the rock samples are crushed with help of a porcelain mortar and pestle or just with hammer and anvil.
- Harder rocks are fragmented in an electrical crusher.

The accepted compromise when crushing concerns the possible damaging of vulnerable material.

1.3.3 Carbonates – Hydrochloric acid (HCl)

- In order to dissolve carbonates, HCl is used.
- Any acid could be used.
- Since most samples contain both carbonates and silicates, it seems easy to use HF to dissolve them.
- **Unfortunately carbonates will precipitate the insoluble mineral CaF with the Fluor.**

The accepted compromise using HCl concerns the loss of all calcareous dinoflagellates.

When all carbonates are consumed, the liquid – holding the unwanted Ca^{++}-ions – should be separated from the residue. This separation is effectuated by way of decanting after settling of the material. The settling is obtained by first leaving the material standing one night over (at least 8 hours). After that by centrifuging to get all the Ca^{++}-ions out.

The accepted compromise of decanting concern
After settling overnight:

- ***Prolongation of the total processing time.***
- ***The possible selective loss of small and easily floating material after improper decantation.***
- ***Too much solvent (containing unwanted ions) left after improper decantation.***

After centrifuging:

- ***More manual action in the laboratory.***
- ***The damaging of vulnerable material when centrifuging.***

1.3.4 Silicates – Hydrofluoric acid (HF)

- In order to dissolve silicates HF is used.
- Since glass is SiO_2 the HF treatment should be performed in a fume cupboard with a sash window of plastic and also the plates in the fume cupboard and no other glass components.
- The reaction of HF with silicates forms SiF_4. SiF_4 is undesirable because it "protects" the material against dissolving chemicals; in a later stage of processing, SiF_4 hampers the sieving. To rid the material of SiF_4, the samples should be shaken regularly. The easiest way is to use an orbital shaking apparatus.

The accepted compromises of adding HF concern:

- ***The formation of SiF_4 which covers both mineral and organic particles.***
- ***The danger of working with an extreme poisonous reagent.***

If the reaction of the HF is finished (after a minimum of 2 hours) is filled up with water and leave overnight to settle. The liquid should be separated from the residue by way of decanting.

The accepted compromise of decanting concern
After settling overnight:

- ***Prolongation of the total processing time.***
- ***The possible selective loss of small and easily floating material after improper decantation.***
- ***Too much solvent (containing unwanted ions) left after improper decantation.***

After centrifuging:

- ***More manual action in the laboratory.***
- ***The damaging of vulnerable material when centrifuging.***

1.3.5 SiF_4 – Hydrochloric acid

- In order to dissolve SiF_4, HCl is used.
- The SiF_4 dissolves immediately after adding the HCl, fill up with water.
- Centrifuge.
- The liquid should be separated from the residue by way of decanting.

The accepted compromise of decanting concern
After settling overnight:

- ***Prolongation of the total processing time.***
- ***The possible selective loss of small and easily floating material after improper decantation.***
- ***Too much solvent (containing unwanted ions) left after improper decantation.***

After centrifuging:

- ***More manual action in the laboratory.***
- ***The damaging of vulnerable material when centrifuging.***

1.3.6 Sieving

- The size of palynomorphs ranges from approximately 5 µm to > 200 µm with an optimum around 80 µm (Gauss curve).
- Without sieving with a 250 µm mesh sieve, the residue may contain organic material and megaspores which will completely fill the image under the microscope.
- Elimination of the oversized organic material prevents this.
- Without sieving with a 10 to 25 µm mesh sieve, a cloud of organic material from 0.1 µm to 10 µm will show up in the residue and microscope slides.
- The used mesh size depends the goal of the research and the expected size of palynomorphs and other particles.

  - 10 µm or less: takes a long time to finish sieving properly.
  - 15/18 µm: possible loss of smaller palynomorphs.
  - 30 µm: loss of important palynomorphs, but a very clean residue.

The accepted compromise of sieving is selective loss of small palynomorphs.

During sieving a small part of the residue is transferred on a object glass to check the residue. After that you can continue and make a standard preparation slide.

If the residue needs other treatments you can make first a standard slide to compare the deferens between the standard slide and the one that been treated.

Palynological processing is making decisions.

After analyzing this standard slide preparation new decisions are to be made concerning the continuation of the processing with the sieved residue.

1. Processing was satisfactory.
2. The residue still contains minerals.
3. The residue contains organic like minerals (like Pyrites an mica's).
4. The residue contains Structureless Organic Matter (SOM).
5. The residue contains carbonized palynomorphs and coal particles.
6. Other.

	ANALYZE	DECISIONS
1	processing was satisfactory	both slides can be mounted
2	residue contains still minerals	apply heavy liquid separation
3	residue contains organic-like light minerals	apply bleaching in 30% or 70% HNO_3
4	residue contains SOM	a - bleaching by oxidation or reduction b - ultrasonic treatment c - combination of a and b d - new strategies are needed
5	residue contains carbonized palynomorphs and coal particles	bleaching - mostly with Schulze's reagent
6	other	new strategies are needed

1.3.7 Mineral – Heavy liquid separation ($ZnCl_2$)

- In the heavy liquid, the heavy minerals will sink while the lighter organic material keeps floating.

The accepted compromise is possible loss of palynomorphs due to its weight and/or floating abilities and little bit of bleaching.

1.3.8 Pyrite, SOM, coal fragments – Bleaching

- Bleaching is done as careful as possible.
- The choice of oxidizing reagents will be:
  - Thin household bleach.
  - HNO_3 30%.
  - HNO_3 70%.
  - HNO_3 98% (fuming).
  - KOH 10%.
  - Schulze's reagent.

The choice is dependent of the state of the material and choice of reagent needs experience of the processor.

The accepted compromise of bleaching are color changes, the possible damaging and/or loss of material.

Slides for the microscope should be perfect!

2 Standard palynological rock sample processing method.

What is palynological processing?
Palynological processing is isolating organic material from sediments
Palynological processing implies, finding solutions for problems.
Palynological processing is making decisions about solutions.
Palynological processing is accepting compromises.

Palynology is processing!

The procedures described in the following pages applies specifically the Utrecht Laboratory (Geolab). They are based on experience and equipment gained over the last years.
All procedures ultimately are compromises depending specific research goals available amount of money, available amount of working space, time, laboratory equipment, etc.

2.1 About using a centrifuge

- Before using chemicals to a sample it is necessary to remove the preciously used chemicals or water.
- In order to reach that goal a separation of the sediment and the liquids by decantation is needed.
- Careful decantation is possible after leaving the material standing over one night.
- To increase the settling rate (to about four hours) the specific gravity of the liquid (sg of HCl and HF is 1.2) should be decreased by diluting the liquid with at least twice the volume with water.
- The use of a centrifuge is only a way to increase the settling rate (5-10 minutes).
- The disadvantage of using the centrifuge is, however, that the force exerted on the material might damage it.
- Depending on the temperament of the processor, the time available and expected fragility of the material the best way of separation of sediment and liquid is chosen.
- Centrifugation is prohibited with HF, only if there is no other option. You can centrifuge with HCl.

- The centrifuge is used to obtain a rapid settling.
- The speed (RPM) used depends on the centrifugal force (RCF) according to the following table concerning the MSE centrifuges "Mistral" and "Centaur".

FORCE RCF	**MISTRAL SPEED RPM**	**CENTAUR SPEED RPM**	**FORCE RCF**
170	850	1000	170
370	1300	1500	370
680	1700	2000	680
1000	2100	2500	1000
1500	2600	3000	1500

- Centrifuging is generally performed at a force of **2200 RPM**. Heavy liquid separation ($ZnCl_2$) is performed at a force of **1100 RPM**.
- The shaking apparatus is used to obtain 100% contact surface between material and Fluoric acids.
- The vortex is used for homogenization (to loosen the bottom before adding chemicals).
- The ultrasonic bath is used to disintegrate clusters and lumps of small particles, and to clean the sieves.

3 From sediments to palynological preparation slides for the light microscope.

3.1 This are the steps.

1. **Drying or not drying samples.**
2. **Preparing samples.**
3. **Removal of contaminants from the rock sample.**
4. **Mechanical disaggregation of rock samples.**
5. **Dissolution and removal of carbonates.**
6. **Dissolution and removal of silicates and minerals.**
7. **Dissolution and removal of SiF_4.**
8. **Repeating step 6 and 7**
9. **Sieving**
10. **Making residues.**
11. **Separation of organic material from remaining unsolved mineral matter.**
12. **Bleaching.**
13. **Preparation of slides for light microscope.**
14. **Storage**

3.1.1 Step 1 Drying or not drying samples

Requirements: what do you need?

- Oven on 60º C or freeze dryer

3.1.2 Step 2 Preparing samples

- If you need an oven, use for the samples, labeled plastic petri dishes. Go to step 3.1.3. follow it further.
- If you need to freeze dry, first label the 180 ml sample pots (pot and lid) and weigh the pots empty (with lid). After that go further to step 3.1.3 and 3.1.4, by step 4 when you have crushed your sample put it in the 180 ml sample pot, weigh the sample roughly on an upper scale. After that on an analytic balance for the precise weight. Everything is then with lid.
- If you doing pilot samples, you can do it quick and dirty. No drying and roughly weighing on a upper scale balance, use 30% HCl.

3.1.3 Step 3 Removal or contaminants from rock samples

Requirements: what do you need?

- Potato knife
- Point extraction

- Clean the sample carefully by scraping with a potato knife above a trash bin, and if it is very dusty also work under a point extraction.

3.1.4 Step 4 Mechanical disaggregation of rock samples

Requirements: what do you need?

- Porcelain mortar and pestle
- Tea towels
- Upper scale balance
- Sample pots 180 ml PP, lid LDPE
- Edding pen
- Tray to put your samples pots on
- Hammer/fist hammer and anvil
- Analytical balance
- Point extraction
- Petri dishes (plastic)

- Ordinary plastic bags and Geobags
- Weighing paper
- Water
- Brush
- Paper from the paper roll

- Label the 180 ml sample pots (pot and lid).
- Crush between 0-20 grams (depending on the expected amount of palynomorphs) of consolidated rocks to ± 2-5 mm^2 sized particles. NO POWDER!
- Use porcelain mortar and pestle, if the material is to hard use a hammer/fist hammer and anvil by putting in an ordinary plastic bags or Geobag.
- If you used an oven; your samples are in labeled plastic petri dishes and leave them open with lid underneath in the oven on 60º C for a night.
- Next day; fold weighing papers, place your pots ready by the analytic balance, find the right Excel file and get it ready. Get your samples out of the oven.
- Open the pot and put it on the scale and set on zero, get the pot out place the weighing paper into the pot and with help of the weighing paper you put your sample in the pot. You can throw the petri dishes and weighing paper in the trash bin.
- Put the pot and sample on the scale and weight that again.
- Put the lid on the pot, do that with all the samples and then you are finished to start step 5, the chemical part.

3.1.5 Step 5 Dissolution and removal of carbonates

- Lycopodium spore tablets
- Agepon 1:200 (Wetting agent)
- Hydrochloric acid (HCl) 10% and/or 30%
- Alcohol 96%
- Water
- Water jug
- Small trash bin
- Waste bin for chemicals (use the right one!!!), already been labelled, ± 10% HCl
- Funnel
- Storage shelf to put up your samples on
- Neoprene green gloves + neoprene black gloves (lab coat and safety glasses)

- Open the waste bin and place the funnel on the waste bin.
- Take the spray bottle (s) of HCl and place the nozzle above the small waste container.
- Open de pots in the fume cupboard (lid behind the pot and as far as possible in to the back of the fume cupboard).
- Add with a tweezer one lycopodium spore tablet and let it fall in the middle (note later which one you use).
- Moisten the samples with Agepon 1: 200 (wetting agent) and also go over the lycopodium spore tablet. Do not use too much, it is a soap solution.
- Add a little bit of 10% HCl from the side and then the middle (NOT TO MUCH).
- Let it react with the 10% HCl, swirl (grab the pot as low as possible, the vortex stops at the height where you hold the pot with your fingers highest).
- Add another little bit of 10% HCl at your sample and swirl, the same as what you already did before.
- Be sure that the bottom is now completely loose.
- DON'T CONTINUOUSLY ADD 10% HCl, LET SAMPLE FIRST REACT! AND WHEN IT FALLS A BIT OF DEATH, SWIRL, NO REACTION, ADD 10% HCl.
- If you keep adding acid, the lycopodium can also become saturated.
- Prevent strong reaction by slowly adding 10% HCl.
- Do not use more than half of your pot with 10% HCl, see marking on the pot what the top is (See picture "Top of the pot").

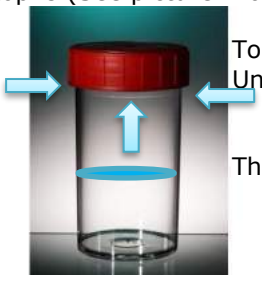

Top of the pot.
Underneath the lid you see a line, that is the top of pot.

This is half of the pot.

- If the reaction is to strong, you can use some drops of ethanol/alcohol 96%.Do not use too much, you will stop the whole reaction.
- If the reaction is finished, fill up the pot with water with a water jug. Fill up ± a centimeter under the top. Put the lid on the pot.
- Leave the sample settle overnight, on the storage self.
- Decant after sedimentation and fill up again with water (see previous how you fill it up).

Transport samples to the HF lab.

- Do not put on the acid apron and sleeves just yet, because you are not yet working with HF.
- Place the sample pots on the transport trolley and bring them to the HF lab.
- Place the samples in the centrifuge as explained at step 6.
- If you are completely finished at the HCl fume hood, put then the acid apron and sleeves on (because you are now stay in the HF lab).
- It is not allowed to come into the other room 5.26 when you have the acid apron and sleeves on.

3.1.6 Step 6 Dissolution and removal of silicates and minerals

<u>Requirements: what do you need?</u>

- Transport trolley + tray to put your samples on
- Hydrofluoric acid (HF) ± 40%
- Water + water spray bottle
- Centrifuge + buckets and inserts
- Balance to weigh the buckets with inserts
- Water jug
- Vortex
- Shaking machines
- Storage racks to put up your samples on
- Neoprene green gloves + neoprene black gloves, acid apron, acid sleeves (safety glasses and lab coat).

- Make the balance that you put on the buckets and inserts equal that the needle is in the middle. If the needle is moving too much, open de window till "working height" and step back to see if the needle comes to rest in the middle. If not fill up the one that is less heavy until the needle is in the middle.
- Place the buckets with insert on the balance just outside of the middle.
- Open the sample pot and put the lid next to the bucket on the scale. Grab the sample pot by the screw rim and guide it into the insert. Do that also with the other sample pots.
- Make the sample pots equal by adding water and repeat it for all the sample pots. If the needle is moving too much, open de window till "working height" and step back to see if the needle comes to rest in the middle. If not fill up the one that is less heavy until the needle is in the middle.
- Grab the sample pot by the screw rim to get it out of the bucket, put the lid on the sample. Make sure your lid is a little bit open for the centrifugal force.
- Put the sample pot with lid back in the bucket, grab it just under the lid (lid is loose!!!), and guide it in the bucket (do not drop it). Repeat that also with the other sample pot.
- Put in centrifuge on the opposite of each other, and then close the lid of the centrifuge.
- Centrifuge, speed 2200 RPM for 5 minutes, acc 9, dec 6
- Centrifuge finished ("End of run", open lid.
- Grab lid of the sample pot and immediately the pot (lid is loose!!!). Place the sample pot on the edge of the centrifuge and close the lid of the sample pot.
- Place it by the side window, to transfer it to the middle fume hood.
- Place another run in the centrifuge, till all runs are finished.
- If you were completely finished in the HCl fume hood, you can put now the acid apron and sleeves on.
- Decant, as far as possible (ideal is completely).
- Loosen the bottom with the vortex (if there is still liquid in it, mix it), make sure you have the lid on the pot.

- Add the HF ± 40% in 4 steps. There is a lot of degrees of heat what the HF can be, from cold to boiling.
    - First step: Add about 5 drops combined of HF ± 40%. Mix and DO NOT look into it (can react heavily and might be boiling and then if you look into it, it comes boiling towards you and you let it fall).
    - Second step: Mix and then add the HF ± 40% to one centimeter to another half a centimeter, mix. Check the bottom if it is completely loose.
    - Third step: Fill up to a quarter.
    - Fourth step: Fill up to under half.
- Place the lid on the jar and move it to the shaking machine.
- Place the jars (with a temperature of ± shower heat) on the shaking machine with a good twist (more then with the centrifuge). Make a row of sample pots and fix the bars tightly that they do not dance (move).
- Shake, speed 250 RPM for 120 minutes (2 hours).
- Finished with shaking, remove the sample pots, one by one, and close lids immediately.
- Remove the black belt with a water spray bottle and fill up the pot with water till a centimeter under the top (see picture "top of the pot").
- Leave the samples to settle overnight (At least 8 hours).

3.1.7 Step 7 Dissolution and removal of SiF_4

Requirements: what do you need?

- Hydrochloric acid (HCl) 30%
- Water + water spray bottle
- Centrifuge + buckets and inserts
- Balance to weigh the buckets with inserts
- Water jug
- Neoprene green gloves + neoprene black gloves, acid apron, acid sleeves (safety glasses and lab coat).

- Decant, as far as possible (ideal is completely).
- Loosen the bottom to mix.
- Add an excess of 30% HCl (3x the amount what already is in the pot, sample and liquid) and if there is room for it, fill it up with water to a centimeter below the top.
- Make the balance that you put on the buckets and inserts equal that the needle is in the middle. If the needle is moving too much, open de window till "working height" and step back to see if the needle comes to rest in the middle. If not fill up the one that is less heavy until the needle is in the middle.
- Place the buckets with insert on the balance just outside of the middle.
- Open the sample pot and put the lid next to the bucket on the scale. Grab the sample pot by the screw rim and guide it into the insert. Do that also with the other sample pots.
- Make the sample pots equal by adding water and repeat it for all the sample pots. If the needle is moving too much, open de window till "working height" and step back to see if the needle comes to rest in the middle. If not fill up the one that is less heavy until the needle is in the middle.
- Grab the sample pot by the screw rim to get it out of the bucket, put the lid on the sample. Make sure your lid is a little bit open for the centrifugal force.
- Put the sample pot with lid back in the bucket, grab it just under the lid (lid is loose!!!), and guide it in the bucket (do not drop it). Repeat that also with the other sample pot.
- Put in centrifuge on the opposite of each other, and then close the lid of the centrifuge.
- Centrifuge, speed 2200 RPM for 5 minutes, acc 9, dec 6. Make sure your lid is little bit open for the centrifugal force.
- Centrifuge finished ("End of run", open lid.
- Grab lid of the sample pot and immediately the pot (lid is loose!!!). Place the sample pot on the edge of the centrifuge and close the lid of the sample pot.
- Place it by the side window, to transfer it to the middle fume hood.
- Place another run in the centrifuge, till all runs are finished.
- Decant, as far as possible (ideal is completely).

3.1.8 Step 8 Repeating step 6 and step 7

See for requirement step 6 and step 7.

- Loosen the bottom with the vortex (if there is still liquid in it, mix it), make sure you have the lid on the pot.
- Put a little bit of HF ± 40% on your sample, mix it, and get loosen the bottom completely.
- Fourth step of step 6: Fill up to under half.
- Follow everything of step 7.
- And end with a centimeter of water.

3.1.9 Step 9 Sieving

Requirements: what do you need?

- Box where you put your sample pots in
- Test tubes 15 ml glass
- Test tube racks
- Dust covers
- Marker
- Ultrasonic bath
- Porcelain bowl
- Sieves (10, 15, 250 µm)
- Beaker (white, old HF bottle, top cut off)
- Water + water spray bottle
- Sobo S Gold
- Agepon 1:200
- Vibraguard glove
- Neoprene green gloves (safety glasses and lab coat)
- Centrifuge + buckets and inserts

- Put a neoprene gloves (green) on and one bigger size over the Vibraguard glove. Put the Vibraguard glove off and ready.
- First clean the ultrasonic bath.
- Close the tap of the ultrasonic bath.
- Fill the ultrasonic bath with cold water to operating level.
- Lay sieve 250 µm on top of the ultrasonic bath on its side. And sieve 10 µm number 1 left, and sieve 10 µm number 2 right underneath that on its side (See picture).

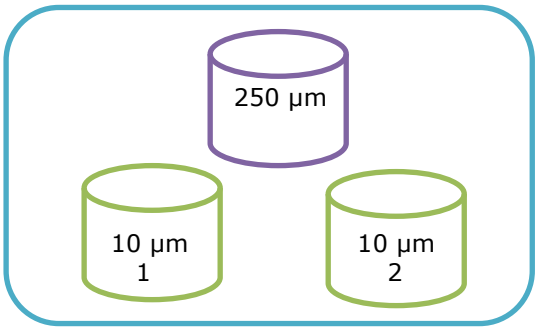

- Turn on the ultrasonic bath for 5 minutes, put the lid and tea towel back on the ultrasonic bath. Cleaning of the sieves.
- Label the test tubes and put them upside down in a test tube holder with dust cover. Grab an extra test tube holder.
- Clean the white beaker with soap, brush and warm water.
- Clean the porcelain bowl.
- Empty the water spray bottle, rinse it, and fill up with new water.
- Now we can start.
- Grab the sample pot you want to start with out of the box says "Box samples to sieve".

- Rinse the sieve 250 µm with water. And the sieve cloth by squeezing the hose with a hard jet of water.
- Take the clean white beaker and place the rinsed 250 µm sieve on top of it (it doesn't fit inside). Be sure that the sieve is more horizontal instead of diagonal.
- First loosen the bottom of the sample in the pot.
- Open the lid of the sample pot.
- Clean the lid above the 250 µm sieve.
- Turn on the tap (not too hard, just that the air is out of the hose). Fill up the pot via the sides and then in the middle, until a 1 cm under the top.
- Decant the pot over the 250 µm sieve.
- Hold the pot close to the bottom. Now you going to pour out, clean and turn through your fingers until it is completely clean.
- Rinse the pot again with the hose. First along the sides and then by squeezing the hose with the hard jet of water. Pour immediately over the 250 µm sieve. Repeat filling up with the hard water jet again. Pour immediately over the 250 µm sieve.
- You can now throw the pot away.
- Use the water spray bottle to clean the inside sides and the sieve cloth of the sieve.
- Rinse the sieve 250 µm with water. And the sieve cloth by squeezing the hose with a hard jet of water. And then put it back in the ultrasonic bath.
- Clean the sink, also the mat and underneath what is in the sink.
- Place the white beaker in the sink, go through the sides of the beaker with the water hose. Do not use too much water, the white beaker is now half / three quarters full. Remove the white beaker from the sink and put it on the table.
- Take the 10 µm number 1 or 15 µm number 1 sieve from the ultrasonic bath and rinse it, the same as what you did with the 250 µm sieve.
- As an option you can dry the outside of the side of the sieve.
- Pour (dash on the side of the white beaker, pouring edge) no more than half of your sieve with the water and sample over your sieve.
- Sieving: By making a slow circular motion from the wrist and tapping hard, firm and fast with the other hand with your fingers.
- You continue until your white beaker is empty.
- Place the sieve on the table just over the edge.
- Clean the white beaker with the water spray bottle, first the side and then the bottom and then pour and clean completely.
- If necessary, turn and tap the sieve again.
- ALWAYS MAKE SURE YOUR WATER SPRAY BOTTLE IS FULL!!!
- Place the sieve in the back of the sink (slightly slanted), rinse the white beaker 3 times by squeezing the hard water jet with as little water as possible.
- Turn and tap the sieve again.
- Remove the other sieves from the ultrasonic bath and place them upside down on the tea towel.
    A. Put on the Vibraguard glove.
    B. Make a circular motion with the sieve with the hand without the Vibraguard glove in the ultrasonic bath, and ensure that no air remains under the sieve.
    C. Put the sieve in the hand where you have the Vibraguard glove on.
    D. Put the ultrasonic bath on (minutes or on hold).
    E. Let it vibrate so that the remaining organic stuff falls apart. Lift the sieve up a bit so that it draws vacuum and the water goes out. Then let water flow in again by lowering the sieve. Repeat this a few times, until no brown / black clouds come under the sieve.
    F. Then view the material in the sieve to see how it looks. Looks like dots then you can continue, if you see fluffy stuff then you should continue with the ultrasonic bath with vibrating.
    G. If you can continue, go further with H.
    H. Get the water out (make sure that no air comes under the sieve).
    I. Clean the side of the inside of the sieve with the water spray bottle (make sure that no air comes under the sieve).
    J. Get the water out (make sure that no air comes under the sieve).
    K. Sieve can now come out of the ultrasonic bath and the ultrasonic bath can now be switched off.
    L. Dry the porcelain bowl with a piece of paper.

M. Place your fingers under the sieve and your thumb on it.

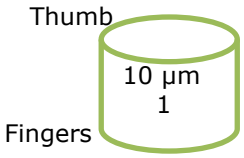

N. Make a "Z" with the water spray bottle on the sieve to bring everything down.
O. Pour the sample in the porcelain bowl.
P. Use hard bumps against the sieve cloth with the water spray bottle to clean the sieve cloth as far as possible.
Q. Spray with the water spray bottle from the nozzle and inside of the sieve (for cleaning and there must be water in the sieve).
R. Repeat A. to P., this is a cleaning step of the sieve, to have everything in the porcelain bowl.
S. Homogenize the material in the porcelain bowl (but not too full, otherwise it can sink!).
T. Place the sieves what is on the tea towel back in the ultrasonic bath.
U. Carefully place the porcelain bowl in the ultrasonic bath (do not drop it in the ultrasonic bath).
V. Put the lid on the ultrasonic bath and turn the ultrasonic bath on for ± 5 minutes, then place the tea towel over the ultrasonic bath.
W. Re-homogenize after ± 2½ minutes, place the tea towel over the ultrasonic bath.
X. After the ± 5 minutes have elapsed, remove the tea towel and lid. And then remove the porcelain bowl from the ultrasonic bath.
Y. Hold the porcelain bowl completely above the sieve.
Z. Do not pour the material into the porcelain bowl too quickly or slowly, stop when you see a haze of brown / black stuff.
AA. Clean the bottom of the porcelain bowl with the water spray bottle above the sieve.
BB. Spray with the water spray bottle from the nozzle and side of the inside of the porcelain bowl, to fill it up and homogenize again.
CC. Carefully place the porcelain bowl in the ultrasonic bath (do not drop it in the ultrasonic bath).
DD. Put the ultrasonic bath on (minutes or on hold), this step is done fairly briefly, until there is a nice separation again between the heavy part and the floating part.
EE. After leaving it for a short time in the ultrasonic bath, remove the porcelain bowl from the ultrasonic bath.
FF. Hold the porcelain bowl completely above the sieve and then you can continue pouring (slowly!). If you do that the flow will stop automatically.
GG. Clean the bottom of the porcelain bowl with the water spray bottle above the sieve.
HH. Remove the other sieves from the ultrasonic bath and place them upside down on the tea towel.
II. Check the residue that is now in the sieve into a water slide if other action is needed. More ultrasonic bath, Sobo (is only rinsing in the sieve), Agepon (is only rinsing in the sieve), Schulz, HNO_3, KOH, heavy liquid ($ZnCl_2$) or maybe something else.
JJ. Repeat A. to Q., but instead of porcelain bowl we use test tube.
KK. With L. you prepare the test tube.
LL. And between N. and P., place the nozzle on the test tube and make a path from outside to inside with as little water as possible.
MM. Do not use more than half of the test tube.
NN. Repeat A. to P., but now it follows the path that you already made.
OO. Rinse the sieve and put it back in the ultrasonic bath.
PP. Place the other sieves that is on the tea towel back in the ultrasonic bath.
QQ. Finished, you can start with the next sample to sieve.

- Centrifugation of the test tubes:

- When you are done with sieving for the day, it is desirable that you centrifuge the test tubes. You can also centrifuge the test tubes in between, for example during a break.
- Prepare the balance that you put on the buckets and inserts equal that the needle is in the middle.
- Place the buckets with insert on the balance with your tubes. The tubes have to be diagonal equal to each other.

Picture 1

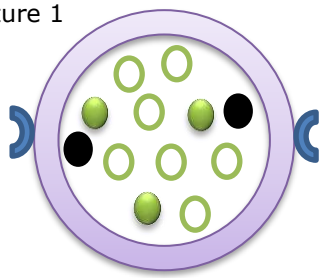

= Where you grab the insert.

= Empty holes where you can put test tubes.

= Full with a test tube.

= Place where you hang the bucket in the centrifuge.

Always use 2 dummy test tubes to make the buckets, insert and test tubes equal.
On the bucket itself you have 2 have moons where you put the things that you grab the insert.
The test tubes in both buckets + inserts are placed in the same place.
Then turn both buckets inside or outside. Hang them then the same as you have it now in the centrifuge (see picture 1 and 2).

Picture 2

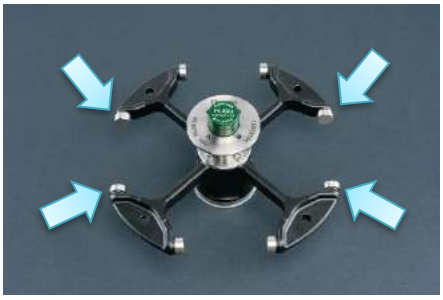

= Where you hang the buckets.

- Centrifuge, speed 2200 RPM for 5 minutes, acc 9, dec 0.

3.1.10 Step 10 Making residues

Requirements: what do you need?

- Centrifuge + buckets and inserts
- Water spray bottle
- Balance for buckets
- Residue vials
- Labels
- Adhesive tape
- Corks
- Safe lock tubes (1,5 ml)
- Pasteur pipettes
- Deionized water
- Pasteur pipettes balloon
- Glycerin water
- Lab dancer
- Water
- Demineralized water

➢ After centrifugation it depends on what slides you are going to make. Glycerin gelatin (with cover varnish or candle wax) or permanent mounting. And whether you need to do other analyzes such as heavy liquid (too much minerals left in

relation with the organic matter) bleaching (too much Structureless Organic Matter (SOM), too many carbonized palynomorphs and coal particles) etc.
- Pipette off the water from the test tube or decant. If there is very little residue or making permanent mounting slides pipette with Pasteur pipette.
- If there is no action needed go further with 3.1.10.1 or 3.1.10.2.
- If there is action needed go further with 3.1.11 and/or 3.1.12.

3.1.10.1 Preparing for glycerin gelatin slides with cover varnish or candle wax

Preparing for glycerin gelatin slides with cover varnish

- First label the residue vials with your label and adhesive tape, and place them in a residue vial holder.
- After centrifuging, pipette off or decant the water that is in the test tube.
- Dry the outside of the test tube after you decanted the test tube.
- Make sure you always pour on the same side of the test tube.
- Drop about 5 drops of glycerin water into the test tube and mix (make family).
- Take the residue vial and tilt it, vortex the test tube on the lab dancer.
- Now place the test tube on the residue vial and pour until the liquid is on the rim, and then pour on.
- Place the residue vial if you are right-handed in front on the right-hand side, if you are left-handed on the left-hand side in the holder.
- Clean the test tube with as little of glycerin water as possible and as many times as possible.
- Drop just below where the liquid of the water was, do not use more than 5 drops at a time. Spread the drops over the entire side of the inside of the test tube.
- If it is greasy on the inside, keep the test tube slightly horizontal and let the liquid go from the bottom to the edge where the water in the test tube was filled and go back, turn the test tube a little bit. Then you continue until you have had the whole tube.
- Mix the residue and liquid with lab dancer or in your hand.
- You can now leave the residue vial in the residue vials holder and pour into the residue vial.
- Keep repeating this until the residue vial is almost full and the cork still fits on it.
- Repeat this for all your samples.
- Centrifuge the residue vials, speed 2200 RPM for 5 minutes, acc 9, dec 0.
- The explanation how, you see how you centrifuge the tubes. Only now you use the dummy residue's or safe lock tubes. And place them on the tray before the buckets to make them equal and not in the insert.
- After centrifuging, pipette off or decant the liquid that is in the residue vial.
- Dry the outside of the residue vial after you decanted the residue vial.
- Put the cork on the residue vial.
- Finished to make glycerin gelatin slides.

Preparing for glycerin gelatin with candle wax

- First label the safe lock tubes with your label and adhesive tape, and place them in a residue vial holder.
- After centrifuging, pipette off or decant the water that is in the test tube (see also here above how).
- Make sure you always pour on the same side of the test tube.
- Take the safe lock tube and tilt it, vortex the test tube on the lab dancer.
- Now place the test tube on the safe lock tube and pour until the liquid is on the rim, and then pour on.
- Place the safe lock tube if you are right-handed in front on the right-hand side, if you are left-handed on the left-hand side in the holder.
- Clean the test tube with as little of water as possible and as many times as possible.
- Drop just below where the liquid of the water was, do not use more than 5 drops at a time. Spread the drops over the entire side of the inside of the test tube.
- If it is greasy on the inside, keep the test tube slightly horizontal and let the liquid go from the bottom to the edge where the water in the test tube was filled and go back. Then you continue until you have had the whole tube.
- Mix with lab dancer or in your hand.

- You can now leave the safe lock tube in the residue vial holder and pour into the safe lock tube.
- Keep repeating this until the safe lock tube is almost full until the lid still fits on it.
- Repeat this for all your samples.
- Centrifuge the safe lock tubes, speed 2200 RPM for 5 minutes, acc 9, dec 0.
- When the safe lock tubes come out of the centrifuge, bring them to the correct water level in the safe lock tubes. You bring them to 1 ml.

3.1.10.2 Preparing for permanent mounting slides

- First label the safe lock tubes with your label and adhesive tape, and place them in a residue vials holder. Immediately get the same number of safe lock tubes for making slides.
- After centrifuging, pipette off or decant the water that is in the test tube.
- Make sure you always pour on the same side of the test tube.
- Drop about 5 drops of deionized water into the test tube and mix (make family).
- Take the safe lock tube and tilt it, vortex the test tube on the lab dancer.
- Now place the test tube on the safe lock tube and pour until the liquid is on the rim, and then pour on.
- Place the safe lock tube if you are right-handed in front on the right-hand side, if you are left-handed on the left-hand side in the holder.
- Clean the test tube with as little of deionized water as possible and as many times as possible.
- Drop just below where the liquid of the water was, do not use more than 5 drops at a time. Spread the drops over the entire side of the inside of the test tube.
- If it is greasy on the inside, keep the test tube slightly horizontal and let the liquid go from the bottom to the edge where the water in the test tube was filled and go back. Then you continue until you have had the whole tube.
- Mix with lab dancer or in your hand.
- You can now leave the safe lock tube in the residue vials holder and pour into the safe lock tube.
- Keep repeating this until the safe lock tube is almost full until the lid still fits on it.
- Repeat this for all your samples.
- Centrifuge the safe lock tubes, speed 2200 RPM for 5 minutes, acc 9, dec 0.
- Finished to make permanent mounting slides.

3.1.11 Step 11 Separation of organic material from remaining unsolved mineral matter

- Add approximately 8 ml of heavy liquid ($ZnCl_2$) to the constantly homogenized residue with a lab dancer and allow the samples to stand overnight or centrifuge with as little as possible acceleration for 10 minutes without a break. Centrifuge, speed 1100 RPM, for 10 minutes, acc 1, dec 0.
- Use fairly hot water to pipette off the organic material that floats on the heavy liquid.
- Carefully add about 1 ml of fairly hot water to the floating organic material.
- Transport the floating material with a Pasteur pipette to a white beaker. Place the Pasteur pipette on the separation of organic material with fairly hot water and the heavy liquid ($ZnCl_2$) and pipette it off. Also transfer the column of the solution to the white beaker. And fill up with fairly hot water to about half / three quarters.
- Continue with step 9 Sieving, throw away the pellet of the heavy material and follow those steps and continue further with the other steps. You can use the same test tube for the residue when it is empty.

3.1.12 Step 12 Bleaching

- First find out which method of bleaching you need. HNO_3, KOH, Schulz, etc.
- Add approximately 5-10 ml of oxidizing reagent to the homogeneous residue, it depends what you going to use.
- If necessary, you can also heat it in a heating block. Place the test tubes in the heating block for about 1-10 minutes. The time and temperature depends on the effect of the specific sample. The sample with the test tube must be exactly below or equal the level of the heat block, and not above it.
- You can stop the reaction of, for example, HNO_3 or Schulz with 10% KOH, fill the test tube completely.

- Centrifuge.
- Transfer the residue to a white beaker and fill up with water to half / three quarters.
- Continue with step 9 Sieving and follow those steps and continue further with the other steps.

3.1.13 Step 13 Preparation of slides for the light microscope

- It depends what kind of slides you want to make, glycerin gelatin slides or permanent mounting slides.

3.1.13.1 Making glycerin gelatin slides with cover varnish or candle wax

Requirements: what do you need for slides with cover varnish?

- Burner with methylated spirits
- Methylated spirits
- Lighter
- Pasteur pipette
- Pasteur pipette balloon
- Glycerin water
- Glycerin gelatin
- Cover glasses 20x20 mm
- Object glasses
- Cardboard folder(s)
- Tissues
- 1 Straight preparation needle
- 1 with hook preparation needle
- 1 lancet preparation needle (looks like a scalpel)
- Point extraction
- Cover varnish
- Razorblade
- Labels
- Residues
- Wooden sticks
- Slide box

- Start by filling the burner with methylated spirits.
- Take the object glasses (without a frosted edge), coverslips 20x20 mm, glycerin water and cardboard folder(s).
- Take the preparation needles that you are going to use from the tray. Clean them with a tissue, do NOT put them through the flame.
- Take the glycerin gelatin and make small cubes that are exactly for each sample. Check your sample how much you need. Too much you have to focus too much with the microscope, too less you get very watery slides.
- Light the burner with methylated spirits.
- Place an object glass under the point extraction. Put the coverslips ready for use.
- NEVER GRAB THE OBJECT GLASS AND COVERSLIPS ON THE GLASS, PUT ON THE SIDE OF IT.
- Take the first sample residue, remove the cork and place it upside down on the table.
- Place a balloon on a Pasteur pipette. Hold the Pasteur pipette completely in your hand, so that you only use your thumb and index finger to release and close the balloon.
- Push the balloon shut and place the tip of the Pasteur pipette in the residue, by constantly sucking it up and putting it back again you homogenize the sample.
- Check the concentration of the residue, if it is too dark add glycerin water. Add drop by drop, after every drop mix and check. Look in the thinnest part of the Pasteur pipette, if you see the light through it and the particles are neatly next to each other, it's good (but it's pure guesswork).
- Once you have the correct dilution, homogenize the residue (described above) close to the object glass underneath the point extraction.
- Pick up a small portion and make sure there are no air bubbles in it, and that you have the residue in the thinnest part of the Pasteur pipette.
- Let a drop fall just outside the middle.

- Heat the drop, but do not let it boil until it is syrupy watery. Be sure that you have enough water to stir the glycerin gelatin is to the sample.
- Take a cube of glycerin gelatin with the straight preparation needle (make sure you don't poke it but leave it hanging on it) and place it on your sample on the object glass.
- Let the cube melt (still watch that it does not boil).
- Quickly stir the molten cube of glycerin gelatin through your sample, the drop may be larger than it was, and then end in the middle.
- Grab a cover slip and hold it against the flame, you see a haze go over it.
- You now use the preparation needle with the hook.
- Hold the coverslip on the side in the middle, place one side on the object glass and on the other side you can lower it slowly and carefully with the preparation needle with hook.
- Let it completely flow under the coverslip. If that doesn't work, you can heat it lightly and/or use a wooden stick.
- Stick the label on the object glass and let it solidify in the cardboard folder.
- Finished making slides, place the cardboard folder under the point extraction(as low as possible) with a piece of paper with your name on it.
- Usually after one night, you can clean the slide with a razorblade, and seal it with cover varnish.
  How do you do that.
  - Prepare 2 tissues. One tissue for wipe the excess sample/glycerin gelatin. Second tissue for underneath the object glass to apply cover varnish.
  - First place the razorblade in an angle of 45º on the object glass against the coverslip, be careful that you not pock with the tip underneath the coverslip. The razorblade has to be horizontal with the coverslip and wipe the access off. After every wipe clean the razorblade on the tissue. Clean also on top of the coverslip but be careful do not push too hard (to get the excess sample/glycerin gelatin)
  - Add the coverslip varnish. Take a big drop of cover varnish and start in the middle of the edge of the coverslip. Pull (so do not wipe) the drop to each slides. Cover only the edges + corners and seal the coverslip. You only seal the transition from coverslip to object glass. Leave a big square left in the middle to count, because under the cover varnish you cannot count. Leave the cardboard folder underneath the point extraction (as low as possible) to dry, with your name on a tissue.

<u>Requirements: what do you need for slides with candle wax?</u>

- Heating plate
- Candle wax
- 2x Eppendorf pipettes (1x 200-1000 µl + 1x 5-50 µl)
- Eppendorf pipettes point (Yellow + blue)
- Water
- Propanol
- Burner with methylated spirits
- Methylated spirits
- Lighter
- Glycerin gelatin
- Cover glasses 24x32 mm
- Object glasses
- Tissues
- 1 Straight preparation needle
- 1 with hook preparation needle
- 1 lancet preparation needle (looks like a scalpel)
- Point extraction
- Razorblade
- Labels
- Residues (safe lock tubes)
- Wooden sticks
- Slide box
- Vortex

- Start by filling the burner with methylated spirits.

- Turn on the heating plate till high (± 50ºC degrees).
- Take the object glasses (without a frosted edge), coverslips 24x32 mm, water and slide box.
- Place the amount of object glasses (slides) what you need on the heating plate, be sure that a piece of the object glass sticks out.
- Take the preparation needles that you are going to use from the tray. Clean them with a tissue, you do NOT have to get them through the flame.
- Take the glycerin gelatin and make small cubes that are exactly for each sample. They are smaller than with glycerin water samples.
- Light the burner with spirit.
- Place on an object glass the small piece of glycerin gelatin just outside the middle on a heating plate, object glass sticks out over the edge. Let de cube melt.
- Put in a blue Eppendorf tip water and place it over the edge of the table (that is for rinsing).
- Mix the safe lock tube with the vortex.
- Take the Eppendorf pipette 5-50 µl, and draw up 10 µl in a yellow Eppendorf pipette tip.
- Carefully remove the Eppendorf pipette tip from the Eppendorf pipette, the liquid with sample as to come down by pushing it down with your finger. And place it over the edge of the table.
- If glycerin gelatin cube is melted. Gently drop 1 drop onto the glycerin gelatin block.
- Stir the sample through it quickly, making sure that the drop does not become too large.
- Allow the water to evaporate before adding another drop. You can check that to put a clean coverslip above the sample, if you still see a haze then it not done.
- Continue until the Eppendorf point is completely empty.
- Add 1 drop of water from the blue Eppendorf tip to the yellow one (cleaning). Push the drop down with your finger, be careful not to push too hard that the liquid is going out.
- Repeat what you have already done with your sample.
- Stir the sample through the glycerin gelatin for the last time.
- Now wait until all the water has evaporated. You can test it by holding a cold cover slip above the material.
- When it is ready and all the water has evaporated, you can lightly heat a cover slip (hold it against the flame) and carefully lower the cover slip with a preparation needle with a hook.
- Heat with the flame a part of the coverslip that is opposite where you going to put the label. Then hold the candle wax against the coverslip and let it flow under the coverslip, now you can place it on the heating plate, as soon as it comes to the other side of the drop use the wooden sticks to extract the air. The drop needs to be closed by the candle wax.
- Then place the slide on the table (because it is cool) to solidify it.
- Remove the remaining candle wax with a razorblade, and then clean it with a piece of paper with propanol.
- Stick the label on it and then you can store it in a slide box.
- Repeat this with all the samples/slides.
- You know that the slides are good, add to your safe lock tubes 3 drops of 10% HCl.
- Finished!

3.1.13.2 Making permanent mounting slides

<u>Requirements: what do you need?</u>

- Heating plate
- UV-light (fake money detector)
- Aluminum foil (tinfoil)
- Burner with methylated spirits
- Methylated spirits
- Lighter
- Cover glasses 24x32 mm
- Object glasses
- Tissues
- Labels

- Residues (safe lock tubes)
- Wooden sticks
- Slide box
- Glue for glass
- PVA (Poly Vinyl Alcohol)
- Demineralized water
- Marker
- Hand soap
- Pasteur pipettes
- Pasteur pipette balloons
- Extra safe lock tubes
- Vortex

- Start by filling the burner with methylated spirits.
- Take the object glasses (without a frosted edge), coverslips 24x32 mm, demineralized water, PVA, UV-light, hot plate with very flat aluminum foil(tinfoil) on top, extra safe lock tubes labeled, labels and slide box.
- First you start by placing the aluminum foil (tinfoil) over the heating plate, make sure it is as flat as possible (no bumps and wrinkles).
- Turn the heating plate on and at a temperature of 35ºC degrees.
- Reduce the volume in the safe lock tubes to approximately 0.5-1 ml. It depends on the amount of sample in the safe lock tube.
- Pass the coverslips through the flame, keeping a haze over the coverslip. This is to remove the fat and filth.
- Then place the coverslips on the hotplate and ensure that they are labeled on the aluminum foil next to the coverslip.
- Put in the extra safe lock tube with a Pasteur pipette ± 3 drops of the homogenized sample/demineralized water.
- Add 3 drops of PVA, dilute it with demineralized water until you see the light through it in the thin part of a Pasteur pipette and you have the particles neatly next to each other.
- Homogenize the mixture well, suck up the mixture, but make sure you do not get any air bubbles in the thin part of the Pasteur pipette.
- Place a drop of the sample on the 4 points of the clean and dry coverslip. Then connect the dots in a square with each other, and continue filling the middle part with the rest of the material.
- Leave it on the heating plate for at least 30 minutes or more before continuing.
- When the demineralized water has completely evaporated, first start the object glasses with whatever you have done with the coverslip, hold against the flame to remove grease and filth and dry.
- Put 3 drops of "Glue for Glass" on the object glass just outside the middle.
- Turn the coverslip so that the material gets on the glue. Then let it flow out completely under the coverslip.
- Turn on the UV lamp. Hold the object glass with your coverslip for ± 10 seconds under the lamp. Check if the coverslip is stuck, you do that with your thumb over the coverslip.
- Is it good. Put some soap on the slide and use a brush and water to completely clean it.
- Stick the label on it and then you can place it in a slide box.
- Repeat this for all slides.
- You know that the slides are good, add to your safe lock tubes 3 drops of 10% HCl.
- Finished!

3.1.14 Storage

- The raw material and residues are given to the supervisors. These ensure that it is stored.

WORKING SCHEME PROCESSING ROCK SAMPLES FOR PALYNOLOGY														
Section/core			Age:			Country:			Supervisor:			Name:		
Depth	Gr	HCl-H_2O	H_2O +	HF-H_2O	HCl-H_2O	HF-H_2O	HCl-H_2O	Sieve ...μm	Standard slide	$ZnCl_2$	HNO_3 ..... %	Schulze's or KOH .... %	Other	Slide

REMARKS:

Appendix 3

Age Model

NZ-80b																	
Top Depth of interval (cm)	Bottom Depth of interval (cm)	Average Depth of interval (cm)	Bulk Density (g/cm3)	210Pbxs Activity (dpm/g)	Decay Corrected 210Pbxs Activity (dpm/g)	Decay Corrected 210Pbxs error (dpm/g)	137Cs Activity (dpm/g)	137Cs error (dpm/g)	Year, Top of Interval (cm)	Year, Bottom of Interval (cm)	Year, Average of Interval (cm)	Year Std. Dev.	Year Std. Dev /2	LAR (cm/yr)	MAR (g/cm3/yr)	MAR (g/cm3/yr) Std. Dev.	MAR Std. Dev./2
0,00	0,20	0,10	0,24	12,96	12,96	0,45	0,00	0,00	2020,12	2019,89	2020,01	3,25	1,63	0,89	0,21	0,04	0,02
0,20	0,40	0,30	0,15	12,57					2019,89	2019,76	2019,83	3,26	1,63	1,12	0,16	0,04	0,02
0,40	0,60	0,50	0,21	12,18					2019,76	2019,57	2019,67	3,26	1,63	1,10	0,23	0,04	0,02
0,60	0,80	0,70	0,26	11,79					2019,57	2019,35	2019,46	3,26	1,63	1,04	0,27	0,04	0,02
0,80	1,00	0,90	0,31	11,40					2019,35	2019,09	2019,22	3,27	1,64	0,97	0,30	0,04	0,02
1,00	1,20	1,10	0,29	11,01					2019,09	2018,85	2018,97	3,28	1,64	0,95	0,27	0,04	0,02
1,20	1,40	1,30	0,29	10,61					2018,85	2018,62	2018,74	3,28	1,64	0,93	0,27	0,04	0,02
1,40	1,60	1,50	0,33	10,22					2018,62	2018,36	2018,49	3,29	1,64	0,91	0,30	0,04	0,02
1,60	1,80	1,70	0,40	9,83					2018,36	2018,06	2018,21	3,30	1,65	0,88	0,35	0,04	0,02
1,80	2,00	1,90	0,39	9,44					2018,06	2017,78	2017,92	3,30	1,65	0,86	0,33	0,04	0,02
2,00	2,50	2,25	0,32	9,05	9,05	0,35	0,17	0,03	2017,78	2017,21	2017,50	3,32	1,66	0,86	0,28	0,04	0,02
2,50	3,00	2,75	0,38	8,96					2017,21	2016,54	2016,88	3,33	1,67	0,84	0,32	0,04	0,02
3,00	3,50	3,25	0,45	8,87					2016,54	2015,72	2016,13	3,35	1,68	0,80	0,36	0,04	0,02
3,50	4,00	3,75	0,41	8,78					2015,72	2014,98	2015,35	3,37	1,69	0,78	0,32	0,04	0,02
4,00	4,50	4,25	0,38	8,69					2014,98	2014,27	2014,63	3,39	1,70	0,77	0,30	0,04	0,02
4,50	5,00	4,75	0,43	8,60					2014,27	2013,46	2013,86	3,42	1,71	0,75	0,33	0,04	0,02
5,00	5,50	5,25	0,45	8,51					2013,46	2012,59	2013,02	3,44	1,72	0,73	0,33	0,04	0,02
5,50	6,00	5,75	0,48	8,42					2012,59	2011,66	2012,12	3,47	1,74	0,71	0,34	0,04	0,02
6,00	6,50	6,25	0,36	8,33	8,33	0,31	0,10	0,02	2011,66	2010,94	2011,30	3,50	1,75	0,71	0,26	0,04	0,02
6,50	7,00	6,75	0,43	8,23					2010,94	2010,08	2010,51	3,53	1,76	0,70	0,30	0,04	0,02
7,00	7,50	7,25	0,44	8,13					2010,08	2009,19	2009,63	3,56	1,78	0,69	0,30	0,04	0,02
7,50	8,00	7,75	0,46	8,03					2009,19	2008,24	2008,71	3,59	1,80	0,67	0,31	0,03	0,02
8,00	8,50	8,25	0,45	7,93					2008,24	2007,31	2007,77	3,63	1,82	0,66	0,30	0,03	0,02
8,50	9,00	8,75	0,49	7,83					2007,31	2006,27	2006,79	3,68	1,84	0,65	0,32	0,03	0,02
9,00	9,50	9,25	0,42	7,74					2006,27	2005,36	2005,81	3,72	1,86	0,64	0,27	0,03	0,02
9,50	10,00	9,75	0,46	7,64					2005,36	2004,34	2004,85	3,77	1,88	0,63	0,29	0,03	0,01
10,00	11,00	10,50	0,47	7,54	7,54	0,20	0,09	0,01	2004,34	2002,19	2003,26	3,86	1,93	0,61	0,29	0,03	0,01
11,00	12,00	11,50	0,52	6,79					2002,19	1999,90	2001,04	3,98	1,99	0,59	0,31	0,03	0,02
12,00	13,00	12,50	0,44	6,04					1999,90	1998,06	1998,98	4,10	2,05	0,59	0,26	0,04	0,02
13,00	14,00	13,50	0,54	5,29					1998,06	1995,93	1996,99	4,22	2,11	0,58	0,32	0,04	0,02
14,00	15,00	14,50	0,51	4,54					1995,93	1994,10	1995,02	4,33	2,17	0,58	0,30	0,05	0,02
15,00	16,00	15,50	0,58	3,79					1994,10	1992,27	1993,18	4,43	2,22	0,57	0,33	0,06	0,03
16,00	17,00	16,50	0,59	3,04	3,04	0,22	0,00	0,00	1992,27	1990,69	1991,48	4,51	2,26	0,58	0,34	0,07	0,04
17,00	18,00	17,50	0,59	2,91					1990,69	1989,11	1989,90	4,58	2,29	0,58	0,34	0,07	0,04
18,00	19,00	18,50	0,62	2,78					1989,11	1987,44	1988,27	4,67	2,33	0,58	0,36	0,07	0,03
19,00	20,00	19,50	0,62	2,65					1987,44	1985,77	1986,60	4,76	2,38	0,58	0,36	0,06	0,03
20,00	21,00	20,50	0,58	2,52	2,52	0,14	0,00	0,00	1985,77	1984,19	1984,98	4,86	2,43	0,58	0,34	0,06	0,03
21,00	22,00	21,50	0,64	2,44					1984,19	1982,42	1983,31	4,98	2,49	0,58	0,37	0,06	0,03
22,00	23,00	22,50	0,62	2,35					1982,42	1980,68	1981,55	5,09	2,55	0,58	0,36	0,07	0,03
23,00	24,00	23,50	0,66	2,27					1980,68	1978,79	1979,73	5,21	2,60	0,58	0,38	0,08	0,04
24,00	25,00	24,50	0,62	2,19					1978,79	1976,99	1977,89	5,33	2,66	0,58	0,36	0,08	0,04
25,00	26,00	25,50	0,56	2,11					1976,99	1975,31	1976,15	5,43	2,72	0,58	0,33	0,09	0,04
26,00	27,00	26,50	0,66	2,02	2,02	0,19	0,00	0,00	1975,31	1973,31	1974,31	5,54	2,77	0,58	0,38	0,10	0,05
27,00	28,00	27,50	0,61	2,09					1973,31	1971,27	1972,29	5,66	2,83	0,57	0,35	0,09	0,05
28,00	29,00	28,50	0,62	2,15					1971,27	1969,00	1970,14	5,80	2,90	0,57	0,35	0,09	0,05
29,00	30,00	29,50	0,62	2,21					1969,00	1966,49	1967,75	5,98	2,99	0,56	0,35	0,09	0,04
30,00	31,00	30,50	0,57	2,27	2,27	0,19	0,00	0,00	1966,49	1963,93	1965,21	6,19	3,10	0,55	0,31	0,09	0,04
31,00	32,00	31,50	0,62	2,19					1963,93	1961,00	1962,46	6,44	3,22	0,54	0,33	0,09	0,04
32,00	33,00	32,50	0,65	2,12					1961,00	1957,74	1959,37	6,75	3,37	0,53	0,34	0,09	0,04
33,00	34,00	33,50	0,61	2,04					1957,74	1954,46	1956,10	7,10	3,55	0,52	0,32	0,09	0,05
34,00	35,00	34,50	0,60	1,96					1954,46	1951,02	1952,74	7,50	3,75	0,51	0,30	0,09	0,05
35,00	36,00	35,50	0,64	1,89					1951,02	1947,05	1949,04	7,98	3,99	0,49	0,31	0,10	0,05
36,00	37,00	36,50	0,59	1,81	1,81	0,18	0,00	0,00	1947,05	1943,09	1945,07	8,56	4,28	0,48	0,28	0,10	0,05
37,00	38,00	37,50	0,61	1,68					1943,09	1938,76	1940,92	9,22	4,61	0,47	0,28	0,11	0,05
38,00	39,00	38,50	0,64	1,55					1938,76	1933,94	1936,35	10,02	5,01	0,45	0,29	0,12	0,06
39,00	40,00	39,50	0,61	1,41					1933,94	1929,03	1931,49	10,94	5,47	0,44	0,27	0,13	0,07
40,00	41,00	40,50	0,59	1,28					1929,03	1924,01	1926,52	11,98	5,99	0,43	0,25	0,14	0,07
41,00	42,00	41,50	0,64	1,15					1924,01	1918,29	1921,15	13,22	6,61	0,41	0,26	0,16	0,08
42,00	43,00	42,50	0,65	1,02					1918,29	1912,10	1915,20	14,72	7,36	0,40	0,26	0,19	0,09
43,00	44,00	43,50	0,66	0,88					1912,10	1905,43	1908,76	16,52	8,26	0,38	0,25	0,22	0,11
44,00	45,00	44,50	0,64	0,75	0,75				1905,43	1898,59	1902,01	18,58	9,29	0,37	0,24	0,26	0,13
45,00	46,00	45,50	0,65	0,67					1898,59	1890,89	1894,74	21,06		0,36	0,23	0,29	0,14
46,00	47,00	46,50	0,65	0,58					1890,89	1882,19	1886,54	24,29		0,34	0,22	0,33	0,16
47,00	48,00	47,50	0,65	0,50					1882,19	1872,23	1877,21	28,64		0,32	0,21	0,38	0,19
48,00	49,00	48,50	0,65	0,42					1872,23	1860,64	1866,43	34,71		0,31	0,20	0,46	0,23
49,00	50,00	49,50	0,65	0,33					1860,64	1846,91	1853,77	43,57		0,29	0,19	0,57	0,29
50,00	51,00	50,50	0,65	0,25	0,25				1846,91	1830,50	1838,71	56,99		0,27	0,17	0,76	0,38
51,00	52,00	51,50	0,65	0,19					1830,50	1808,25	1819,38	81,39		0,25	0,16	1,02	0,51
52,00	53,00	52,50	0,65	0,13					1808,25	1772,97	1790,61	146,46		0,21	0,14	1,52	0,76
53,00	54,00	53,50	0,65	0,06					1772,97	##########	##########	##########		##########	##########	3,04	1,52
54,00	55,00	54,50	0,65	0,00	0,00				##########	##########	##########	##########		##########	##########	##########	##########

NZ-80b

Top Depth	Bottom De	Average D	Year, Top	Year, Bott	Year, Aver	Year Std. Dev.
0	0,2	0,1	2020,118	2019,894	2020,006	3,25
0,2	0,4	0,3	2019,894	2019,761	2019,828	3,26
0,4	0,6	0,5	2019,761	2019,572	2019,667	3,26
0,6	0,8	0,7	2019,572	2019,35	2019,461	3,26
0,8	1	0,9	2019,35	2019,087	2019,218	3,27
1	1,2	1,1	2019,087	2018,852	2018,969	3,28
1,2	1,4	1,3	2018,852	2018,619	2018,735	3,28
1,4	1,6	1,5	2018,619	2018,364	2018,491	3,29
1,6	1,8	1,7	2018,364	2018,062	2018,213	3,30
1,8	2	1,9	2018,062	2017,782	2017,922	3,30
2	2,5	2,25	2017,782	2017,21	2017,496	3,32
2,5	3	2,75	2017,21	2016,54	2016,875	3,33
3	3,5	3,25	2016,54	2015,723	2016,131	3,35
3,5	4	3,75	2015,723	2014,982	2015,353	3,37
4	4,5	4,25	2014,982	2014,271	2014,627	3,39
4,5	5	4,75	2014,271	2013,456	2013,864	3,42
5	5,5	5,25	2013,456	2012,591	2013,024	3,44
5,5	6	5,75	2012,591	2011,655	2012,123	3,47
6	6,5	6,25	2011,655	2010,94	2011,297	3,50
6,5	7	6,75	2010,94	2010,078	2010,509	3,53
7	7,5	7,25	2010,078	2009,186	2009,632	3,56
7,5	8	7,75	2009,186	2008,243	2008,714	3,59
8	8,5	8,25	2008,243	2007,306	2007,774	3,63
8,5	9	8,75	2007,306	2006,269	2006,787	3,68
9	9,5	9,25	2006,269	2005,357	2005,813	3,72
9,5	10	9,75	2005,357	2004,337	2004,847	3,77
10	11	10,5	2004,337	2002,188	2003,263	3,86
11	12	11,5	2002,188	1999,9	2001,044	3,98
12	13	12,5	1999,9	1998,055	1998,978	4,10
13	14	13,5	1998,055	1995,931	1996,993	4,22
14	15	14,5	1995,931	1994,1	1995,015	4,33
15	16	15,5	1994,1	1992,27	1993,185	4,43
16	17	16,5	1992,27	1990,69	1991,48	4,51
17	18	17,5	1990,69	1989,113	1989,901	4,58
18	19	18,5	1989,113	1987,436	1988,274	4,67
19	20	19,5	1987,436	1985,77	1986,603	4,76
20	21	20,5	1985,77	1984,188	1984,979	4,86
21	22	21,5	1984,188	1982,423	1983,306	4,98
22	23	22,5	1982,423	1980,676	1981,55	5,09
23	24	23,5	1980,676	1978,793	1979,735	5,21
24	25	24,5	1978,793	1976,986	1977,889	5,33
25	26	25,5	1976,986	1975,314	1976,15	5,43
26	27	26,5	1975,314	1973,305	1974,309	5,54
27	28	27,5	1973,305	1971,273	1972,289	5,66
28	29	28,5	1971,273	1969,003	1970,138	5,80
29	30	29,5	1969,003	1966,491	1967,747	5,98
30	31	30,5	1966,491	1963,926	1965,209	6,19
31	32	31,5	1963,926	1961,001	1962,464	6,44
32	33	32,5	1961,001	1957,736	1959,369	6,75
33	34	33,5	1957,736	1954,459	1956,097	7,10
34	35	34,5	1954,459	1951,017	1952,738	7,50
35	36	35,5	1951,017	1947,053	1949,035	7,98
36	37	36,5	1947,053	1943,088	1945,071	8,56
37	38	37,5	1943,088	1938,76	1940,924	9,22
38	39	38,5	1938,76	1933,941	1936,351	10,02
39	40	39,5	1933,941	1929,031	1931,486	10,94
40	41	40,5	1929,031	1924,007	1926,519	11,98
41	42	41,5	1924,007	1918,292	1921,15	13,22
42	43	42,5	1918,292	1912,1	1915,196	14,72
43	44	43,5	1912,1	1905,426	1908,763	16,52
44	45	44,5	1905,426	1898,593	1902,01	18,58
45	46	45,5	1898,593	1890,887	1894,74	21,06
46	47	46,5	1890,887	1882,189	1886,538	24,29
47	48	47,5	1882,189	1872,229	1877,209	28,64
48	49	48,5	1872,229	1860,636	1866,432	34,71
49	50	49,5	1860,636	1846,909	1853,772	43,57
50	51	50,5	1846,909	1830,505	1838,707	56,99
51	52	51,5	1830,505	1808,246	1819,375	81,39
52	53	52,5	1808,246	1772,966	1790,606	146,46
53	54	53,5	1772,966	########	########	########
54	55	54,5	########	########	########	########

Beyond Pb dating

Sample	Average a	st.dev.
0-0,5	2019,892	3,254782
0,5-1	2019,377	3,265013
1-1,5	2018,789	3,280231
1,5-2	2018,136	3,296943
2--3	2017,161	3,317773
3--4	2015,761	3,352035
4--5	2014,219	3,394467
5--6	2012,556	3,443388
6--7	2010,866	3,497923
7--8	2009,16	3,559214
8--9	2007,256	3,634409
9--10	2005,303	3,722412
10--11	2003,263	3,812175
11--12	2001,044	3,918127
12--13	1998,978	4,04138
13-14	1996,993	4,160078
14-15	1995,015	4,275811
15-16	1993,185	4,382974
16-17	1991,48	4,473214
17-18	1989,901	4,548807
18-19	1988,274	4,624961
19-20	1986,603	4,713194
20-21	1984,979	4,812135
21-22	1983,306	4,919874
22-23	1981,55	5,034057
23-24	1979,735	5,151063
24-25	1977,889	5,268383
25-26	1976,15	5,37983
26-27	1974,309	5,485941
27-28	1972,289	5,599118
28-29	1970,138	5,730909
29-30	1967,747	5,891625
31-32	1965,209	6,086195
32-33	1962,464	6,317059
33-34	1959,369	6,595323
34-35	1956,097	6,924289
35-36	1952,738	7,298614
36-37	1949,035	7,738699
37-38	1945,071	8,267858
38-39	1940,924	8,886734
39-40	1936,351	9,617077
40-41	1931,486	10,48021
41-42	1926,519	11,46415
42-43	1921,15	12,60095
43-44	1915,196	13,97089
44-45	1908,763	15,62105

Sample	Average a	st.dev.
0-0,5	2019,892	3,254782
1-1,5	2018,789	3,280231
2--3	2017,161	3,317773
5--6	2012,556	3,443388
8--9	2007,256	3,634409
11--12	2001,044	3,918127
14-15	1995,015	4,275811
17-18	1989,901	4,548807
20-21	1984,979	4,812135
23-24	1979,735	5,151063
26-27	1974,309	5,485941
29-30	1967,747	5,891625
32-33	1962,464	6,317059
35-36	1952,738	7,298614
38-39	1940,924	8,886734
41-42	1926,519	11,46415
44-45	1908,763	15,62105

Appendix 4

Palynology counts (raw data, relative abundances, absolute abundances)

Table 1.1 Dinocyst counts, raw data

Table 1.2 Dinocyst counts, relative abundances

Table 1.3 Dinocyst counts, absolute abundances

Table 2.1 Pollen counts, raw data

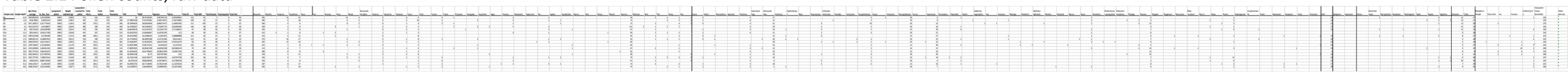

Table 2.2 Pollen counts, relative abundances

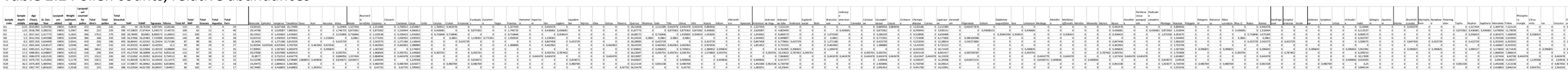

Table 2.3 Pollen counts, absolute abundances

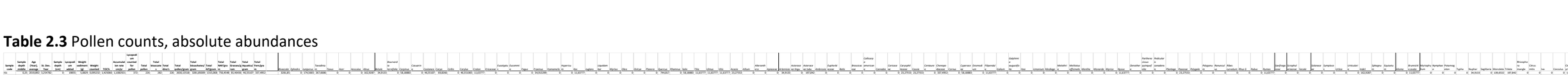

Appendix 5

Choices made in statistical analysis

Choices made for PCA

A note beforehand

Is it even possible to perform a PCA with the amount of samples in my dataset? If there are too little samples, the PCA is bound too much to the limited variation in the dataset.
According to Osborne and Costello (2004), for example, at least 100 samples are needed for accurate PCA results in general. However, this is the statistician's view. In ecological/palynological practice, less samples might be enough. In their book on this subject, Leps and Smilauer (2003) present an ecological presented with only 70 samples and an impressive 285 variables.
According to this criterion, I would not have enough samples. In order to compare palynological and chemical variables, the palynological variables can be interpolated (or a transfer function might be created), so that they yield a value for all 47 datapoints instead of 22. However, this only creates the illusion of more available data: the overall variability for the palynological variables does not change. However, according to Timme Donders (personal communication), it does not matter so much if one performs a PCA on less than 40 datapoints. The crucial point is that the amount of samples has to be quite a bit larger than the amount of variables used per PCA. He recommends a 1:3 2 ratio for variables:samples. Therefore, I will use a maximum of 7-8 variables per PCA when dinoflagellate data is involved (22 samples), 5-6 for pollen data (17 samples) and 15-16 for chemical data (47 samples). If we wanted to be even more strict, Donders recommends a 1:5 ratio. This would mean a maximum of 9-10 variables for chemical data, but only 4-5 dinoflagellate variables and 3-4 for pollen, which is a bit too little, and might prevent us from finding important patterns and correlations.

The small size of my dataset also prevents me from drawing quantitative conclusions from the PCA, as the ratios seen in the plots might not be accurate. However, we can interpret the PCA's results qualitatively.

- **Standarizing variables.**
  To properly conduct a PCA, variables should be comparable. If one variable has an order of magnitude of 100 of 1000, and another varies between -2 and 2, the relationship that will be found by the PCA will be skewed: much more weight will be given to the larger variables. All other variables will be compared to the large variable and less to each other.
  Standarizing the data smoothens this difference as much as possible. Standarized variables will be compared in the same dimension. Standardization is done by substracting the mean of a variable for each of its values, then dividing by the variable's standard deviation:
  Standarized value = (original value - mean)/standard deviation.

- **Using PCA rather than CCA.**
  PCA assumes that variables react linearly to an environmental forcing, while CCA assumes a unimodal reaction, where the variables has an optimum. In this case, using a PCA or CCA does not make much of a difference: I compared the results of some PCA's to the results of a related, unimodal analysis (in which it is assumed the variables react unimodally instead of linearly) using the same variables and datapoints, to see if their results differed. The

difference in results was small.
If we assume a unimodal model, we have to apply this same model to all variables (bron boek van Timme). However, while taxons of dinoflagellates or pollen might have an optimum for a certain environmental forcing, the chemical variables probably have not. If we assume a unimodal model, chemical and palynological variables might not be comparable.
Furthermore, a unimodal model needs all-positive data (boek van Timme). As standardization has caused many values to be negative, a constant should be added in many instances. This is another manipulation of the data, which might obscure original correlations. I want to reduce unnecessary manipulations as much as possible.
Thirdly, I am used to interpreting PCA results, while CCA interpretation is somewhat more arcane to me.
So, I will use a linear model and perform PCA's.

- **Comparison to correlation coefficients (Kendall's tau) when an interesting correlation was suggested by the PCA.**

- **No RDA.**
  RDA is the constrained variant of PCA, used to see how species data react to one specific environmental variable. However, it could not be done using the programs used, or was too complicated and too time-consuming to learn to interpret. So, I sticked with PCA.

- **No log transformation.**
  A log-transform is often used to normalize the data before performing a PCA. However, data does not have to be normally distributed for a PCA, as for example stressed by researchers on the ResearchGate question forum, for example at
  https://www.researchgate.net/post/If_I_dont_have_a_normal_distribution_for_one_or_two_variables_is_it_still_possible_convenient_to_perform_PCA
  and
  https://www.researchgate.net/post/Hello-everyone-Is-it-possible-to-do-PCA-analysis-if-data-is-not-normally-distributed.
  Linearity is far more important than normality. For my variables, the relatively small amount of datapoints increases the likelihood of a non-normal distribution. This was indeed evident from the Shapiro-Wilk normality test (the most commonly used test) for most of my proxies. However, sometimes a log-transform for a specific variable is useful.
  The book by Leps and Smilauer (2003) says (p. 14): "The question of when to apply a log transformation and when to use the original scale is not an easy one to answer and there are almost as many answers as there are statisticians. We advise you not to think so much about distributional properties, at least not in the sense of comparing frequency histograms of the variables with the ideal Gaussian (normal) distribution. **Rather try to work out whether to stay on the original axis or log-transform by using the semantics of the hypothesis you are trying to address.**"
  This means that, if we are looking for a quantitative result (such as "when this variables increases with unit 1, this species increases by 10 percent"), then it is needed to log-transform the response variable (in this case the species variable). However, if the PCA is only used explanatory (qualitatively), as I am using it, transformation is not needed. The

original axis is then preserved.

- **Interpolation of missing values.**
  One common way to deal with missing values is to delete them (Leps and Smilauer, 2003). However, if we wanted to compare chemical data to palynological data, we could only use the 22 datapoints where the palynological variables have a value. We would not use the chemical information of the 25 other datapoints, so that more than half of all information would be missing.
  A better way is to use a transfer function, to generate values for the missing spaces out of the known values. This does not increase the amount of information present, but allows us to compare all 47 datapoints.
  There are several ways to do this, such as substituting the variable's mean for all missing values. However, this would reduce the original variability (Swalin, 2018) which is exactly what we do not want for the PCA, and would change the variable's patterns (as seen in the graph) far too greatly. It is better to use interpolation. This uses the least assumptions about trends in the data and will not change the graph.
  Interpolation is, of course, not ideal: it may change the variable's mean and causes problems in quantitative analysis. But the mean is far less crucial than, for example, the largest amount of information and original variability, and I was not planning on using the PCA for quantitative means anyway.

  Only the record of Atchafalaya nitrate concentration cannot be interpolated, due to two large stretches of missing variables near the end and at the end. We would need extrapolation to fill in these missing values, but this would use assumptions that are too spurious.
  So, whenever this record is compared with other variables in a PCA, I can only use 29 samples (a maximum of 9-10 variables per PCA) instead of 47.

Leps, J., and Peter Smilauer. 2003. Multivariate Analysis of Ecological Data using Canoco. Cambridge: Cambridge University Press.

Osborne, Jason W., and Anna B. Costello. 2004. ample size and subject to item ratio in principal components analysis. Practical Assessment, Research, and Evaluation, Vol. 9, Art. 11. DOI: https://doi.org/10.7275/ktzq-jq66

Swalin, Alvira. 2018. How To Handle Missing Data. Towards Data Science, https://towardsdatascience.com/how-to-handle-missing-data-8646b18db0d4